Université de Montréal

Plasticity of neuroanatomical relationships between cholinergic and dopaminergic axon varicosities and pyramidal cells in the rat medial prefrontal cortex

par

Zi Wei Zhang

Programme de sciences neurologiques, Ph.D.

Faculté de médecine

Thèse présentée à la Faculté des études supérieures

en vue de l'obtention du grade de Philosophiae Doctor (Ph.D.)

en sciences neurologiques

Septembre 15, 2011

Université de Montréal

Faculté des études supérieures et postdoctorales

Cette thèse intitulée:

Plasticity of neuroanatomical relationships between cholinergic and dopaminergic axon varicosities and pyramidal cells in the rat medial prefrontal cortex

Présentée par :

Zi Wei Zhang

a été évaluée par un jury composé des personnes suivantes :

Dr Laurent Descarries, président-rapporteur

Dre Elvire Vaucher, directrice de recherche

Dr Guy Doucet, membre du jury

Dre Kathleen Rockland, examinatrice externe

Dre Hélène Girouard, représentante du doyen de la FES

Résumé

Les systèmes cholinergique et dopaminergique jouent un rôle prépondérant dans les fonctions cognitives. Ce rôle est exercé principalement grâce à leur action modulatrice de l'activité des neurones pyramidaux du cortex préfrontal. L'interaction pharmacologique entre ces systèmes est bien documentée mais les études de leurs interactions neuroanatomiques sont rares, étant donné qu'ils sont impliqués dans une transmission diffuse plutôt que synaptique. Ce travail de thèse visait à développer une expertise pour analyser ce type de transmission diffuse en microscopie confocale.

Nous avons étudié les relations de microproximité entre ces différents systèmes dans le cortex préfrontal médian (mPFC) de rats et souris. En particulier, la densité des varicosités axonales *en passant* a été quantifiée dans les segments des fibres cholinergiques et dopaminergiques à une distance mutuelle de moins de 3 µm ou à moins de 3 µm des somas de cellules pyramidales. Cette microproximité était considérée comme une zone d'interaction probable entre les éléments neuronaux. La quantification était effectuée après triple-marquage par immunofluorescence et acquisition des images de 1 µm par microscopie confocale. Afin d'étudier la plasticité de ces relations de microproximité, cette analyse a été effectuée dans des conditions

témoins, après une activation du mPFC et dans un modèle de schizophrénie par déplétion des neurones cholinergiques du noyau accumbens.

Les résultats démontrent que

1. Les fibres cholinergiques interagissent avec des fibres dopaminergiques et ce sur les mêmes neurones pyramidaux de la couche V du mPFC. Ce résultat suggère différents apports des systèmes cholinergique et dopaminergique dans l'intégration effectuée par une même cellule pyramidale.

2. La densité des varicosités *en passant* cholinergiques et dopaminergiques sur des segments de fibre en microproximité réciproque est plus élevée comparé aux segments plus distants les uns des autres. Ce résultat suggère un enrichissement du nombre de varicosités axonales dans les zones d'interaction.

3. La densité des varicosités *en passant* sur des segments de fibre cholinergique en microproximité de cellules pyramidales, immunoúactives pour c-Fos après une stimulation visuelle et une stimulation électrique des noyaux cholinergiques projetant au mPFC est plus élevée que la densité des varicosités de segments en microproximité de cellules pyramidales non-activées. Ce résultat suggère un enrichissement des varicosités axonales dépendant de l'activité neuronale locale au niveau de la zone d'interaction avec d'autres éléments neuronaux.

4. La densité des varicosités en passant des fibres dopaminergiques a été significativement diminuée dans le mPFC de rats ayant subi une déplétion cholinergique dans le noyau accumbens, comparée aux témoins. Ces résultats supportent des interrelations entre la plasticité structurelle des varicosités dopaminergiques et le fonctionnement cortical.

L'ensemble des donneès démontre une plasticité de la densité locale des varicosités axonales en fonction de l'activité neuronale locale. Cet enrichissement activité-dépendant contribue vraisemblablement au maintien d'une interaction neurochimique entre deux éléments neuronaux.

Mots-clés : acétylcholine, cognition, cortex préfrontal médian, dopamine, glutamate, morphométrie, neurones pyramidaux, transmission diffuse, varicosités axonales, schizophrénie.

Abstract

The cognitive functions of the rat medial prefrontal cortex (mPFC) are modulated by ascending modulatory systems such as the cholinergic and dopaminergic afferent systems. However, despite the well-documented pharmacological interactions between the cholinergic and dopaminergic afferents and pyramidal cells in the PFC, there is only scarce neuroanatomical data on the reciprocal interrelationships between these neuronal elements in the mPFC. This might be due to the diffuse rather than synaptic transmission mode of intercellular communication of the cholinergic system in the mPFC. For these reasons, the neuroanatomical relationships between the cholinergic and dopaminergic systems and pyramidal cells in the mPFC are examined, with an emphasis on the local density of the cholinergic and dopaminergic axon varicosities. To analyze the plasticity of these interrelationships, the two systems were examined in condition of increased neuronal activity in the mPFC, or of decrease dopaminergic activity in a model of schizophrenia.

The microproximity relationships between cholinergic and dopaminergic fibers as well as with pyramidal cells were studied in the mPFC of rats and mice. In particular, the number of axon varicosities in cholinergic and dopaminergic fiber segments within 3 µm from each other or from pyramidal cells were quantified. This microproximity was considered as a possible

interaction zone between two neuronal elements. Quantification was performed using triple immunofluorescence labeling and acquisition of 1 µm optic sections using confocal microscopy. To assess the plasticity of these relationships, the analysis has been performed in control condition as well as after a cortical activation or a decreased dopaminergic input in a schizophrenia model.

Our results demonstrate a neuroanatomical convergence of cholinergic and dopaminergic fibers on the same pyramidal cell from layer V (output) of mPFC, suggestinggests the integration of different types of inputs by the same pyramidal cell, which may be transmitted to subcortical areas to execute prefrontal cognitive control. Close apposition between cholinergic and dopaminergic fibers could also be seen in the mPFC.

There was an increase of the density of cholinergic and dopaminergic en passant varicosities on those fiber segments within microproximity of each other, compared to those outside the reciprocal microproximity, supporting functional importance of the close apposition between those two ascending neuromodulatory systems into the mPFC.

There was enrichment of cholinergic en passant varicosities on the fiber segments within microproximity of c-Fos activated pyramidal cells in the mPFC of visually and HDB electrically stimulated rats, indicating association between axonal varicosity density and the local neuronal activity.

There was decrease of dopaminergic en passant varicosities in the mPFC of rats with ChAT depletion in the N.Acc., compared to controls. This evidence supports the association between dopaminergic axonal varicosities and relevant neuronal activity in a complex neuronal network.

This thesis shows that the density of cholinergic and dopaminergic axonal varicosity density in the mPFC is influenced by and contributes to the relevant local neuronal activity from the interactions of different transmitter systems. Such interactions of different systems in a complex and intricate prefrontal neuronal network endeavour to maintain the delicate balance for cognitive processes.

Keywords: acetylcholine, axon varicosity, cognition, diffuse transmission, dopamine, glutamate, pyramidal cells, medial prefrontal cortex, morphometry, schizophrenia.

TABLE OF CONTENTS

LIST OF TABLES

CHAPTER II

CHAPTER III

CHAPTER IV

LIST OF FIGURES

CHAPTER I

CHAPTER II

CHAPTER III

CHAPTER IV

CHAPTER V

LIST OF ABBREVIATIONS

5-HT	5-hydroxytryptamine
AAV	adeno-associated virus
AC	anterior cingulate cortex
ACh	acetylcholine
AChE	acetylcholinesterase
ADHD	attention deficit hyperactivity disorder
AI	agranular insular cortex
AMPA	α-amino-3-hydroxy-5-methyl-4-isoazolepropionic acid
AO	anterior olfactory nucleus
BF	basal forebrain
BL	basolateral amygdaloid nucleus
Cg1	anterior cingulate cortex
ChAT	choline acetyltransferase
CNS	central nervous system
D_1R	D_1 dopamine receptor
D_2R	D_2 dopamine receptor
D_3R	D_3 dopamine receptor
D_4R	D_4 dopamine receptor
D_5R	D_5 dopamine receptor
DA	dopamine

DAT	dopamine transporter
DR	dorsal raphé
dltn	laterodorsal tegmental nucleus
EAAC1	excitatory amino acid carrier 1 protein
EAATs	excitatory amino-acid transporters
ENT	entorhinal cortex
EPSP	excitatory post-synaptic potential
GABA	γ-aminobutyric acid
GluR1	Glutamate Receptor subtype 1
GluT	glutamate transporter
HDB	horizontal limb nuclei of the diagonal band of Broca
ICj	islands of Calleja
iGluRs	ionotropic glutamate receptors
IL	infralimbic cortex
IP	interpeduncular nucleus
Kainate	2-carboxy-3-carboxymethyl-4-isopropenylpyrrolidine
L	lateral amygdaloid nucleus
LC	locus ceruleus
L-DOPA	L-dyhydroxyphenylalanine
LTP	long term potential
mAChRs	muscarinic ACh receptors
nBM	nucleus basalis magnocellularis
mGluRs	metabotropic glutamate receptors

mPFC	medial prefrontal cortex
MS	medial septum
N.Acc.	nucleus accumbens
nAChRs	nicotinic ACh receptors
NE	norepinephrine
NET	NE transporter
NMDA	N-methyl-D-aspartate
OC	occipital cortex
PCl	lateral precentral cortex
PCm	medial precentral cortex
PIR	piriform cortex
PR	perirhinal cortex
PrL	prelimbic cortex
PV	paraventricular hypothalamic nucleus
ROI	region of interest
RS	retrosplenial cortex
sEPSCs	spontaneous excitatory postsynaptic currents
SI	substantia innominata
SN	substantia nigra
SNc	substantia nigra pars compacta
SS1/SS 2	somatosensory cortex 1 and 2
TE	temporal cortex
TH	tyrosine hydroxylase

VAChT	vesicular acetylcholine transporter
VDB	vertical limb nucleus of diagonal band of Broca
VP	ventral pallidum
VTA	ventral tegmental area

DEDICATION

I dedicate this thesis to my mother and my father.

ACKNOWLEDGEMENTS

I would like to thank my research supervisor, Dre Elvire Vaucher, for giving me this great opportunity to explore into the mechanisms of the brain, and for all her guidance, help and trust in my research work during those past years.

I would like to thank all my team members, collleagues, co-workers and friends, whose generous help, valuable advice, and sincere encouragement are an indispensible part of my Ph.D. research.

I would also like to thank the school of Optometry in the University of Montreal, for providing me not only a great research environment but also generous scholarships during my graduate studies. I will keep those pleasant moments I spent here in my memory.

Last but not least, I would like to thank my mother and my father, whose unconditional love encourages me to believe in myself and be faithful to my dreams, even in situations of adversities. I would also like to thank my brother, whose deep wisdom has helped me to keep growing and improving.

CHAPTER I

General Introduction

The central nervous system (CNS) is a global network wherein the dynamic influences of a variety of neuromodulators on afferent input versus intrinsic input depend on broad and diffuse transmission, which enables the “entire provinces of the CNS” to be in the appropriate functional setting and to work as a unit (Agnati et al., 1995; Descarries et al., 1997; Giocomo and Hasselmo, 2007; Lendvai and Vizi, 2008).

I.1 Introduction to the cerebral cortex

I.1.1 Functional and anatomic organization of the cerebral cortex

The grey matter covering the cerebral hemispheres is the cerebral cortex (Ellis and Keswick, 2011), Figure I.1), which is divided in four anatomically distinct lobes: frontal, parietal, temporal, and occipital (Kandel et al., 2000). A great number of cortical areas have been defined in relation to their functional specialization, from primary sensory areas, to association and motor cortex. The cerebral cortex is primarily responsible for cognitive abilities, integrating information from a diverse range of sources by processing bottom-up sensory signals of relevant behavioral significance, top-down feedback carrying goal-related information, as well as intrinsic horizontal signals carrying contextual information (Miller and Cohen, 2001, Raizada and Grossberg, 2003). Cortical areas are richly interconnected with each other and with subcortical structures, and many mental

functions are processed by the serial and parallel interlinking of several cortical regions and neuronal pathways (Shipp, 2007).

Figure I.1.

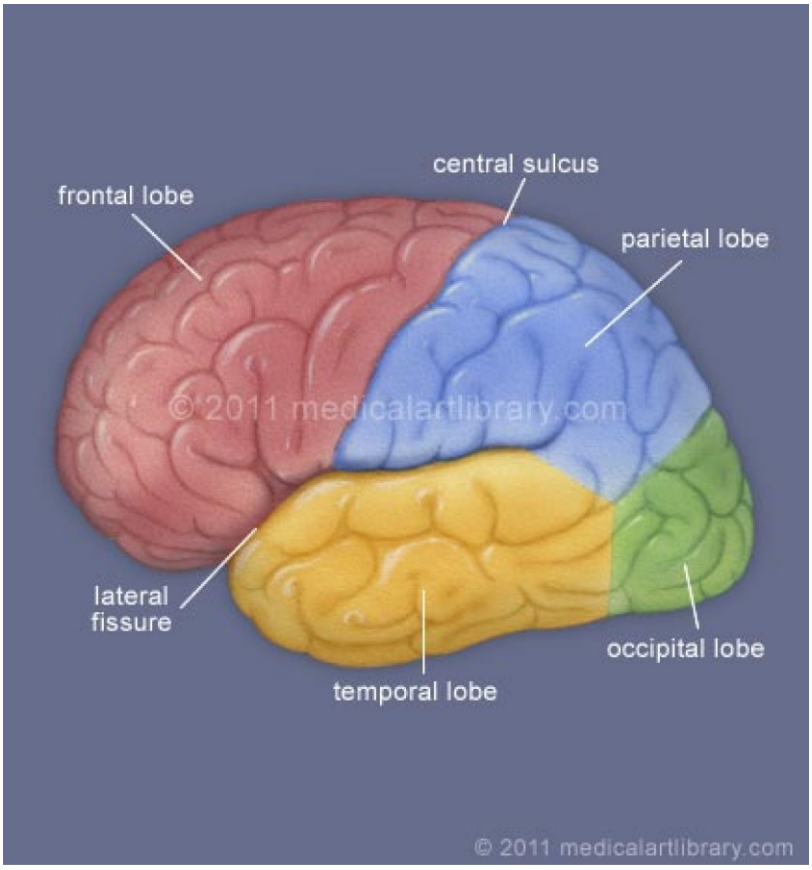

Figure I.1. Representation of the frontal, parietal, temporal, and the occipital lobe of the brain. The cerebral cortex covers the surface of the cerebral hemispheres. Figure from http://www.stockmedicalart.com/medicalartlibrary/brain-lobes.html

The cerebral cortex is organized in functional layers. In general the neocortex has a six-layered structure, although some cortical structures such as the hippocampus have fewer than six layers (Raizada and Grossberg, 2003). The uniformity of this layered pattern suggests cortex's basic "housekeeping" operations that generalize across diverse cortical functions (Shipp, 2007). Generally, neurons in layers II and III tend to form corticocortical connections, those in layers V and VI project to subcortical areas, and those in layers I and IV extend axons locally within the cortex. Different layers have distinctive densities and morphologies of their constituent neurons (Leone et al., 2008). Moreover, different cortical projection systems also demonstrate specific laminar distributions of efferent terminations and their neurons of origin. For example, a study of the occipital lobe from the rhesus monkey demonstrates that, rostrally directed cortical connections originate from neurons in layer IIIc and terminate in layer IV, whereas caudally directed connections originate in layers Vb, VI and IIIa, and terminate in layer I (Rockland and Pandya, 1979). The laminar fate of a neuron is under the control of specific genetic and molecular mechanisms (Yamamori and Rockland, 2006; Leone et al., 2008).

I.1.2 Nerve cells – basic units of the cerebral cortex

The basic units of the brain are individual nerve cells. Four morphologically defined structures in a typical neuron are the cell body, dendrites, the axon, and axon terminals. The cell body or soma surrounds the nucleus, the dendrites are the main target of incoming signals from other nerve cells, whereas the axon carries signals to other neurons by projecting to target cells and the nerve terminals release neurotransmitters (Kandel et al., 2000, Cooper et al., 2003). Axo-axonal and axo-somatic relationship has also been evidenced. There is a large variety of neurons in the cortex with different physiological properties but two maincortical types are classified: interneurons with short axons to process information within local circuits, and projection neurons (pyramidal neurons) with long axons to carry signals from one brain region to another over long distances (Rockland, 1998, Kandel et al., 2000). The interneurons are mostly GABAergic and inhibitory, although spiny stellate cells of layer IV and local pyramidal neurons of layer II-III are glutamatergic. The pyramidal cells are glutamatergic and excitatory.

The neurons communicate together through synaptic transmission and diffuse transmission. Synapses are specialized zones of communication between neurons (Cooper et al., 2003). The presynaptic cell and the postsynaptic cell are separated by the synaptic cleft. When an action potential reaches a neuron's terminal it

stimulates the release of transmitters, which diffuse across the synaptic cleft and bind to receptors in the membrane of the postsynaptic neurons to influence the neuronal activity (Kandel et al., 2000). This synaptic transmission has been extensively described, However, in the past decades, the existence of nonsynaptic interactions or diffuse transmission has also been recognized, whereby the transmitters are released from axon terminals without synaptic contacts, diffuse and stimulate extrasynaptically located receptors to influence the activity of other neurons in their microenvironment (Agnati et al., 1995, Descarries et al., 1997, Lendvai and Vizi, 2008).

I.1.3 Major neurotransmitter systems in the cortex

The complex and subtle control of the state of the nervous system is executed by a wide variety of transmitter systems abundantly distributed in the cortex with region-specific and layer-specific patterns (Eickhoff et al., 2007). Glutamatergic and GABAergic (γ-aminobutyric acid) neurons are among the major cortical neurons (DeFelipe et al., 2002). Transmitters that are more prolonged in duration are typically involved in the control of the state of the executive networks such as arousal and attention, including acetylcholine, norepinephrine, serotonin, dopamine, histamine, adenosine, and probably numerous other agents (McCormick, 1992, Briand et al., 2007). A single neurotransmitter may produce a

diverse range of postsynaptic responses via coupling of different subtypes of receptors to different second messenger systems. (McCormick, 1992).

I.2 The rat medial prefrontal cortex

I.2.1 Neuroanatomy of the medial prefrontal cortex

Located over the medial, orbital, and insular surfaces of the rostral cerebral hemispheres, the prefrontal cortex (PFC) consists of the medial prefrontal cortex (mPFC), the orbital prefrontal cortex, and the lateral or sulcal prefrontal cortex (Heidbreder and Groenewegen, 2003), which process specific aspects of cognitive processing including working memory, behavioral inhibition, attentional processing, and organization, planning and flexibility of behavior (Uylings et al., 2003, Dalley et al., 2004a, Gabbott et al., 2005, Briand et al., 2007). The rodent cortex serves as a good model for analyzing prefrontal functions (Uylings et al., 2003). The connectivity between the PFC with virtually all sensory neocortical regions, motor regions, and subcortical structures (Groenewegen and Uylings, 2000) enables its “top-down” processing of behaviorally relevant sensory stimuli.

The rat medial prefrontal cortex (mPFC) has four main subdivisions: the medial precentral, the anterior cingulate (Cg1), the prelimbic (PrL) and the

infralimbic (IL) areas (Vertes, 2004, Tavares and Correa, 2006). In the rat, Cg1, PrL and IL are typical agranular cortical fields, that is, regions without a layer 4 (Gabbott et al., 1997, Ding et al., 2001). The mPFC in rodents has been suggested to be functionally equivalent to the dorsolateral PFC in primates (Brown and Bowman, 2002, Uylings et al., 2003). Functional differentiation between the dorsal mPFC (Cg1 and the dorsal PrL) and ventral mPFC (IL and the ventral PrL) has been discussed, with the involvement of the dorsal mPFC in the temporal shifting of behavioral sequences, and the role of the ventral mPFC in a flexible shifting to new strategies related to spatial cues (Heidbreder and Groenewegen, 2003, Uylings et al., 2003).

I.2.2 Involvement of the medial prefrontal cortex in a variety of cognitive functions

The mPFC in rodents is involved in a variety of cognitive and emotional processes (Brown and Bowman, 2002, Heidbreder and Groenewegen, 2003), and has been implicated in many of the cognitive and behavioral disturbances associated with major neuropsychiatric disorders, such as ADHD and schizophrenia (Brown and Bowman, 2002, Dalley et al., 2004a). The dorsal mPFC is involved in the temporal patterning of behavioral sequences, whereas the ventral part the mPFC plays an important role in flexible shifting to new strategies, and the preparatory processes of reaction time performance (Heidbreder and

Groenewegen, 2003). Attentional selectivity in the visual domain resides mainly in Cg1 (Dalley et al., 2004b), and the rostral part of the Cg1 responds to electrical stimulation of the visual cortex (Golmayo et al., 2003). The Cg1 is also crucial in processing negative events such as errors and losses of reward, which is involved in initiating increases in attentional effort (Sarter et al., 2006). In contrast, infusions of scopolamine, a muscarinic antagonist, into the rat PrL/IL, results in significant impairments in a spatial working memory task (12-arm radial maze using recognition go/no-go procedure) (Ragozzino and Kesner, 1998). Local lesions of the rat PrL and IL by infusion of ibotenic acid result in selective impairments of extra-dimensional attentional set-shifting (Birrell and Brown, 2000). PrL neuronal activity is modulated by task variables during sustained attentional performance (Gill et al., 2000).

I.2.3 Prefrontal glutamatergic output to the basal forebrain

The PFC sends a glutamatergic output to the basal forebrain (BF), which modulate its activity (Zaborszky et al., 1997, Hur et al., 2009). Projections from the medial and ventral prefrontal areas give rise to dense arborizations in BF, particularly to horizontal limb nuclei of the diagonal band of Broca (HDB) and the region ventral to it (Zaborszky et al., 1997). Descending fibers from neocortical areas to BF are smooth and devoid of terminal varicosities, and contained glutamate immunoreactivity (Zaborszky et al., 1997). Many large Glutamate

Receptor subtype 1 (GluR1) - positive neuronal perikarya and aspiny dendrites are present within the medial septal nucleus, the nucleus of the diagonal band of Broca, and the nucleus basalis of Meynert, as shown in an immunocytochemistry study using antipeptide antibodies that recognized GluR subunit proteins in rat and monkey (Martin et al., 1993).

I.3 Cholinergic system in the medial prefrontal cortex

The cholinergic innervation of the cerebral cortex from the basal forebrain neurons has a strong modulatory role of the cortical activity. It is mostly involved in cognitive functions.

I.3.1 Cholinergic projections

Cholinergic neurons use acetylcholine (ACh) as their neurotransmitter. ACh is synthesized from choline in one single step, in which choline acetyltransferase (ChAT) mediates the transfer of an acetyl group from acetyl coenzyme A to choline (Sarter and Parikh, 2005), and then ACh is pumped into synaptic vesicles by the vesicular ACh transporter (VAChT) (Okuda and Haga, 2003). After ACh is released, it is rapidly metabolized into choline by acetylcholinesterase (AChE) (Nikonenko et al., 2003). ACh is the only classical neurotransmitter to be removed not by reuptake, but via fast hydrolysis by AChE (Silman and Sussman, 2005).

The Na^+-dependent, high-affinity choline transporter in the plasma membrane takes up choline into the presynaptic terminals, which is subsequently used for ACh synthesis. Choline uptake is thought to be the rate limiting step in ACh synthesis (Okuda and Haga, 2003). Measuring ChAT activity is the most specific indicator for monitoring the functional state of cholinergic neurons in the CNS (Trachtenberg et al., 2002). ChAT is a specific marker of cholinergic cells and fibres and allows for a maximal immunocytochemical detection of cholinergic axons and varicosities in the rat neocortex (Umbriaco et al., 1994, Mechawar et al., 2000).

The main nuclei of cholinergic soma are located in the basal forebrain and the pons. They constitutes two major cholinergic projection systems in the rat central nervous system, (Everitt and Robbins, 1997) (Figure I.2). The basal forebrain (BF) within the medial septal nucleus (MS), vertical (VDB) and horizontal (HDB) limb nuclei of the diagonal band of Broca, and the nucleus basalis magnocellularis (nBM) send broad cholinergic projections throughout the cortex and hippocampus. Cholinergic neurons in the pedunculopontine tegmentum and the laterodorsal pontine tegmentum provide widespread projections mainly to the thalamus, midbrain and the brain stem (Everitt and Robbins, 1997, Dani, 2001).

Figure I.2

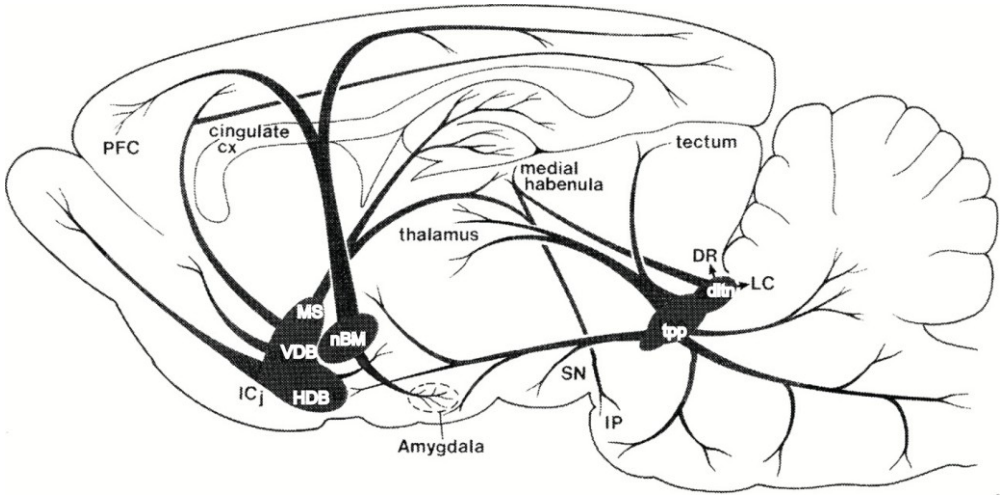

Figure I.2. Distribution of central cholinergic neurons and their projections in the rat brain. (Woolf, 1991) Abbreviations: MS, medial septum; VDB, vertical limb nuclei of the diagonal band of Broca; HDB, horizontal limb nuclei of the diagonal band of Broca; nBM, nucleus basalis magnocellularis; tpp, pedunculopontine tegmental nucleus; dltn, laterodorsal tegmental nucleus; PFC, prefrontal cortex; ICj, islands of Calleja; SN, substantia nigra; IP, interpeduncular nucleus; DR, dorsal raphé; LC, locus ceruleus.

Cholinergic neurons are involved in a wide variety of cognitive functions including attention, learning, memory, arousal, sleep and movement, and their loss of functional deficit are associated with neurological disorders such as attention deficit hyperactivity disorder (ADHD), Alzheimer's disease and schizophrenia (Dunnett et al., 1991, Breese et al., 2000, Sarter and Bruno, 2000, Trachtenberg et al., 2002, Kozak et al., 2006, Zhang, 2006, Bellgrove and Mattingley, 2008, Jones, 2008, Lester et al., 2010, Bohnen and Albin, 2011, Hasselmo and Sarter, 2011, Robinson et al., 2011, Wallace et al., 2011).

I.3.2 Cholinergic receptors

ACh released from the nerve terminals interacts with and activates the ionotropic nicotinic ACh receptors (nAChRs) or the metabotropic muscarinic ACh receptors (mAChRs) (Hasselmo and Sarter, 2011). Although being activated by the same ligand, ACh, nAChRs and mAChRs are members of two quite separate gene superfamilies (Hulme et al., 1990).

Ionotropic nAChRs are pentameric acetylcholine-gated ion-channel receptors which are sensitive to nicotine and mediate fast excitatory synaptic transmission (Zhang, 2006, Albuquerque et al., 2009, Sydserff et al., 2009, Wallace et al., 2011). nAChRs are assembled from twelve subunits, α2-α10 and β2-β4, which combin to form homomeric or heteromeric nAChRs (Anderson et al.,

2009). The heteromeric assembly of α 4β2 subunits (the high-affinity nicotine-binding sites), and the homomeric assembly of α7 subunits (the majority of the a-bungarotoxin binding sites) are the two major types of functional nAChRs within the brain (Dani, 2001, Couey et al., 2007, Albuquerque et al., 2009, Wallace et al., 2011). nAChRs have predominantly modulatory functions in the brain (Livingstone et al., 2010). α4β2 neuronal nicotinic receptors are localized in the dopaminergic-rich brain regions including cerebral cortex, hippocampus, ventral tegmentum and substantia nigra (Gotti et al., 2006), and can exist in high (nM) and low (μM) sensitivity states (Anderson et al., 2009, Wallace et al., 2011). α7 nAChRs are localized almost exclusively in the brain, with high calcium permeability and rapid desensitization upon agonist binding (Wallace et al., 2011).

In contrast, activation of mAChRs induces slower and more sustained response compared to nAChRs. M_1-like (M_1, M_3, and M_5) receptors are coupled to Gq proteins which lead to activation of a phospholipase, and M_2-like (M_2 and M_4) receptors are coupled to Gi proteins which inhibits adenylate cyclase (Hulme et al., 1990, Lester et al., 2010). All of the mAChR subtypes exist in the CNS, with M_1 mAChR as the predominant brain mAChR (Wallace et al., 2011). M_1 and M_3 receptors are necessary for tonic cholinergic signaling (Gulledge et al., 2009).

I.3.3 Basal forebrain projection to the prefrontal cortex

The BF is located close to the medial and ventral surfaces of the cerebral hemispheres (Zaborszky et al., 1997, Zaborszky et al., 1999). The BF areas include the MS, VDB, HDB, sublenticular substantia innominata and pallidal regions (Zaborszky and Duque, 2000). The substantia innominata (SI) was also known as the basal nucleus of Meynert (Heimer and Van Hoesen, 2006), and SI and the ventral pallidum (VP) are often referred to collectively as the magnocellular basal nucleus (MBN). The cholinergic nuclei are located in all of these BF areas (Eckenstein and Sofroniew, 1983, Luiten et al., 1987).

The frontal cortex is the chief target of MBN and HDB projections (Luiten et al., 1987, Gaykema et al., 1990). The posterior MBN projects predominantly to lateral neo- and mesocortex, the anterior MBN sends more fibers to the medial cortical regions, and the HDB projects almost exclusively to the medial mesocortex and provides rich projections to Cg1, PrL and IL (Figure I.3, (Luiten et al., 1987). The BF sends three virtually non-overlapping groups of glutamatergic, GABAergic and cholinergic varicose fiber systems into the PFC. In IL ~19% of BF terminals are cholinergic, ~15% are glutamatergic, and ~52% are GABAergic (Henny and Jones, 2008). In the BF, cholinergic and non-cholinergic projection neurons as well as interneurons are intermingled (Martin et al., 1993, Zaborszky and Duque, 2000, Gritti et al., 2006). γ- aminobutyric acid (GABA) – synthesizing cells in BF also send their projections to the cortex, as well as glutamatergic neurons (Gritti et

al., 2003, Henny and Jones, 2008). The BF projection is the primary source of cortical ACh (Rye et al., 1984, Golmayo et al., 2003).Pyramidal neurons in layers III and V are preferentially innervated by those ascending axons (Briand et al., 2007).

Figure I.3

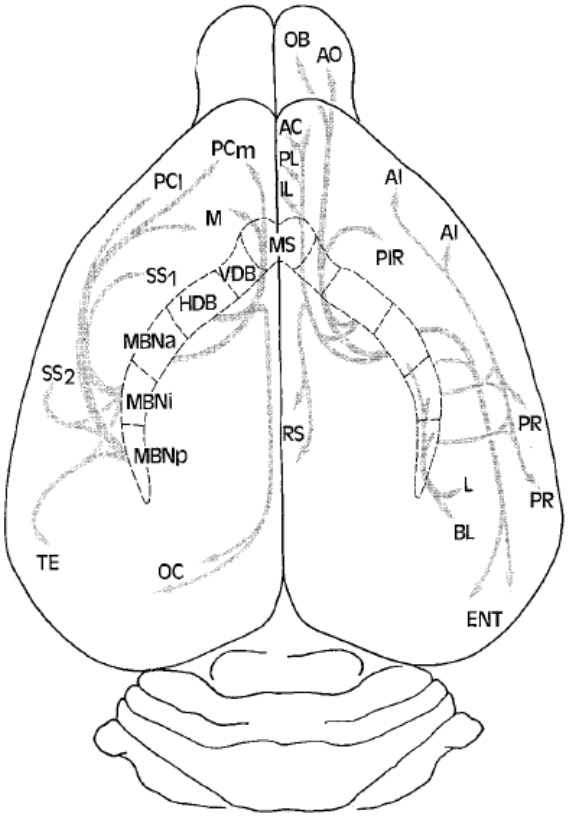

Figure I.3. Major basal forebrain cortical projections. Projections from BF to the various neocortical areas in a dorsal view of the brain found in a study using the anterograde tracer Phaseolus vulgaris leucoagglutinin (PHA-L) (Luiten et al., 1987).

Abbreviations: AC: anterior cingulate cortex; AI: agranular insular cortex: AO anterior olfactory nucleus; BL: basolateral amygdaloid nucleus; ENT: entorhinal cortex; L: lateral amygdaloid nucleus; HDB: horizontal limb nuclei of diagonal band of Broca; MBNa: magnocellular basal nucleus, anterior; MBNi: magnocellular basal nucleus, anterior intermediate; MBNp: magnocellular basal nucleus, posterior; MS: medial septum; OC occipital cortex; PCl: lateral precentral cortex; PCm: medial precentral cortex; PIR: piriform cortex; PL: prelimbic cortex; PR: perirhinal cortex; PV: paraventricular hypothalamic nucleus; RS: retrosplenial cortex; SS1/SS: 2 somatosensory cortex 1 and 2; TE: temporal cortex; VDB: vertical limb nuclei of diagonal band of Broca; VTA: ventral tegmental area

I.3.4 Basal forebrain cholinergic projections to the prefrontal cortex in cognitive functions

The dense cholinergic projections from BF to the PFC have been implicated in a variety of behavioral functions, including attention, learning, , and cortical arousal (Everitt and Robbins, 1997, Golmayo et al., 2003, Sarter et al., 2003, Chudasama et al., 2004, Fournier et al., 2004, Gritti et al., 2006, Briand et al., 2007, Hur et al., 2009). It has been hypothesized that cholinergic inputs to PFC

mediate the ‘recruitment’ of top-down attentional mechanisms underlying increased demands on attentional processes and capacities in challenging conditions (Gill et al., 2000, Sarter et al., 2005, Kozak et al., 2006), and hyperactive cortical cholinergic inputs mediate hyperattentional dysfunctions (Sarter and Bruno, 2000). The BF cortical cholinergic system is robustly activated in attentional performance, and cortical release of ACh increases selective sensory input processing (Golmayo et al., 2003, Sarter et al., 2005).The MBN and HDB cortical projections play an important role in attentional functions (Everitt and Robbins, 1997). In contrast, loss of cortical cholinergic inputs and changes in optimal levels of cortical ACh have detrimental effects on an animal’s performance in attentional tasks (Zaborszky et al., 1999, Gill et al., 2000, Chudasama et al., 2004, Dalley et al., 2004b, Sarter et al., 2005, Kozak et al., 2006). Attentional dysfunction is the most consistent deficit following lesions of the BF-mPFC cholinergic system (Muir et al., 1994, Voytko et al., 1994). The BF cholinergic projection to the cortex is also involved in learning-induced synaptic plasticity in the cortex (Zaborszky et al., 1999, Zaborszky and Duque, 2000). Schizophrenics who smoke demonstrate an overall reduction in the normal up-regulation of high affinity neuronal nicotinic receptors in most brain regions, including the cortex, compared to control smokers (Breese et al., 2000). Particularly, the α7 nAChR is profoundly impaired in patients with schizophrenia (Wallace et al., 2011), and decreased P50 inhibition in schizophrenia is linked to a dinucleotide polymorphism at chromosome 15q13-14, the site of the α7 nAChR (Freedman et al., 1997). The BF facilitates the selective processing by the PFC of behaviorally relevant sensory stimuli (Sarter et al., 2003). This processing capacity

is decreased in a crossmodal divided attention task in rats with 192 IgG-saporin-induced lesions of the cholinergic neurons of the BF (Turchi and Sarter, 1997). Local perfusion with the ionotropic glutamate receptor antagonist kynurenate in the ipsilateral BF attenuates ACh release in the mPFC evoked by behaviorally relevant stimuli in awake rats, whereas perfusion of NMDA in BF following exposure to stimuli enhances both the magnitude and duration of stimulated mPFC ACh efflux (Fadel et al., 2001). BF organization supports selective cortical processing. The BF stimulation results in differential amount of ACh efflux from the visual cortex compared with the somatosensory cortex (Jimenez-Capdeville et al., 1997). Different BF glutamate receptor subtypes differentially mediate ACh release in the mPFC (Fadel et al., 2001). Anatomical studies and microdialysis data suggest that cholinergic BF projections to the cortex are modality and region-specific. Thus, distinct populations of neurons in the BF may be activated by different sensory inputs (Fournier et al., 2004, Robinson et al., 2011).

It has been proposed that novel, salient or unexpected sensory inputs from sensory cortical areas are transferred to the BF via PFC topographic projections (Zaborszky et al., 1999, Golmayo et al., 2003), because BF in rodents does not seem to receive specific sensory inputs from the brainstem or via thalamic sensory areas (Zaborszky et al., 1991). Consistent with this hypothesis, glutamatergic inputs to basal forebrain neurons are a major source of basal forebrain neuronal stimulation in visual attentional task-performing animals (Sarter and Bruno, 2000). In animals performing attention tasks, in addition to the cholinergic transients

mediating cue detection, there is also a more tonic increase in cholinergic activity that remains relatively stable, evoked by the anticipation and/or the initiation of the test session and mediated via projections from the PFC to the BF (Parikh et al., 2010).

I.4 Dopaminergic system in the mPFC

The dopaminergic innervation of the mPFC from the ventral tegmental area facilitates neuronal activity in the mPFC. It modulates cognitive functions including working memory, stress, attention, and reward.

I.4.1 Synthesis and uptake of dopamine

Dopamine is synthesized from the essential amino acid tyrosine. Tyrosine hydroxylase (TH) converts tyrosine to L-dyhydroxyphenylalanine (L-DOPA), which is then decarboxylated into dopamine (DA) and CO_2 (Kandel et al., 2000). DA is removed from the extracellular space and transported back into DA neurons by the DA transporter, DAT. This is an important mechanism for inactivating DA neurotransmission (Zahniser and Sorkin, 2004). TH is the rate-limiting enzyme for the synthesis of both dopamine and norepinephrine (NE). However, in the PFC, only about 10% of the profiles expressing NE transporters (NET) display immunoreactivity for TH, indicating that TH immunoreactivity is primarily

representative of DA rather than NE axons in this cortical region (Miner et al., 2003).

I.4.2 The mesocortical dopaminergic projection

There are two major DA projection systems in the CNS. One is the mesocorticolimbic system. Its dopamine-containing cell bodies are located in the ventral tegmental area (VTA) of the midbrain and project to limbic structures and the mPFC(Siegel et al., 1999) (Figure I.4). The other is the nigrostriatal system, whose dopamine-containing cell bodies are located in the substantia nigra pars compacta (SNc) of the midbrain, and project predominantly to the dorsal striatum (Seamans and Yang, 2004, Lester et al., 2010). The mesocorticolimbic DA system can be further divided into the mesocortical DA pathway and the mesolimbic DA pathway. The dopaminergic projection from the paranigral VTA subdivision to the nucleus accumbens, amygdala, and hippocampus constitutes the mesolimbic DA pathway (Lester et al., 2010). The mesocortical DA pathway consists of DA projections from the parabrachial VTA subdivision that innervate prefrontal cortical structures (Descarries et al., 1987, Tam and Roth, 1997, Tzschentke, 2001, Lester et al., 2010). In a radioautography study, the supragenual cingulate cortex and the anteromedial PFC receive higher DA innervation compared to other cortical areas, with predominance of DA varicosities in the upper layers of cingulate cortex in contrast with their predominance in the deep layers of the anteromedial PFC. The

perithinal and rostl rhinal cortex show moderate DA innervation, the dorsalfrontal, parietal and temporal neocortex show only light innervation, and the primary visual cortex show the smallest number of DA varicosities (Descarries et al., 1987). However, the mean diameter of these varicosities, which is estimated as 0.74 μm, demonstrates little difference across different cortical areas (Descarries et al., 1987). This DA projection facilitates neuronal activity in the mPFC and modulates cognitive functions such as working memory, motor control, attention, stress, and impulsion (Tam and Roth, 1997, Seamans and Yang, 2004, Floresco and Magyar, 2006, Chen et al., 2007, Li et al., 2007, Livingstone et al., 2009, Lester et al., 2010).

Figure I.4

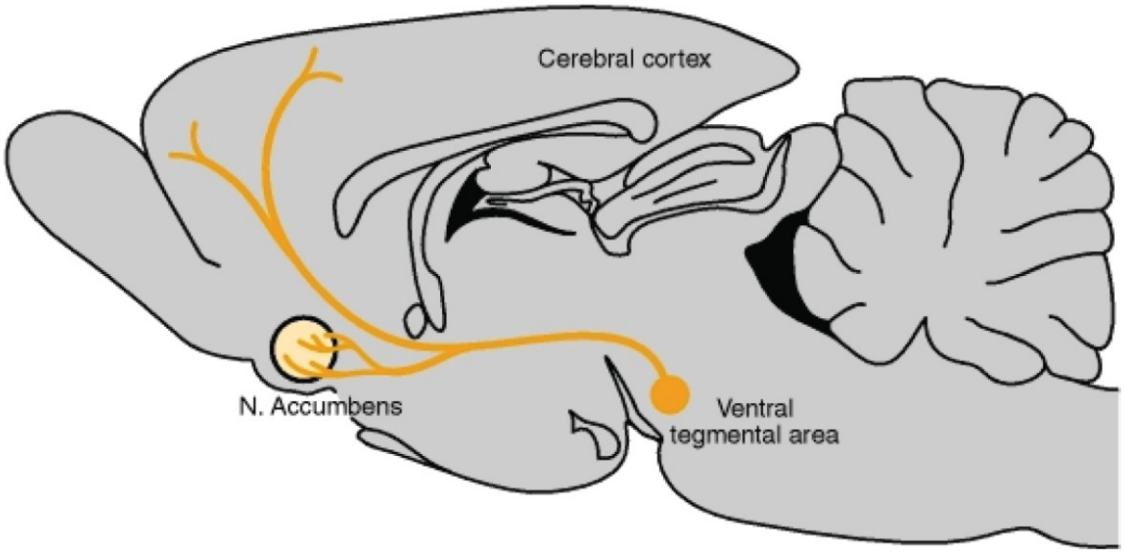

Figure I.4. The mesocorticolimbic dopaminergic projection orginates from cell bodies in the ventral tegmental area and innervates the frontal cortex and limbic forebrain. (George J Siegel et al., 1999)

I.4.3 Dopaminergic receptors

All the DA receptors are slow, metabotropic, G-protein-coupled receptors that functionally modulate other receptor systems and ion channels. There are five DA receptor subtypes in the CNS, named (D_1R), D_5 (D_5R) (Kostrzewa, 1995, Seamans and Yang, 2004). D_1R and D_5R belong to the G_s-, G_q-, or G_{Olf}- coupled D_1 family, whereas D_2R, D_3R and D_4R belong to G_i-/$_o$ D_2 family (Seamans and Yang, 2004). D_5R have a much higher affinity for DA than D_1R (Sunahara et al., 1991), and D_3R and D_4R have a higher affinity than D_2R (Sokoloff et al., 1990). Since DA receptors have different affinities and their expression levels and neuronal localization in the cortex vary, the effects are determined by both the receptor subtype as well as the amount of DA released . Lower concentrations of DA preferentially activate D_1R, but higher concentrations activate both D_1R and D_2R (Trantham-Davidson et al., 2004). Different types of executive functions engage different patterns of activation of DA receptors in the PFC. D_1R activity mediates working memory, whereas the cooperation of D_1R and D_2R mediates behavioral flexibility (Floresco and Magyar, 2006). It has been suggested that D_2R are expressed in both pyramidal and nonpyramidal cells, whereas D_1R are expressed predominantly in non-pyramidal cells (Vincent et al., 1995, Tzschentke, 2001). D_2R activation is thought to decrease inhibition of PFC pyramidal neurons (Seamans and Yang, 2004, Trantham-Davidson et al., 2004). There is an inverted-'U' function for DA related to cognitive performance. Deviation from the critical levels of PFC DA can disrupt cognitive processes (Seamans and Yang, 2004).

I.4.4 Role of the mesocortical DA system in cognitive functions

The mesocortical DA system has been implicated in cognitive functions including working memory, stress, attention, and reward (Schultz, 2002). Event unpredictability in a wide range of stimuli with rewarding characteristics is an important feature to activate dopamine neurons (Schultz et al., 1997). DA plays an important role in goal-directed behaviors (Kiyatkin and Rebec, 2001). The D_2/D_3 receptor antagonist S33138 elevates extracellular levels of ACh in the frontal cortex, and reverses the effect of scopolamine in social recognition (Millan et al., 2008, Wallace et al., 2011). DA is also involved in attention, especially when novel stimuli or positive reward is involved (Schultz, 1997, Robbins, 2005). Impairments in set shifting in patients with schizophrenia or ADHD are due in part to alterations in mesocortical DA activity (Floresco and Magyar, 2006). In marmosets PFC DA improves attentional set-shifting, and frontal DA system in rats with high performance is recruited effectively to optimize attentional task performance (Goto and Grace, 2005, Robbins, 2005). Infusion of 0.06 μg/side dose of DA agonist into the rat PrL enhances the accuracy of attentional performance. In contrast, intracortical infusion of 0.3 μg of the D_1 antagonist produces selective impairments of performance accuracy (Granon et al., 2000). An association was found between ADHD and DAT_1 440-bp polymorphism (Todd et al., 2005).

I.5. Pyramidal cells in the mPFC

I.5.1 Glutamate

Pyramidal cells are abundant in brain structures such as the cerebral cortex and the hippocampus (Spruston, 2008). Pyramidal neurons typically have a prominent apical dendrite (Shipp, 2007), and are likely to use glutamate as their neurotransmitter (Kandel et al., 2000, Lewis et al., 2003). In the brain, glutamate can be synthesized from glucose via the Krebs cycle and the transamination of α-oxoglutarate, or recycled through the glutamate/glutamine cycle (Sanacora et al., 2008). The glutamate/glutamine cycle' involves a rapid uptake of glutamate from the synaptic cleft mainly into the astrocytes, where glutamate is converted into glutamine and further transferred to nerve terminals (Nieoullon et al., 2006). Glutamate is transported into synaptic vesicles by vesicular glutamate transporters. Glutamate is cleared from the extracellular space via high-affinity excitatory amino-acid transporters (EAATs). Uptake by the EAATs is the primary mechanism to terminate action of extracellular glutamate (Sanacora et al., 2008). Glutamate is the major mediator of excitatory synaptic transmission in the brain (Tzschentke, 2002, Sanacora et al., 2008), and pyramidal cells are the targets of the majority of glutamate-containing axon terminals (Lewis et al., 2003). Among the different populations in the mPFC, about 85% of total neurons are pyramidal projection

cells, and 15% are GABAergic interneurons (DeFelipe et al., 2002). Glutamate is the main transmitter of the efferent mPFC projections (Tzschentke, 2001).

I.5.2 Glutamate receptors

Glutamate is the ligand of two main classes of receptors: the ionotropic glutamate receptors (iGluRs) displaying rapid signaling and the metabotropic glutamate receptors (mGluRs) involved in more sustained actions. There are three types of iGluRs, N-methyl-D-aspartate (NMDA), α-amino-3-hydroxy-5-methyl-4-isoazolepropionic acid (AMPA) and 2-carboxy-3-carboxymethyl-4-isopropenylpyrrolidine (kainate) receptors, as well as eight types of the G-protein-coupled mGluRs (mGluR1-8) (Kew, 2004).

I.5.3 Roles of prefrontal pyramidal cells in brain functions

Glutamate-containing neuronal systems support rapid transfer of excitatory information in neuronal networks and are involved in most of the brain processes associated with sensorimotor, neurovegetative, limbic and cognitive functions (Nieoullon et al., 2006). They are the basic components of neuronal plasticity supporting learning and memory (Nieoullon et al., 2006). Pyramidal cells are major recipients of inputs and the major source of outputs for the PFC. They transmit activity in local circuits (Rotaru et al., 2007), and the projections from pyramidal

neurons in deep layers V and VI transmit neural information processed by the PFC to the neural networks in subcortical sites (Carr and Sesack, 2000, DeFelipe et al., 2002, Gabbott et al., 2005). mPFC glutamate neurotransmission plays an important role in response selection and inhibition. Intra-mPFC infusions of NMDA and AMPA receptor antagonists disrupt attentional set shifting (Murphy et al., 2005). PFC glutamatergic projections into the BF likely influence cortically projecting cholinergic neurons (Zaborszky et al., 1997). Glutamate is also a potent neuronal excitotoxin triggering neurotoxicity in pathological conditions. Failure of the EAATs to effectively clear glutamate from the extracellular space leads to various forms of cellular damage (Sanacora et al., 2008). Abnormal function of the glutamatergic system has been implicated in the pathophysiology of many disorders including Alzheimer's disease, schizophrenia and anxiety disorders (Tzschentke, 2002, Sanacora et al., 2008, Javitt, 2010).

I.6. Relationship between the cholinergic and dopaminergic afferents and pyramidal cells

I.6.1 An intricate and complex neuron network

The neuronal basis of the role of the PFC in cognitive functions is an intricate and extensive neuronal network (Agnati et al., 2006, Semyanov, 2008), where the regulation of PFC function by the interaction between the ascending

neuromodulators such as DA and ACh plays an important role (Robbins, 2005). Neuronal elements are not isolated but interact in a intricate and complex network. Pyramidal cells are the skeleton of the basic cortical microcircuit composed of a large number of different elements in this network, with multiple connections between inputs and outputs (DeFelipe et al., 2002). A number of neurotransmitter agents including GABA, serotonin, and adenosine may increase potassium conductance in cortical pyramidal cells, and a number of different neurotransmitters such as ACh and serotonin may block the M-current. This allows the ascending modulatory transmitter systems to control the excitability and responsiveness of cortical pyramidal neurons (McCormick, 1992). The PFC integrates widespread glutamatergic inputs from sensorimotor and limbic regions to perform executive functions, with mesocortical dopamine projections and basal forebrain cholinergic projections exerting important and distinct modulatory influences on PFC functions (Robbins, 2005, Livingstone et al., 2010). Abnormal interactions among those ascending neuromodulatory systems lead to disrupted PFC function in many neurological, psychiatric and drug-addictive disorders (Briand et al., 2007). Restoration of the dynamic balance between these neurotransmitter systems is the main approach for treating such disorders (Lester et al., 2010). The idea that the actions of one type of neurotransmitter must be viewed within a wider context of interactions with other neurotransmitter systems is an important development of insight into these cognitive diseases (Goldman-Rakic, 1996). Indeed, reciprocal modulation between the dopaminergic and cholinergic

systems and pyramidal cells have been documented in a variety of pharmacological and electrophysiological studies, as discussed below.

I.6.2 Reciprocal modulation between the prefrontal dopaminergic and cholinergic system

The modulation of the prefrontal dopaminergic response by acetylcholine is well documented. Parasynaptic and preterminal nAChRs modulate the release of all the major neurotransmitters that have been tested such as dopamine, norepinephrine, serotonin, GABA, and glutamate (Dani, 2001). Activation of presynaptic nicotinic receptors can evoke the release of various monoamines from brain slices (Lendvai et al., 2000, De Paola et al., 2003, Vizi et al., 2004). Nicotine inhaled during smoking results in the release of excitatory amino acids and NE, DA, or 5-HT, which can diffuse to affect tonically the release of other transmitters or the firing rate of other circuitries (Vizi, 2000). Due to nicotinic modulation of dopamine release, nAChRs are therapeutic targets for pathological conditions involving dopaminergic dysfunction, including schizophrenia, ADHD, Parkinson's disease, and Alzheimer's disease (Livingstone and Wonnacott, 2009). Different nicotinic ACh receptor subtypes modulate dopamine release from the PFC and striatum. A selective nAChR antagonist, MG 624, inhibits cortical DA by 53%, but has no effect on striatal release (Cao et al., 2005). The highly sensitive, but not the low sensitive, form of α4β2 nAChR mediates [^{3}H]dopamine release from slices of

rat prefrontal cortex and striatum (Anderson et al., 2009). Low doses of AZD0328, a partial agonist of α7 neuronal nicotinic receptor, increase the firing of dopamine neurons in VTA, and improve novel object recognition in mice (Sydserff et al., 2009). In the mPFC, α7 nAChRs present on glutamate terminals increase glutamate release which could coordinately enhance dopamine release from neighboring boutons (Livingstone et al., 2010). Intracellular recordings in horizontal slices of ventral midbrain from adult male rats demonstrated the increase of potassium conductance resulting from release of calcium from internal stores via activation of muscarinic receptors on DA neurons by ACh application (Fiorillo and Williams, 2000). In awake, freely moving rats, the muscarinic M_1 receptor agonist AC260584, xanomeline and sabcomeline enhance cortical ACh and DA efflux in mPFC (Li et al., 2007, Li et al., 2008). The inhibition of cholinesterase elevated the extracellular level of cortical dopamine by 80% (Giacobini et al., 1996).

In the PFC, DA also exerts its influence on the cholinergic system. Prefrontal dopaminergic activity mediates particularly the amplitude of α7 nAChR-evoked ACh release (Parikh et al., 2010). D_1R exerts a tonic, facilitatory influence upon cholinergic transmission. The D_1R agonist, SKF82958, robustly increases the extracellular levels of ACh in the PFC of freely moving rats, whereas the D_1R antagonist SCH 23390 decreases the levels of ACh and abolishes the facilitatory influence of SKF 82958 upon ACh levels (Di Cara et al., 2007). The systemic administration of two selective D_3R antagonists, SB-277011A and SB-414796A, produces a significant increase in extracellular levels of ACh compared to vehicle-

treated animals (Lacroix et al., 2006). The associations between polymorphisms of the DAT_1 or DRD_4 genes and ADHD were strengthened in children whose mothers smoked during their pregnancy (Neuman et al., 2007). Selective blockade of D_3R elicits dose-dependent, pronounced and sustained elevations of extracellular ACh levels in the frontal cortex and improves social learning in rats (Millan et al., 2007). The DA uptake blocker nomifensine increases extracellular ACh concentrations in the PFC at all days of treatment in awake rats (Hernandez et al., 2008). The release of AChE is regulated by extracellular DA as well. Local administration of D-amphetamine and the inhibitor of dopamine uptake GBR12909 both significantly increases the spontaneous release of ACHE in the rat substantia nigra (Dally et al., 1996).

I.6.3 Reciprocal modulation between PFC pyramidal cells and the cholinergic system

Acetylcholine release regulates the output of neocortical pyramidal neurons. Individual cortical pyramidal neurons faithfully respond to phasic and tonic ACh release in the cortex (Gulledge and Stuart, 2005, Parikh et al., 2007). Nicotine increases the frequency and amplitude of spontaneous excitatory postsynaptic currents in pyramidal cells in mouse PFC (Couey et al., 2007). Multiple subtypes of nAChR regulate glutamate release (Wonnacott et al., 2006). Nicotine evokes [^{3}H]D-aspartate (a surrogate for glutamate) release from rat synaptosomes, which

are sensitive to both DHβE and α-bungarotoxin (Marchi et al., 2002, Rousseau et al., 2005). Application of nicotine induced a large increase in glutamate release onto layer V pyramidal neurons, as measured by an increase in spontaneous excitatory postsynaptic currents (sEPSCs) (Lambe et al., 2003). The interaction between the α7 nAChR and glutamatergic neurons is important for cellular events underlying executive functions (Livingstone et al., 2010). Both α7 and β2 receptor agonists evoked release of glutamate (Dickinson et al., 2008). The α4β2 nAChR agonist, ABT-089 evokes potent glutamate release (Parikh and Sarter, 2008). Via muscarinic acetylcholine receptor activation, ACh can directly inhibit the output of neocortical layer V pyramidal neurons (Gulledge and Stuart, 2005). Whole-cell recordings of layer V pyramidal neurons in cortical slices demonstrate strong and direct inhibition of neocortical pyramidal neurons by transient mAChR activation by agonists (Gulledge and Stuart, 2005). M_1 receptor stimulation in layer V pyramidal cells of the rodent PrL/IL produces a strong depolarization, leads to tonic firing, and dramatically enhances the summation of excitatory synaptic potentials (Carr and Surmeier, 2007). Both M_1R and M_3R regulate the output of cortical pyramidal neurons (Gulledge et al., 2009). Layer V pyramidal neurons are modulated by ACh and carbachol to a greater degree than neurons in layer II/III (Gulledge et al., 2007).

Reciprocally, glutamatergic mechanisms modulate the cholinergic effects in the PFC. As demonstrated by a microdialysis study, the AMPA receptor antagonist DNQX and the NMDA receptor antagonist APV attenuate cholinergic signals

evoked by the α4β2 nAChR agonist, ABT-089 (Parikh and Sarter, 2008). The NMDA receptor antagonist CPP decreases the improvement in attentional function produced by nicotine (Quarta et al., 2007). Lack of β2-containing nAChRs leads to partial attenuation of both cholinergic and glutamatergic transients evoked by nicotine, and complete attenuation evoked by ABT-089, indicating that the amplitude of glutamatergic transients controls the amplitude of cholinergic transients (Parikh et al., 2010). Activation of α4β2 nAChRs residing on prefrontal dopaminergic and glutamatergic afferents could evoke ACh release in the PFC (Briand et al., 2007, Parikh and Sarter, 2008). An electron microscopic study of vesicular glutamate transporters (Vglut1 and Vglut2) and ChAT in BF demonstrated that Vglut1 and Vglut2 boutons synapse with cholinergic dendrites (Hur et al., 2009).

I.6.4 Reciprocal modulation between PFC pyramidal cells and the dopaminergic system

The output of cortical pyramidal cells is also modulated by dopaminergic afferents to the mPFC. Prefrontal pyramidal cells are the primary targets of the ascending dopaminergic fibers (Tzschentke, 2001). Application of the D_1R agonist SKF 81297 attenuates simulated EPSP (sEPSP) amplification in layer 5 pyramidal neurons in rat mPFC at depolarized potentials in a concentration-dependent manner. The effects of different concentrations of SKF81297 on sEPSP area are

well fitted by a sigmoideal function, and ~1.3 μm of the SKF81297 concentration produces 50% of the maximum effect. The SKF81297 effects are abolished by the D_1R antagonist SCH23390 (Rotaru et al., 2007). NMDA, AMPA, and the D_1R agonist SKF38393 increase the excitability of deep layer pyramidal neurons in PFC in a concentration-dependent manner, whereas the D_2R agonist quinpirole induces the opposite effect (Tseng et al., 2007). D_2R activation was shown to decrease inhibition of PFC pyramidal neurons (Seamans and Yang, 2004, Trantham-Davidson et al., 2004), and excessive activation of D_2R is detrimental to induction of long term potentiation (LTP) in the PFC (Xu et al., 2009). The inhibitory D_2R effects on pyramidal cell excitability may be important cellular mechanisms for the selection of relevant information in the PFC (Tseng and O'Donnell, 2004).

On the other hand, glutamate exerts a local modulation on DA release in the PFC (Del Arco et al., 2003). Prefrontal glutamate ionotropic receptors seem to have a local inhibitory modulation on DA release in the PFC. Local perfusion of ketamine, a non-competitive NMDA receptor antagonist, enhances DA release within the mPFC, while NMDA decreases DA release (Lorrain et al., 2003). Local infusion of the AMPA/kainate antagonist CNQX produces a 40% increase in dopamine levels in the mPFC (Wu et al., 2002). Prefrontal perfusion of NMDA decreases the basal release of dopamine, and significantly reduces dopamine release stimulated by stress (Del Arco and Mora, 2001), suggesting an inhibitory role for NMDA receptors on dopamine release. NMDA and AMPA prefrontal activation could also inhibit dopamine release indirectly via GABA receptors

located on dopamine terminals (Del Arco and Mora, 2005). A balanced prefrontal glutamate-dopamine interaction is crucial to the function and activity of PFC and other interconnected brain areas such as nucleus accumbens (Del Arco and Mora, 2005).

I.7 Diffuse transmission

I.7.1 Synaptic versus diffuse transmission

Classical synaptic transmission and diffuse transmission are the two main modes of intercellular communication that have been proposed in the CNS (Umbriaco et al., 1994, Descarries et al., 1997, Zoli et al., 1999, Descarries and Mechawar, 2000, Vizi et al., 2004, Agnati et al., 2006). Synaptic transmission, or wired transmission, occurs when a cell is connected to another cell via a physically distinct communication channel, such as a synapse, a gap-junction or membrane juxtapositions (Agnati et al., 2006). In contrast, in diffuse transmission, there are no synaptic contacts or appositions of a postsynaptic density. Transmitters are released from axon terminals into the extracellular space, diffuse, and stimulate extrasynaptically located receptors to influence the activity of other neurons (Lendvai and Vizi, 2008). Compared to classic synaptic transmission, diffuse transmission has longer transmission delay, more than one target, and a lower

energy cost (Agnati et al., 2006). Diffuse transmission allows a global mode of operation for the CNS, setting the CNS to the appropriate functional state so that it works as a unit (Agnati et al., 1995). The dynamic influences of neuromodulators depend on their broad and diffuse transmission (Giocomo and Hasselmo, 2007). Many transmitters such as norepinephrine, serotonin, ACh, glutamate, GABA, and nitirc oxide have been implicated in diffuse transmission (Umbriaco et al., 1994, Descarries et al., 1997, Huang, 1998, Cragg et al., 2001, Lapish et al., 2007). They can be released nonsynaptically (Descarries et al., 1997, Isaacson, 2000), and virtually all the transmitters are found in the extracellular fluid, as indicated in microdialysis studies (Garris and Wightman, 1994, Del Arco et al., 2003). The existence of nonsynaptic varicosities is a quite general feature of the CNS (Vizi, 2000, Descarries et al., 2008). Although the receptors involved in diffuse transmission are hypothesized to be mainly high-affinity metabotropic receptors (Kiss et al., 1999), extrasynaptic locations have been demonstrated for cholinergic, peptidergic, monoamine and glutamatergic ion channel-gated receptors (Jacob and Berg, 1983, Yung et al., 1995). Most presynaptic receptors are nonsynaptic and regulate the tonic release of transmitters (Vizi et al., 2004).

I.7.2 The brain extracellular space

The structure of the brain extracellular space supports the feasibility of diffuse transmission (Nicholson and Sykova, 1998). 20% of the brain volume is

extracellular space, which provides a significant extracellular microenvironment and acts as communication channels between cells in diffuse transmission (Nicholson and Sykova, 1998). Repetitive neuronal activity and pathological states can lead to long-term changes in the properties of the extracellular space (Nicholson and Sykova, 1998), thus affecting diffuse transmission of various neuromodulators. Neurotransmitters diffuse in their 3D microenvironment in preferential pathways, because tortuosity and volume fraction, the two main features of the cerebral microenvironment, are not uniform in different regions and various physiopathological conditions (Agnati et al., 1995). The tortuosity is the length of the diffusion path for a molecule in a given medium with respect to free medium (Agnati et al., 1995), a measure of how diffusing molecules are hindered by cellular obstructions (Nicholson and Sykova, 1998). The volume fraction represents the amount of volume in which an extracellular molecule can diffuse with respect to the overall volume of the brain region (Agnati et al., 1995). Different chemical-physical phenomena such as intracranial pressure waves, temperature and concentration gradients could also exert their influence in volume transmission (Fiorillo and Williams, 2000, Santha et al., 2001).

I.7.3 Role of diffuse transmission in brain function

The view has been developed in recent years that alterations in the diffuse transmission of neurotransmitters contribute more to dysregulations and

pathological disorders in the brain than the cessation of their actions at synaptic release sites (Meshul et al., 1999, Marti et al., 2000, Sykova and Chvatal, 2000, Del Arco et al., 2003). Many functions of the nervous system are influenced by the presynaptic modulation of transmitter release and postsynaptic effects of endogenous molecules released from far away varicosities (Vizi et al., 2004). Besides, extrasynaptic receptors are among the primary targets of medicine, partly due to the reason that micromolar blood concentrations of drugs require high affinity receptors (Zoli et al., 1999, Vizi, 2000). These drugs diffuse in the cerebral extracellular space and interact more effectively with diffuse transmission than synaptic transmission (Zoli et al., 1999).

I.7.4 Diffuse transmission of ACh

Diffuse transmission is proposed to be the major mode of neuronal communication for ACh in the PFC (Umbriaco et al., 1994, Descarries et al., 1997, Descarries and Mechawar, 2000). Little evidence has been shown for classical nicotinic synaptic transmission in the CNS (McGehee, 1995). In contrast, many features of ACh transmission support diffuse transmission. The majority of cholinergic boutons in the CNS do not make synaptic contacts (Umbriaco et al., 1994, Descarries et al., 1997, Mechawar et al., 2000). Both muscarinic (Yamasaki et al., 2010) and nicotinic AChRs such as α7 (Duffy et al., 2009) and high-affinity type of α 4 β 2 (Hill et al., 1993, Ullian and Sargent, 1995, Lendvai and Vizi, 2008)

have been implicated in diffuse transmission. nAChRs were mainly found in nonsynaptic sites (Fabian-Fine et al., 2001, Jones and Wonnacott, 2004). Electron microscopic immunolabeling of the α7nAChR and vesicular acetylcholine transporter (VAChT) in single sections through the PFC demonstrated that, in rat and mouse, there were no recognizable synaptic specializations in the spatial or intracellular relationship between α7nAChR and VAChT-containing axonal profiles (Duffy et al., 2009). In the chick lateral spiriform nucleus, most clusters of α5 and β2 are extrasynaptic, as demonstrated by double-label immunofluorescence with mAbs to AChRs and to synaptic vesicle antigens (Ullian and Sargent, 1995). M_1R likely mediate cholinergic diffuse transmission in the cortex by sensing the ambient ACh. M_1R were found to be preferentially expressed in pyramidal cells, far more outnumbered cholinergic varicosities and localized widely on the extrasynaptic membrane (Yamasaki et al., 2010). The cholinergic system modulates cortical functions via axo-axonic interactions. Extracellular and intracellular recordings in rat cortical slices from rat piriform cortex demonstrated that cholinergic agonists suppress synaptic transmission through a presynaptic mechanism via M_1R (Hasselmo and Bower, 1992).

I.7.5 Diffuse transmission despite ACh hydrolysis by AChE

It has been proposed that cholinergic varicosities should be in close proximity to target elements in diffuse transmission (Lendvai and Vizi, 2008)in

regard to its fast hydrolysis by AChE (Descarries et al., 1997, Descarries, 1998, Sarter et al., 2009b), However, it has been argued by (Descarries et al., 1997) that the main action of AChE in CNS is to keep the extrasynaptic, ambient level of ACh within physiological limits (Descarries et al., 1997, Descarries, 1998, Lendvai and Vizi, 2008). In any event, since inhibition of AChE is correlated with the increase of extracellular concentration of ACh in cortex, it may have an impact on cognitive function (Giacobini et al., 1996, Giacobini, 1998). The soluble form of AChE and its "excess substrate inhibition" also provide selective flexibility to the cholinergic system (Descarries et al., 1997, Descarries, 1998, Lendvai and Vizi, 2008).

I.7.6 Synaptic nature of DA transmission in the mPFC

Diffuse transmission has been suggested for DA due to their spatially diffusible release, and slow long-term modulations of the neuronal activity of entire networks (Agnati et al., 1995, Cass and Gerhardt, 1995, Mundorf et al., 2001, Lapish et al., 2007). Compared with the striatum, in PFC there was relatively low levels of DAT proteins, distant localization of DAT from synaptic release sites, and less DA uptake by DAT (Garris and Wightman, 1994, Cass and Gerhardt, 1995, Sesack et al., 1998). A junctional complex exists on only 56% in the suprarhinal cortex (Seguela et al., 1988), suggesting existence coexistence of non-synaptic and synaptic transmission of DA in the PFC.

However, DA transmission in the mPFC is mainly synaptic. In the rat anteromedial PFC, a junctional complex is observed on 93% of the DA varicosities, demonstrated by an electron microscopic study using immunocytochemical staining with a highly specific polyclonal antiserum directed against DA-glutaraldehyde-lysyl-protein conjugate (Seguela et al., 1988).

I.7.7 Diffuse transmission of glutamate

Extracellular variations of glutamate are regarded as an index of diffuse transmission mediated actions (Del Arco et al., 2003). Synaptically released glutamate could spill over to extrasynaptic regions to activate nonsynaptic receptors and exert remote effects (Scanziani et al., 1997, Rusakov and Kullmann, 1998, Bergles et al., 1999, Isaacson, 2000, Giocomo and Hasselmo, 2007). Glutamate can also be released by astrocytes through glutamate receptors by previous activation of adjacent neurons, and act on neuronal extrasynaptic receptors to modulate neurotransmission (Del Arco et al., 2003). There are also glutamate receptors (Scanziani et al., 1997, Rusakov and Kullmann, 1998) located on glutamatergic axon terminals (autoreceptors), on astrocytes and on other neurotransmitter system terminals such as dopaminergic terminals (heteroreceptors), and both metabotropic glutamate receptors and ionotropic glutamate receptors are involved in diffuse transmission (Scanziani et al., 1997, Rusakov and Kullmann, 1998, Del Arco et al., 2003, Semyanov, 2008).

I.8. Plasticity of axon varicosities

I.8.1 Axon varicosities

Varicosities or boutons are dilated regions of the axon where vesicles containing transmitter substance accumulate (Cooper et al., 2003). *En passant* varicosities are studded along the axonal branches and are of great interest in diffuse transmission since most of them do not make synaptic contacts (Vizi, 2000). *En passant* varicosities and terminal varicosities may be intermingled along the same axon (Anderson and Martin, 2001), and different types of axons have distinct densities of varicosities (De Paola et al., 2006). The distribution of varicosities is uneven along the axons and can be quite specific (Shepherd and Raastad, 2003), suggesting that there are regions in which the local concentration of transmitters could be much higher (Vizi, 2000). Formation of varicosities are not random but might be intrinsic to axons (Sabo et al., 2006), as well as shaped by activities and experiences throughout life (Colicos et al., 2001, Trachtenberg et al., 2002, Nikonenko et al., 2003, Galimberti et al., 2006).

I.8.2 Structural plasticity of axon varicosities

Axon varicosities exhibit vigorous structural plasticity in the brain (De Paola et al., 2003, De Paola et al., 2006, Stettler et al., 2006, Gogolla et al., 2007). Extrinsic experiences may induce changes in the numbers of axon varicosities.Chronic imaging of neuronal structure in vivo via injecting adeno-associated virus (AAV) carrying the EGFP gene has demonstrated axonal bouton turnover dynamics in V1 during the functional reorganization following retinal lesions. A significantly higher turnover rate was observed after the lesion, and initially more boutons appeared than disappeared, followed by elimination of more boutons until a return of the bouton density to the level seen prior to the lesion (Yamahachi et al., 2009). A two-photon microscopy imaging of pyramidal neurons in the developing rat barrel cortex demonstrated the structural dynamics of dendritic spines and filopodia driven by sensory experience. During a critical period around postnatal days, sensory deprivation markedly reduced protrusive motility in deprived regions of the barrel cortex (Lendvai et al., 2000). Dynamics in the number of varicosities may be induced by the activity of postsynaptic elements. A study using confocal imaging of DiI-labeled axons demonstrated that short anoxia/hypoglycemia and theta burst stimulation induced rapid remodeling of presynaptic varicosities (Nikonenko et al., 2003). Studies using cultured hippocampal neurons via live imaging and retrospective immunohistochemical methodologies demonstrated that functional presynaptic boutons can form within

25-30 min of the establishment of an axodendritic contact, some of which were recruited from SVs of nearby preexisting boutons (Friedman et al., 2000).

There is also evidence for a spontaneous turnover rate of the axon varicosities. In mature hippocampal networks, a fraction of *en passant* varicosities along mossy fibers demonstrated a turnover within a period of several days (De Paola et al., 2003). In the intact adult barrel cortex of GFP transgenic mice, the axon varicosities appeared and disappeared over times of days and stable and dynamic varicosities intermingled along the axons, as shown via two-photon microscopy (De Paola et al., 2006). In anesthetized Macaca fascicularis monkeys and mice injected with AAV.EGFP, two-photon imaging sessions of their V1 showed frequent bouton addition and elimination along collaterals over 1 week interval (Stettler et al., 2006).

The mechanisms underlying changes in the density of axon varicosities are not clear, but increases in the number of axon varicosities may result from either the formation of new varicosities or the mobilization of previously existing ones to new sites (Friedman et al., 2000, Trachtenberg et al., 2002).

I.8.3 Structural plasticity of axon varicosities in brain diseases

Changes in axonal varicosities have been implicated in pathological conditions. In mild to moderate Alzheimer disease, ChAT axonal varicosities in the frontal cortex were less and abnormally enlarged compared to healthy controls (Ikonomovic et al., 2007). A lower density of parvalbumin-immunoreactive varicosities was found in the middle cortical layers in prefrontal cortex of schizophrenic patients (Lewis et al., 2001). Compared to young cognitively unimpaired rats, there was an increase in the density of dopaminergic varicosities in layer V of the prefrontal cortex in aged cognitively unimpaired rats, but a decrease in layer III in aged cognitively impaired rats (Allard et al., 2010).

I.9 Summary

The functions of the rat medial prefrontal cortex are modulated by ascending modulatory systems such as the ACh and DA afferent systems, in which diffuse transmission play an important role. The horizontal nucleus of the diagonal band of Broca in the basal forebrain sends prominent projections to Cg1, PrL and IL, the subregions of mPFC. Pyramidal neurons in layers III and V were preferentially innervated by those ascending axons. PFC and BF are reciprocally involved in the processing of behaviorally relevant sensory stimuli. The level of PFC DA is critical for modulating normal cognitive and behavioral processes. In the mesocortical DA

pathway, DA projections from the parabrachial VTA subdivision innervate prefrontal cortical structures and enhance neuronal activity in the mPFC. Pyramidal cells use glutamate as their neurotransmitter and are abundant in brain structures associated with advanced cognitive functions such as the cerebral cortex. Glutamate is the main transmitter of the efferent mPFC projections. PFC pyramidal cells transmit activity in local circuits, as well as neural information processed by the PFC to the neural networks in subcortical sites. Glutamate-containing neuronal systems support rapid transfer of excitatory information in neuronal networks.

The interrelationships between the ascending cholinergic and dopaminergic systems and pyramidal cells in the mPFC in rodents have been involved in a variety of cognitive and emotional processes including attention, learning and plasticity, as well as in cognitive and behavioral disturbances associated with major neuropsychiatric disorders such as ADHD and schizophrenia.

The neuronal basis of the role of the PFC in cognitive functions is an intricate and extensive neuronal network, in which the regulation of PFC function by the interaction between the ascending neuromodulators such as DA and ACh plays an important role. Pyramidal cells are the skeleton of the basic cortical microcircuit composed of a large number of different elements, and their intrinsic and extrinsic connections. The PFC integrates widespread glutamatergic inputs from sensorimotor and limbic regions to perform executive functions, with mesocortical dopamine projections and basal forebrain cholinergic projections

exerting important and distinct modulatory influences on PFC functions. The reciprocal modulation among prefrontal ACh, DA and pyramidal cells has been reported in a number of pharmacological and electrophysiological studies. A balanced interaction among the three neuronal elements is crucial to the function and activity of PFC and other interconnected brain areas. Abnormal interactions among those ascending neuromodulatory systems and pyramidal cells lead to disrupted PFC function in many neurological, psychiatric and drug-addictive disorders, and restorations of the dynamic balance between these neurotransmitter systems are the main approach for treating such disorders.

Diffuse transmission, an important mode of intercellular communication, allows a global mode of operation for the CNS and sets the CNS to an appropriate functional state so that the CNS neuronal elements work as a unit. In diffuse transmission, there are no synaptic contacts. Instead, neurotransmitters are released from axon terminals into the extracellular space, diffuse, and stimulate extrasynaptically located receptors to influence the activity of other neurons. Diffuse transmission is crucial for the communication for cortical ACh and DA, and enables the dynamic influences of those neurotransmitters on cognitive functions. Many features of ACh transmission suggest this system uses a fast form of diffuse transmission, in which the axon varicosities must be in relatively close proximity to their target elements. DA release is spatially diffuse and prolonged, tonically stimulates extrasynaptic receptors in a high affinity state, and exerts slow, long-term modulatory effects on target neurons. However, the heterogeneity of DA

concentration in its microenvironment might limit effective DA diffuse transmission to a few micrometers.

Axon varicosities are of great interest in diffuse transmission since most of them do not make synaptic contacts. The uneven distribution of varicosities along axons suggests heterogeneity in the local concentration of transmitters in the extracellular space. The formation of varicosities is not random, but shaped by extrinsic sensory experiences throughout life. Thus axon varicosities exhibit vigorous structural plasticity in the brain. Changes in axonvaricosities have been implicated in pathological conditions such as Alzheimer disease and schizophrenia.

I.10 Objectives of the studies

Despite the well-documented interactions between the cholinergic, and dopaminergic afferents and pyramidal cells in the PFC, there is only scarce neuroanatomical data depicting the reciprocal interrelationships between these neuronal elements in the mPFC. Facts and principles of such a network organization are also scant (Rockland, 1998).

For these reasons, we examined the ultrastructural neuroanatomical relationship between the cholinergic and dopaminergic systems and pyramidal

cells in the mPFC, with an emphasis on the structural plasticity of the cholinergic and dopaminergic axon varicosities at the subcellular level. These interrelationships were also examined in association with neuronal activity in the mPFC.

Several questions were thus answered:

(1) Do cholinergic and dopaminergic fibers within the mPFC converge on the same pyramidal neurons from layer V (output) in the mPFC?

(2) Are there close appositions between cholinergic and dopaminergic fibers in the mPFC?

(3) Is there any functional importance to the close appositions between cholinergic fiber segments and dopaminergic fiber segments, particularly, is there structural plasticity of axon varicosities on those fiber segments apposing to each other?

(4) Does the activation of pyramidal cells in the mPFC induce changes of varicosity density on cholinergic fiber segments in their vicinity?

(5) Does the dopaminergic system in the mPFC demonstrate this plasticity of varicosity density induced by neuronal activity as well?

CHAPTER II

Confocal analysis of cholinergic and dopaminergic inputs onto pyramidal cells in the prefrontal cortex of rodents

Front Neuroanat. 2010 Jun 14;4:21. Published online: 14 June 2010

*Zi-Wei Zhang[1,2], Mark W. Burke[1], Nicole Calakos[3], Jean-Martin Beaulieu[4] and Elvire Vaucher[1]**

[1] School of Optometry, Université de Montréal, Montréal, QC, Canada

[2] Department of Physiology, Université de Montréal, Montréal, QC, Canada

[3] Department of Neurobiology, Division of Neurology, Center for Translational Neuroscience, Duke University, Durham, NC, USA

[4] Department of Psychiatry and Neuroscience, Université de Laval/Centre de recherche Université Laval Robert-Giffard, Québec, QC, Canada

Contributions:

I contributed to the design, experiment, statistical analysis, production, and revision of this article.

Dr. Elvire Vaucher supervised, contributed to the design, statistical analysis, production, and revision of this article.

Dr. Mark W. Burke contributed to the revision this article, and provided valuable advice.

Dr. Nicole Calakos and Dr. Jean-Martin Beaulieu provided the Drd_1a-tdTomato/Drd_2-EGFP double BAC-transgenic mice and valuable advice.

Abstract

Cholinergic and dopaminergic projections to the rat medial prefrontal cortex (mPFC) are both involved in cognitive functions including attention. These neuronal systems modulate mPFC neuronal activity mainly through diffuse transmission. In order to better understand the anatomical level of influence of these systems, confocal microscopy with triple-fluorescent immunolabeling was used in three subregions of the mPFC of rats and *Drd1a*-tdTomato/*Drd2*-EGFP transgenic mice. The zone of interaction was defined as a reciprocal microproximity between dopaminergic and cholinergic axonal segments as well as pyramidal neurons. The density of varicosities, along these segments was considered as a possible activity-dependant morphological feature. The percentage of cholinergic and dopaminergic fibers in microproximity ranged from 12 to 40% depending on the layer and mPFC subregion. The cholinergic system appeared to have more influence on dopaminergic fibers since a larger proportion of the dopaminergic fibers were within microproximity to cholinergic fibers. The density of both cholinergic and dopaminergic varicosities was significantly elevated within microproximities. The main results indicate that the cholinergic and dopaminergic systems converge on pyramidal cells in mPFC particularly in the layer V. In transgenic mice 93% of the pyramidal cells expressed the transgenic marker for *Drd2* expression, but only 22% expressed the maker for *Drd1a*r expression. Data presented here suggest that the modulation of mPFC by dopaminergic fibers would be mostly inhibitory and localized at the output level whereas the cholinergic

modulation would be exerted at the input and output level both through direct interaction with pyramidal cells and dopaminergic fibers.

Introduction

The rat medial prefrontal cortex (mPFC) is involved in a variety of cognitive functions including attentional processes, working memory, behavioral flexibility and inhibition (Heidbreder and Groenewegen, 2003, Gabbott et al., 2005, Briand et al., 2007). Its three main anatomical subdivisions, the anterior cingulate (Cg1), the prelimbic (PrL) and the infralimbic (IL) areas (Vertes, 2004, Tavares and Correa, 2006, Vertes, 2006) receive long ascending projections from cholinergic neurons of the basal forebrain (BF) (Golmayo et al., 2003, Henny and Jones, 2008) and from dopaminergic neurons of the ventral tegmental area (VTA). Both neuronal systems modulate mPFC activity and attentional performance (Gill et al., 2000, Golmayo et al., 2003, Sarter et al., 2003, Chudasama et al., 2004, Dalley et al., 2004b, Sarter et al., 2005, Goto et al., 2007, Del Arco and Mora, 2009). Particularly, acetylcholine (ACh) plays an essential role in the top-down control of attention (Sarter et al., 2006), orienting and retention in working memory tasks (Broersen et al., 1995, Steckler et al., 1998, Thienel et al., 2009). Dopamine (DA) plays a major role in motor control, selective attention, impulsivity, executive control (Robbins, 2005, Chen et al., 2007, Lapish et al., 2007, Li et al., 2007, Thienel et al., 2009) and has a “fine-tuning” effect for optimum cognitive performance (Granon et al., 2000, Tzschentke, 2001). Both ACh and DA systems are involved in pathologies such as Alzheimer’s disease, attention deficit hyperactivity disorder and schizophrenia.

There is a growing body of pharmacological evidence supporting the interaction between ACh and DA in the rat prefrontal cortex. Increase of DA release by ACh in the prefrontal cortex seems to happen at a local level through nicotinic receptors (nAChR) (Rao et al., 2003, Cao et al., 2005, Rossi et al., 2005, Shearman et al., 2005). Inhibition of ACh esterase (Shearman et al., 2006) or stimulation of muscarinic receptors (Perry et al., 2001, Ichikawa et al., 2002) also induced the release of DA in the mPFC. Likewise, DA has been shown to influence ACh transmission (Laplante et al., 2004). Activation of D_1 dopaminergic receptors (D_1R) has been proposed to exert a tonic, facilitatory influence upon cholinergic transmission (Yang and Mogenson, 1990). Extracellular levels of ACh were robustly enhanced in the PFC following systemic administration of the D_1R agonist SKF82958 (Di Cara et al., 2007) and the D_3R antagonists (Lacroix et al., 2006). However, due to the systemic infusion of these dopamine agonists/antagonists, it is not clear if the modulation of ACh release by DA in these experiments occurred at a local level or is part of a larger neural circuitry modulation.

It has also been shown that both DA and ACh modulate the activity of pyramidal neurons and the functional output of the mPFC (Spruston, 2008). The excitatory post-synaptic potential (EPSP) of pyramidal neurons in layer V of the rat mPFC can be attenuated by the D_1R agonist SKF 81297 *in vitro* (Rotaru et al., 2007). DA has been shown to have an inhibitory effect on layer V pyramidal cells in the rat mPFC through D_2R activation *in vitro* (Gulledge and Jaffe, 1998, Steketee, 2003) and *in vivo* (Goto and Grace, 2005*)*. In addition, M_1 mAChR stimulation in

layer V pyramidal cells of the rodent PrL/IL cortex produces a strong depolarization and leads to tonic firing by dramatically enhancing the summation of EPSP (Carr and Surmeier, 2007). In slices from rat PrL, nicotinic and muscarinic agonists modulate excitatory synaptic transmission, indicating the ascending cholinergic systems might participate in information processing in the PrL via control of ongoing excitation to pyramidal cells (Vidal and Hidalgo, 1993).

Evidence for the physiological basis for the interaction between ACh, DA, and glutamatergic pyramidal cells is extensive, however the neuroanatomical correlate within the mPFC supporting this interaction has not been established. Diffuse transmission, rather than synaptic transmission, is a widely occurring and well-documented phenomenon for ACh and DA in mPFC (Descarries et al., 1997, Descarries, 1998, Descarries and Mechawar, 2000, Yamasaki et al., 2010). The current study investigated the three-dimensional anatomical relationship among the cholinergic system, dopaminergic system, and pyramidal cells by quantifying the microproximity among these three neuronal elements in the mPFC of rats using confocal laser-scanning microscopy. Microproximity between dopaminergic and cholinergic fibers or pyramidal cells (defined as relationships with a gap less than 3 μm between two neuronal elements) was considered as a possible functional interaction zone. As the axonal varicosities are the site of neurotransmitters release, the number of *en passant* varicosities within the axonal segments sharing microproximity was quantified, as an index of possible functional activity. As well, the expression of D_1aR and D_2R by pyramidal cells and cholinergic fibers within the

mPFC was examined since these receptors are implicated in the top-down modulation of subcortical areas via descending PFC (Onn et al., 2006, Del Arco and Mora, 2009). For this purpose we used *Drd1a*-tdTomato/*Drd2*-EGFP double BAC-transgenic mice (Gong et al., 2003, Shuen et al., 2008) expressing tdTomato as a reporter for D_1aR-expressing neurons and EGFP as a reporter for D_2R-expressing neurons. These mice enabled us to overcome limitations imposed by the lack of readily available antibodies that discriminate between these receptor subtypes. Anatomical relationships were investigated within different subregions of the mPFC (PrL, IL, Cg1) as well as in the layer receiving cortico-cortical input (II/III) and the output layer (V) of the mPFC to determine a possible regional specificity of the different neuronal systems.

Materials and Methods

Animal Preparation

Six Male Long Evans rats (300–325 g, Université de Montréal obtained from Charles River Canada (St-Constant, Québec, Canada) and three *Drd1a*-tdTomato *Drd2*-EGFP double transgenic mice (Gong et al., 2003, Shuen et al., 2008) (Université Laval) were housed in a temperature-controlled room (21–25°C) under natural daylight, and had free access to food and water. Animals were deeply anesthetized with pentobarbital (54 mg/kg body weight i.p.) and then were perfused transcardially with 4% paraformaldehyde at room temperature. After perfusion, brains were harvested and post fixed for 2 h in fresh fixative. Serial coronal vibratome sections (35-µm thick) were cut and collected in 0.1 M phosphate buffer (PBS, pH = 7.4), then stored in antifreeze (30% glycerol, 30% ethylene glycol, 40% NaPB 0.24 M) solution at –20°C until further use. All procedures were approved by the local Animal Care Committee Université de Montréal (rats) and Université Laval (mice) and were conducted in accordance with the guidelines of the Canadian Council on Animal Care.

Immunocytochemistry

Sections were thoroughly washed in 0.1 M PBS, and then incubated in 0.3% H_2O_2 in 0.1 M PBS. The sections were then washed and incubated in 1.5% donkey serum in PBS-T (0.1 M phosphate buffer, pH 7.4 and 0.25% triton x-100) for 1 h. Rat brain sections were incubated in a cocktail of primary antibodies for 48 h at 4°C (Table 1): anti-choline acetyltransferase (ChAT, 1:200; Chemicon, Billerica, MA, USA) for cholinergic fibers (Vaucher et al., 1997, Dotigny et al., 2008); anti-tyrosine hydroxylase (TH, 1:1000; Pel-Freez Biologicals, Rogers, AR, USA) for dopaminergic fibers (Miner et al., 2003) and anti-glutamate transporter (EAAC1, excitatory amino acid carrier 1 protein, 1:1000, Chemicon, Billerica, MA, USA) for pyramidal cells (Rothstein et al., 1994, He et al., 2000, Furuta et al., 2003, Dotigny et al., 2008). Moreover, the pyramidal cell analysis was performed based on the pyramidal morphology of the EAAC1 stained cells. Triple immunolabeling of D_1aR-expressing neurons (amplification of the TomatoRed signal with anti-DsRed Polyclonal Antibody Rabbit, 1:200, Clonetech, Mountain View, CA, USA), D_2R-expressing neurons (amplification of the GFP signal with monoclonal mouse anti-GFP (B-2), 1:100, SantaCruz, Santa Cruz, CA, USA), and either pyramidal cells or ChAT fibers were carried out on adjacent sections. After washing, the sections were incubated in secondary antibodies conjugated with fluorophore CY3, FITC, CY5 (Jackson Immunoresearch, West Grove, PA, USA) for 2 h and 30 min. Mouse tissue was incubated with Drd1a labeled with CY5, Drd2 labeled with FITC, and ChAT and pyramidal cells labeled with CY3 (Table 1). Then the sections were

washed and mounted onto slides with anti-fading mounting medium and coverslipped (ProLong Antifade Kit P7481, Molecular Probe, Carlsbad, CA, USA). Adjacent sections were stained with cresyl violet to delineate cortical layers.

Table 1. Combination of primary and secondary antibodies for triple-fluorescent staining procedures.

Series	Primary antibodies (48 h)			Secondary antibodies (2 h 30)	
	Antigen	AB host	Dilution	IgG (Donkey)	Dilution
ChAT fibers/TH fibers/pyramidal cells in rats	ChAT	goat	1:200	Anti-goat-FITC	1:200
	TH	rabbit	1:1000	Anti-rabbit-CY5	1:200
	EAAC1	mouse	1:1000	Anti-mouse-CY3	1:200
Drd_1a/Drd_2/pyramidal cells in mice	DsRed	rabbit	1:200	Anti-rabbit-CY5	1:200
	GFP	goat	1:100	Anti-goat-FITC	1:200
	EAAC1	mouse	1:1000	Anti-mouse-CY3	1:200
Drd_1a/Drd_2/ChAT fibers in mice	DsRed	rabbit	1:200	Anti-rabbit-CY5	1:200
	GFP	mouse	1:100	Anti-mouse-FITC	1:200
	ChAT	goat	1:200	Anti-goat-CY3	1:200

Abbreviations: ChAT: choline acetyltransferase; EAAC1: excitatory amino acid carrier 1 protein; TH: tyrosine hydroxylase.

Confocal Microscopy and Quantification

Based on functional or anatomical relationship between the mPFC and BF (Golmayo et al., 2003, Vertes, 2004, Henny and Jones, 2008), Cg1, PrL and IL in rats or mice were analyzed. The relationships within layer II/III and V were quantified because they constitute the receiving layer of the cortical input (the thalamic input is almost absent in this cortex) and the output layer, respectively and because the EAAC1 pyramidal cells are present only in these layers. The analysis was conducted on two consecutive coronal sections (rats: +2.76 mm from Bregma (Paxinos and Watson, 1997); mice: (+1.94 to +1.70 mm from Bregma; (Franklin and Paxinos, 2007) per animal using the Leica SP2 confocal microscope (Leica Microsystems, Wetzlar, Germany). Argon laser (excitation at 488 nm) was used for excitation of FITC, Helium Neon laser (excitation at 543 nm) was used for excitation of CY3 and Helium Neon laser (excitation at 633 nm) was used for excitation of CY5. Z-series of images were taken using 100 × oil lenses in sequential scanning mode for each channel and captured by Leica Confocal Software (LCS lite). Z-series of images were randomly taken every 200 µm, starting at 0.1 mm above the ventral border of the IL cortex to the dorsal border of Cg1 in each layer (Figure 1). A projection was defined as a series of horizontal optical scanning sections in the same image. When a projection was generated, the sampling points of the individual images superimposed along the projection axis were examined throughout all optical sections. In a maximum projection, the maximum intensity value was displayed. Each Z-series maximal projection was

composed of an average of three optical sections for fiber microproximity analysis in rats, and four optical sections for the pyramidal cells analysis in rats, to ensure the full capture of pyramidal cells. The step size between any two consecutive optical sections was set at 1 μm. In total, 28 images were taken for each section (6 from IL, 10 from PrL, and 12 from Cg1) and a total of 336 neurons from the six rats were analyzed.

To investigate the anatomical relationship between cholinergic and dopaminergic fibers, a randomly-chosen region of interest (ROI) of 12500.00 μm^2 on the maximum projection of three consecutive optical scanning sections in each image was examined using LCS Lite. Because the step size was set at 1 μm, the depth of the ROI on this projection was 3 μm, and the distance between two visible fibers did not span more than 3 μm in the z-axis. The total length of dopaminergic (TH) and cholinergic nerve fibers (ChAT) were evaluated in ROIs with ImagePro using manual tracing (Figure 2). The fiber density ($\mu m/\mu m^3$) in each ROI was determined by dividing the total cholinergic or dopaminergic fiber density over the ROI volume. The volume of the ROI on each image was obtained by multiplying the area of the ROI (12500.00 μm^2) with the depth of the ROI.

Cholinergic and dopaminergic fiber microproximity were quantified semi-manually using LCS lite (Figure 1). For convergence of dopaminergic and cholinergic fibers on mPFC pyramidal neurons, one pyramidal cell per image was analyzed (Figure 1). All single optical scanning sections containing that cell were

examined to avoid overcounting. Microproximity for cholinergic, dopaminergic and pyramidal neurons was operationally defined as relationship between axonal segments or axonal segments/pyramidal cell perikaryon with a distance of 3 μm or less. This was considered a conservative within-limit distance for the possibility of occurrence of diffuse transmission given that extracellular ACh may diffuse over short distances and maintain a fast form of non-synaptic transmission, due to the ACh esterase activity and high sensitivity of nAChR (Lendvai and Vizi, 2008, Sarter et al., 2009b). As well, DA transmission between elements distant from 2 to 10 μm has been shown. The median diffusion distance of dopamine was estimated as 4.8 μm in the striatum, and extracellular dopamine concentration was spatially heterogeneous on a dimensional scale commensurate with this diffusion distance of individual dopamine molecules (Peters and Michael, 2000).

The total length of ChAT fibers within microproximity of TH fibers was measured by manual tracing within each layer of each ROI and the percentage of microproximity per mm of axonal length was calculated. In cases where the microproximity between two fibers did not span more than 3 μm on the *x*-*y* axis, more than three consecutive optical sections composing the image were examined sequentially to ensure the apposition between the two fibers span more than 3 μm in *z*-axis. The same analysis was made for TH fibers in microproximity of ChAT fibers. Furthermore, in order to detect potential activity-related morphological structures of axons, the density and diameter of TH and ChAT varicosities within or outside the microproximity was evaluated using LCS lite. The varicosities were

defined as ellipsoid swelling with a transverse diameter larger than 500 nm (Mechawar et al., 2000). Fiber segments were analyzed for TH varicosities within microproximity of ChAT fibers, TH varicosities outside microproximity of ChAT fibers, ChAT varicosities within microproximity of TH fibers, ChAT varicosities outside microproximity of TH fibers. Fiber segments were randomly analyzed in Layers V and II/III of PrL and Cg1 and IL. In total, 1208 fiber segments were randomly chosen and analyzed in the rat mPFC, with a total length of 10296.65 µm.

Two mouse brain sections at the level of IL, PrL and Cg1 were analyzed using 100× oil lens in sequential scanning mode and captured by LCS lite. Two ROI's were randomly chosen within each layer of each subregion. To ensure sufficient sampling through the *z*-axis, sections with triple immunolabeling for Drd_1a, Drd_2, and pyramidal cells were composed of five optical sections, and each section immunolabeled for *Drd1a*, *Drd2*, and ChAT fibers was composed of ten optical sections. The step size between any two consecutive optical sections was set at 1 µm. The images of triple staining of *Drd1a*, *Drd2* and pyramidal cells were exported to Photoshop CS3 and the presence of *Drd1a* and *Drd2* on pyramidal cells were quantified by manual counting within the ROI. A total of 1810 pyramidal cells were examined. Only pyramidal cells with a clear outline and complete shapes were examined. These pyramidal cells were examined both on the five single optical sections and the overlay projection to ensure validity of the measurements. Colocalization of Drd_1a and Drd_2 on the images of triple labeling of

Drd1a, *Drd2*, and pyramidal cells, as well as *Drd1a* and ChAT, and *Drd2* and ChAT on the images of triple immunostaining of *Drd1a, Drd2*, and ChAT were quantified using the plugin of Intensity Correlation Analysis (Li et al., 2004) in the ImageJ software (Collins, 2007). Mander's Overlap coefficient (*R*) was used to indicate the colocalization of the two neuronal elements (Manders et al., 1992), with *R* ranges between 1 and 0 with 1 being high-colocalization and 0 being low. Each single optical section was examined with ImageJ to avoid overcounting. Background was subtracted using areas that did not contain labeled cells or fibers on the same section.

Statistical Analysis

SPSS (17.0) Wilcoxon signed ranks test ($p < 0.05$, two tailed) was used to compare the regional effects among IL, PrL and Cg1 and the laminar effects between layer V and layer II/III in the rats and mice. Pearson correlation ($p < 0.05$, two tailed) was used to evaluate the correlation between the incidents of microproximity with fiber density in the rats. Paired student *t* test ($p < 0.05$, two-tailed) was used to compare the density and diameter of varicosities inside microproximity and those outside microproximity, as well as the laminar distribution. An ANOVA ($p < 0.05$, two tailed) was used to evaluate the regional difference in the density and diameter of varicosities.

FIGURE 1

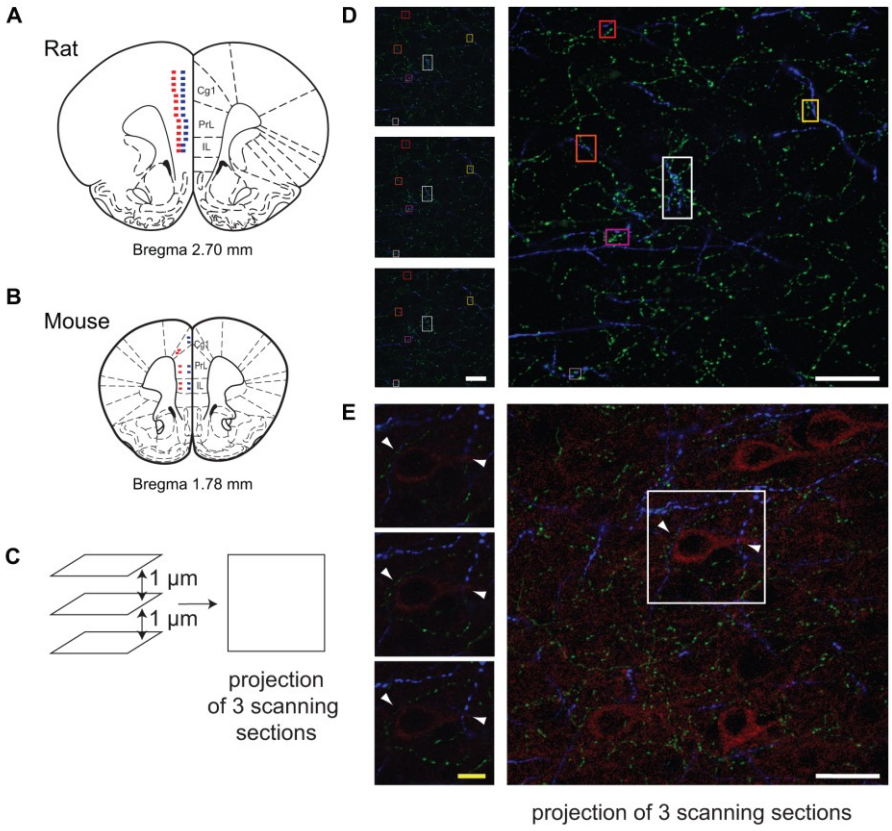

Figure 1. Methodology for quantification of micropoximities with the Leica confocal microscope. Images of the regions of interest (Cg1, PrL, IL) were randomly taken using 100× oil lens in sequential scanning mode on the coronal sections of rats (**A,** Bregma, +2.7 mm) and mice (**B,** Bregma, +1.8 mm). Microphotographs were taken every 200 µm, starting at 0.1 mm above the ventral border of the IL cortex to the dorsal border of Cg1 in each layer **(A, B)**. Red squares indicate location of scanning in Layer V, and blue squares indicate

location of scanning in Layer II/III. In the BAC *Drd1a*-tdTomato and GENSAT BAC *Drd2*-EGFP double transgenic mice, two images were taken in each layer in each subregion of the mPFC **(B)**. The close appositions (within 3 μm in 3D) among cholinergic (green), dopaminergic (blue) fibers, and pyramidal (red) cells were examined on the projection image of three consecutive scanning sections (step size of 1 μm) as well as each single scanning section **(C–E)**. Representative examples of ChAT and TH fibers microproximity are shown (squares in **D**). Arrows showed examples of pyramidal cells within microproximity of ChAT fibers and TH fibers **(E)**. White scale bar: 25 μm; Yellow scale bar: 5 μm.

FIGURE 2

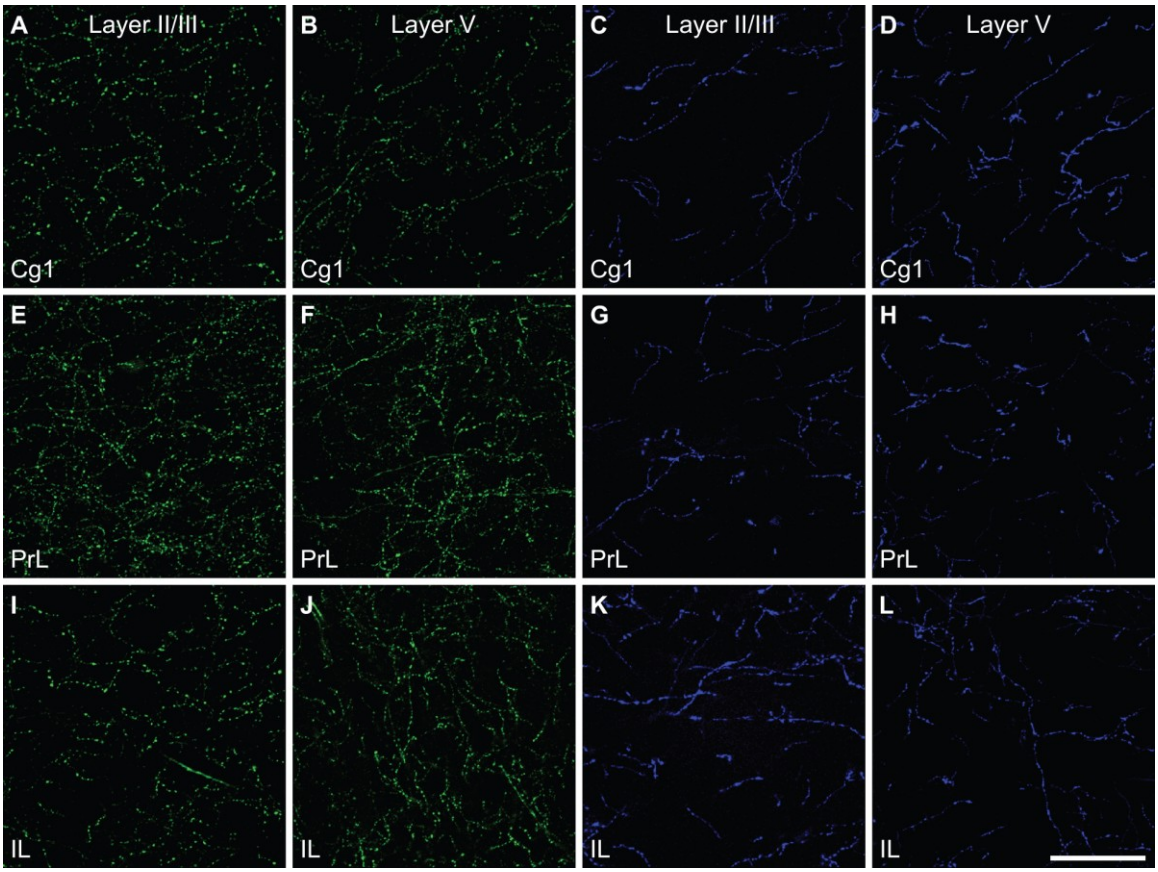

Figure 2. Density of the ChAT (green) fibers (A,B,E,F,I,J) and TH (blue) fibers (C,D,G,H,K,L) in Layer II/III and Layer V of cingulate cortex (Cg1, A–D), prelimbic (PrL, E–H) and infralimbic (IL, I–L) subregions of the medial prefrontal cortex in rats. The density of ChAT fibers was greater than those of TH fibers and showed regional differences. Scale bar: 50 μm.

Results

Cholinergic and Dopaminergic Innervation of IL, PrL and Cg1 Cortical areas in Rats

Prominent innervations of IL, PrL and Cg1 by both ChAT and TH fibers were observed (Figure 2). The density of TH fibers ranged from 0.008 μm/μm^3 in Cg1 to 0.020 μm/μm^3 in IL, and the density of ChAT fibers ranged from 0.021 μm/μm^3 in Cg1 to 0.044 μm/μm^3 in PrL (Table 2). ChAT fibers were significantly denser than TH fibers in most subregions in both layers of mPFC, except in layer V of IL, where significant level was not reached ($p < 0.05$). Cg1 had significantly smaller TH and ChAT fiber density compared to IL and PrL in both layers ($p < 0.05$). Part of the ChAT fibers could be attributed to the intracortical cholinergic neurons but this did not represent more than 10% of the fibers (the ChAT staining was almost absent following BF quisqualic acid lesion; data not shown, but see (Vaucher et al., 1995).

Table 2. Dopaminergic and cholinergic fiber density in the mPFC of rats.

	Infralimbic Ctx	Prelimbic Ctx	Cingulate Ctx
Layer II/III			
TH fiber density	1.56 ± 0.32$^{*\&+}$	1.35 ± 0.30$^{*\&}$	0.79 ± 0.20$^{*\&}$
ChAT fiber density	3.53 ± 1.03$^{*\&+}$	4.44 ± 1.00$^{*\&+}$	2.52 ± 0.43$^{*\&+}$
Layer V			
TH fiber density	1.95 ± 0.39^{*+}	1.79 ± 0.48$^{*\&}$	0.79 ± 0.10$^{*\&}$
ChAT fiber density	2.50 ± 0.79^{*+}	3.24 ± 0.63$^{*\&+}$	2.12 ± 0.37$^{*\&+}$

All values are means ± SEM expressed in 10^{-2}µm/µm^3 from 6 animals. Abbreviations: ChAT: choline acetyltransferase; Ctx: cortex; TH: tyrosine hydroxylase.

$^{\&}$ Wilcoxon test, $p < 0.05$, two-tailed, ChAT vs TH fibers

* Wilcoxon test, $p < 0.05$, two-tailed, Region-specific difference

$^{+}$ Wilcoxon test, $p < 0.05$, two-tailed, Layer-specific difference

Microproximity between ChAT and TH Fibers in IL, PrL and Cg1 of Rats

The proportion of the ChAT fibers within the microproximity of TH fibers (Figure 3 , Table 3), ranged from 12–18% in layer V of the rat mPFC and 8–13% in layer II/III. Layer V of each subregion in mPFC had a significantly larger proportion of ChAT fibers close to TH fibers compared to layer II/III ($p < 0.05$), with the exception of IL. In addition, both Cg1 and IL had a significantly larger proportion of ChAT fibers in microproximity to TH fibers than PrL in both layers V and II/III. In contrast, 21–40% of the TH fibers in layer V as well as II/III shared relationship with ChAT fibers (Figure 3; Table 3). Cg1 had a significantly larger proportion of TH fibers in microproximity with ChAT fibers compared to IL or PrL in both layers V and II/III ($p < 0.05$). In each subregion of each layer in the mPFC, the proportion of TH fibers in microproximity with ChAT fibers was significantly higher than the proportion of ChAT fibers in microproximity to TH fibers, with the exception of Layer V of IL ($p < 0.05$). Because the tortuosity and density of TH and ChAT fibers were different as well as the fiber density for each neuronal system, the length of TH and ChAT microproximities was not symmetrical.

FIGURE 3

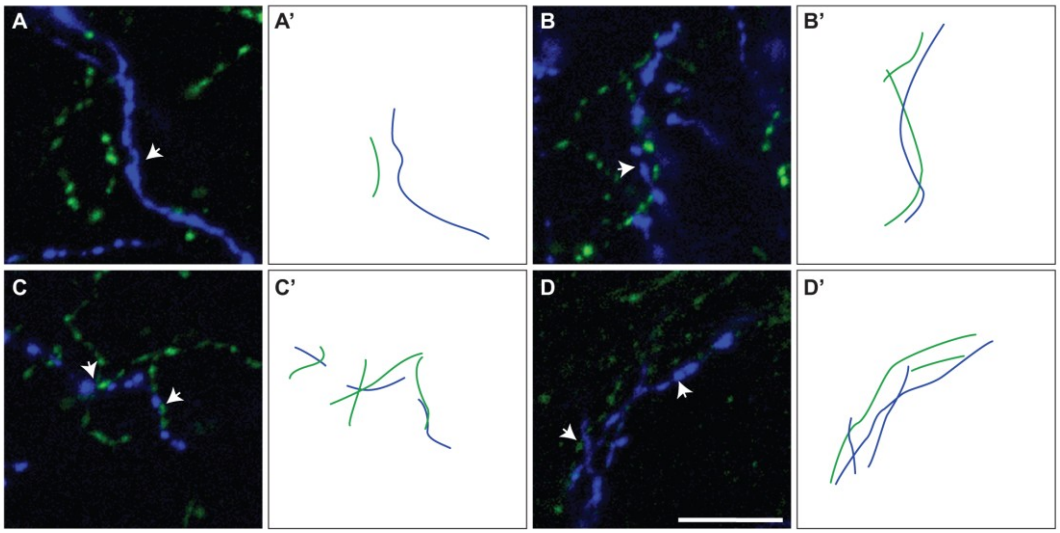

Figure 3. Representative examples of ChAT/TH fibers within microproximity of each other (arrows) (A–D). The measured lengths of microproximity segments are illustrated by drawing of ChAT (green lines) and TH (blue lines) fibers **(A'–D')**. Scale bar: 5 μm.

Table 3. Microproximity between ChAT and TH fibers in the mPFC of rats.

	Infralimbic Ctx	Prelimbic Ctx	Cingulate Ctx
Layer II/III			
ChAT fibers to TH fibers	12.2$^{*+\&}$	8.8$^{*+\&}$	12.3$^{*+\&}$
TH fibers to ChAT fibers	23.9$^{*\&}$	28.1$^{*\&}$	39.6$^{*\&}$
Layer V			
ChAT fibers to TH fibers	17.9^{*+}	12.9$^{*+\&}$	15.5$^{*+\&}$
TH fibers to ChAT fibers	21.4*	22.8$^{*\&}$	40.1$^{*\&}$

All values are percentage of axonal segment in microproximity over total fiber length from 6 animals. Abbreviations: ChAT: choline acetyltransferase; Ctx: cortex; TH: tyrosine hydroxylase.

$^{\&}$ Wilcoxon test, $p < 0.05$, two-tailed, ChAT vs TH fibers

* Wilcoxon test, $p < 0.05$, two-tailed, Region-specific difference

$^{+}$ Wilcoxon test, $p < 0.05$, two-tailed, Layer-specific difference

TH and ChAT Varicosities Density and Morphology within the Microproximity Segment or Intersegment in IL, PrL and Cg1 of Rats

The density of both TH and ChAT varicosities (Figure 4) was significantly elevated within microproximity of the other fiber system in each subregion of both Layer V (ChAT: 0.59 ± 0.03 per μm of ChAT fiber length; TH: 0.53 ± 0.04 per μm of TH fiber length) and Layer II/III (ChAT: 0.56 ± 0.03, TH: 0.52 ± 0.02) in the rat mPFC compared to those outside microproximity (ChAT: 0.43 ± 0.06, TH: 0.36 ± 0.03; $p < 0.05$; Table 4; Figure 4). The ChAT varicosity diameter within microproximity (664 ± 21 nm) compared to that outside microproximity (646 ± 25 nm) was significantly larger ($p = 0.001$). The TH varicosity diameter (677 ± 23 nm) within microproximity compared to that outside microproximity was also significantly larger ($p = 0.016$). TH varicosity diameter within microproximity in layer V (685 ± 34 nm) was significantly larger than that in layer II/III (670 ± 17 nm; $p = 0.001$, Table 5).

FIGURE 4

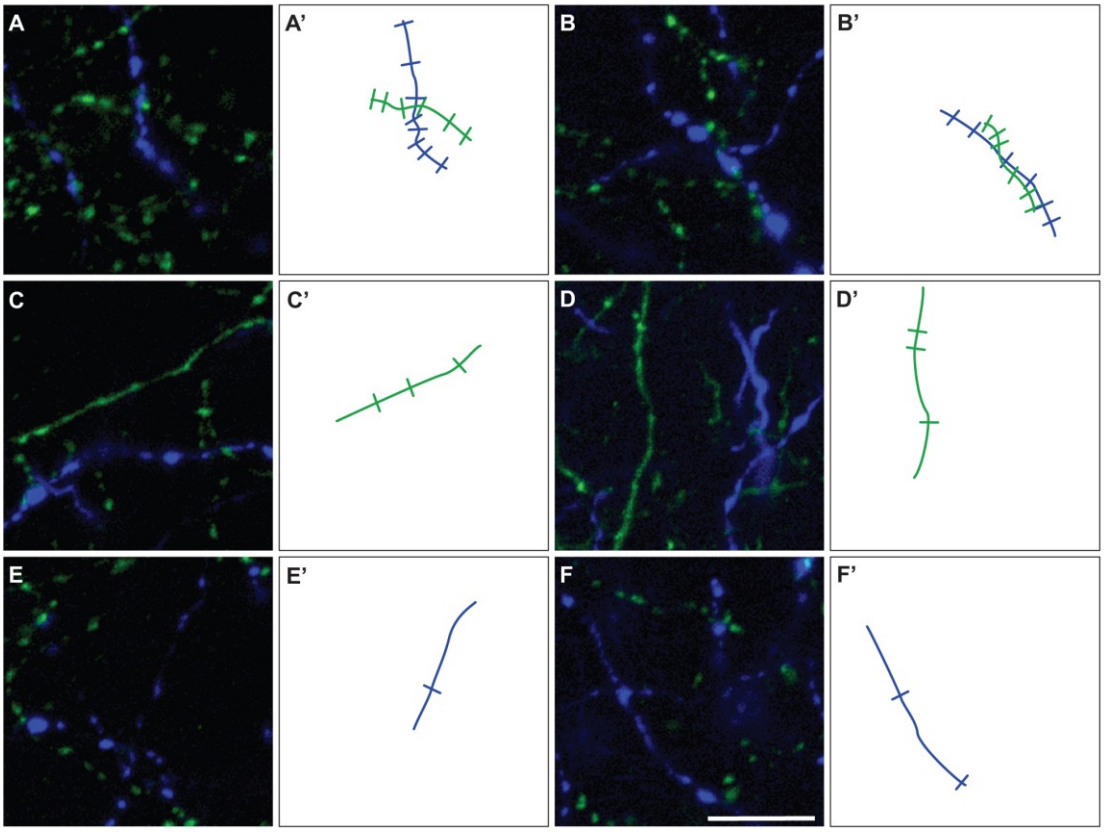

Figure 4. Representative examples of ChAT (green) and TH (blue) varicosities on fiber segments within (A,B) or outside (C–F) the microproximity of the other fiber system in rat mPFC. Note that an increased density of varicosities was seen in segments in microproximity. The number of varicosities counted on microproximity segments are illustrated by indentations on drawing of ChAT (green lines) and TH (blue lines) fibers **(A'–F')**. Scale bar: 10 μm.

Table 4. Number and diameter of TH and ChAT varicosities within or outside microproximity in the mPFC of rats.

	Infralimbic Ctx	Prelimbic Ctx	Cingulate Ctx
Layer II/III			
TH varicosities within microproximity	$0.52 \pm 0.03^{\Delta}$ (666 ± 28)	$0.53 \pm 0.04^{\Delta\&}$ ($689 \pm 44^{\&\Delta}$)	$0.50 \pm 0.04^{\Delta}$ (656 ± 44)
TH varicosities outside microproximity	$0.26 \pm 0.03^{\Delta *+}$ ($672 \pm 62^{*+}$)	$0.33 \pm 0.04^{\Delta\&*+}$ ($608 \pm 37^{\Delta+}$)	$0.31 \pm 0.04^{\Delta+}$ ($601 \pm 12^{*+}$)
ChAT varicosities within microproximity	$0.53 \pm 0.01^{\Delta}$ ($664 \pm 45^{+}$)	$0.59 \pm 0.03^{\Delta\&}$ ($641 \pm 09^{\&\Delta+}$)	$0.54 \pm 0.04^{\Delta}$ (641 ± 23)
ChAT varicosities outside microproximity	$0.38 \pm 0.13^{\Delta}$ ($654 \pm 29^{+}$)	$0.38 \pm 0.02^{\Delta\&+}$ ($620 \pm 12^{\Delta+}$)	$0.35 \pm 0.03^{\Delta+}$ (626 ± 24)
Layer V			
TH varicosities within microproximity	$0.49 \pm 0.06^{\Delta}$ (688 ± 75)	$0.56 \pm 0.02^{\Delta}$ (717 ± 36)	$0.53\pm 0.03^{\Delta\&}$ ($649 \pm 16^{\Delta}$)
TH varicosities outside microproximity	$0.33 \pm 0.02^{\Delta *+}$ ($639 \pm 44^{*+}$)	$0.39 \pm 0.04^{\Delta\&*+}$ ($697 \pm 40^{*+}$)	$0.37 \pm 0.05^{\Delta *+}$ ($627 \pm 13^{*\Delta+}$)
ChAT varicosities within microproximity	$0.57 \pm 0.05^{\Delta *}$ ($665 \pm 21^{\Delta+}$)	$0.61 \pm 0.04^{\Delta *}$ ($704 \pm 35^{+}$)	$0.59 \pm 0.02^{\Delta\&}$ (671 ± 19)
ChAT varicosities outside microproximity	$0.36 \pm 0.02^{\Delta}$ ($627 \pm 28^{*\Delta+}$)	$0.49 \pm 0.06^{\Delta\&+}$ ($690 \pm 42^{*+}$)	$0.42 \pm 0.03^{\Delta+}$ (657 ± 26)

All values are means ± SEM expressed in number of varicosities /µm or (diameter) expressed in nm from 6 animals. Abbreviations: ChAT: choline acetyltransferase; Ctx: cortex; TH: tyrosine hydroxylase.

[&] Paired student t test, $p < 0.05$, two-tailed, ChAT vs TH varicosities

[Δ] Paired student t test, $p < 0.05$, two-tailed, within compared outside microproximity

* One-Way Anova, $p < 0.05$, two-tailed, Region-specific difference

[+] Paired student t test, $p < 0.05$, two-tailed, Layer-specific difference

Table 5. Percentage of pyramidal cells within the microproximity of ChAT and/or TH fibers in the mPFC of rats.

	Infralimbic Ctx	Prelimbic Ctx	Cingulate Ctx
Layer II/III			
ChAT fibers	80.6	86.7	90.3
TH fibers	69.4	65.0	61.1^{+}
ChAT and TH fibers	63.9	56.7	55.6^{+}
Layer V			
ChAT fibers	77.8*	90.0*	88.9*
TH fibers	86.1	80.0	87.5^{+}
ChAT and TH fibers	72.2	70.0	80.6^{+}

All values are mean percentage of pyramidal cells within the microproximity of fibers from 6 animals.

* Wilcoxon test, $p < 0.05$, two-tailed, Region-specific difference in fiber density

$^{+}$ Wilcoxon test, $p < 0.05$, two-tailed, Layer-specific difference of fiber density

Microproximity between Pyramidal Cells and Cholinergic and Dopaminergic Fibers in IL, PrL and Cg1 of Rats

The majority of pyramidal cells were found in close proximity with cholinergic fibers both in layer V and II/III of the three regions examined (Figure 5). In layer V, 78% of the pyramidal cells examined in IL, 90% in PrL, and 89% in Cg1 were in close microproximity with cholinergic fibers (Table 5). In layer II/III these percentages reached 81% in IL, 87% in PrL, and 90% in Cg1. PrL and Cg1 of layer V had significantly more pyramidal cells innervated by ChAT fibers than layer V of IL ($p < 0.05$). As well, the majority of pyramidal cells were found in close proximity with dopaminergic fibers both in layer V and II/III of the three regions examined. In layer V, 86% of pyramidal cells examined in IL, 80% in PrL, and 87% in Cg1 were in microproximity with dopaminergic fibers. In layer II/III, these numbers were 69% in IL, 65% in PrL, and 61% in Cg1 (Table 5). There were no regional differences but there was significantly more pyramidal cells innervated by TH fibers in layer V of Cg1 than in Layer II/III of Cg1 ($p < 0.05$).

FIGURE 5

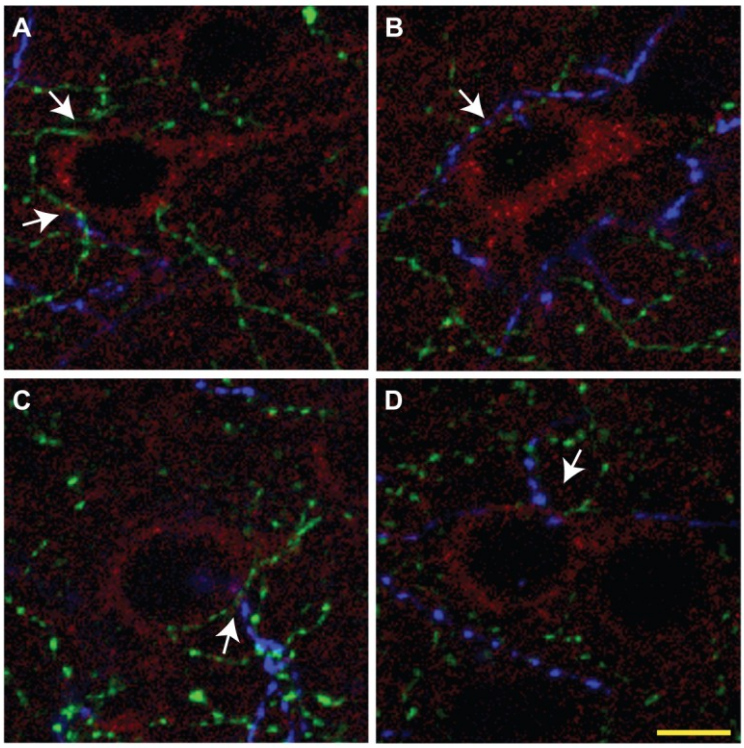

Figure 5. Representative overlay projection images (A–D) of triple immunolabeling of ChAT (green), TH (blue) fibers, and pyramidal cells (red) from three consecutive optic sections in rat mPFC. Arrows show examples of microproximities. Most pyramidal cells were within microproximity of both ChAT and TH fibers. Scale bar: 5 μm.

Most pyramidal cells examined were within the microproximity of both cholinergic and dopaminergic fibers. In layer V, 72% of pyramidal cells examined in IL, 70% in PrL, and 80% in Cg1 showed microproximity with both cholinergic and dopaminergic fibers. In layer II/III these numbers were 64% in IL, 57% in PrL, and 56% in Cg1 (Table 5). There were no regional differences, but there were significantly more pyramidal cells innervated by both ChAT and TH fibers in layer V of Cg1 than in Layer II/III of Cg1 ($p < 0.05$). In layer V, microproximity of cholinergic or dopaminergic fibers with pyramidal cells were observed mainly at the level of the cell soma, less frequently at their apical dendrites and only scarcely at their basal dendrites (Table 6). There was no difference in the preferred localization of the zone of contact of the pyramidal cell by cholinergic or dopaminergic fibers.

Table 6. Percentage of pyramidal cells innervated at their soma/apical dendrites/basal dendrites in Layer V of the mPFC of rats.

	Infralimbic Ctx	Prelimbic Ctx	Cingulate Ctx
Innervation by ChAT fibers			
soma	39.3	51.9	51.6
apical dendrites	28.6	35.2	37.5
basal dendrites	0.0	7.4	3.1
Innervation by TH fibers			
soma	54.8	64.6	54.0
apical dendrites	22.6	31.3	31.8
basal dendrites	0.0	0.0	6.4

All values are means percentage of pyramidal cells innervated at submorphological compartment from 6 animals.

The proportion of pyramidal cells innervated by TH and ChAT fibers was not positively correlated with the fiber density in most regions in either layer, indicating that the innervations were not random ($p < 0.05$, r ranged from −0.636 to +0.636). The only exception was between the proportion of pyramidal cells innervated by ChAT fibers and ChAT fiber density in Cg1 of layer II/III (Pearson correlation, $p = 0.031$, $r = 0.852$). Moreover, a negative correlation was found between the proportion of pyramidal cells innervated by both fiber systems and TH fiber density in IL of Layer V (Pearson correlation, $p = 0.036$, $r = -0.840$).

Presence of D_1a and D_2 Receptors (D_1aR and D_2R) on Pyramidal Cells and ChAT Fibers in IL, PrL and Cg1 of Mice

Most pyramidal cells (~ 92% to 95%) in the mPFC of mice were stained for GFP, i.e. expressing D_2R. However, only a small proportion of pyramidal cells (~ 16% to 26%) were stained for TdTomato, i.e. expressing D_1aR (Figure 6). About 15% to 25% of pyramidal cells expressed both EGFP and TdTomato (Table 7). No significant region-specific or layer-specific difference was found ($p > 0.05$). The expression of either D_1aR or D_2R by cholinergic fibers in the subregions of mPFC of mice was low, with the Mander's coefficient of colocalization of TdTomato and ChAT ranging from ~0.10 to 0.13 and of GFP and ChAT ranging from 0.22 to 0.27 (Figure 7). No significant region-specific or layer-specific difference was found ($p > 0.05$).

FIGURE 6

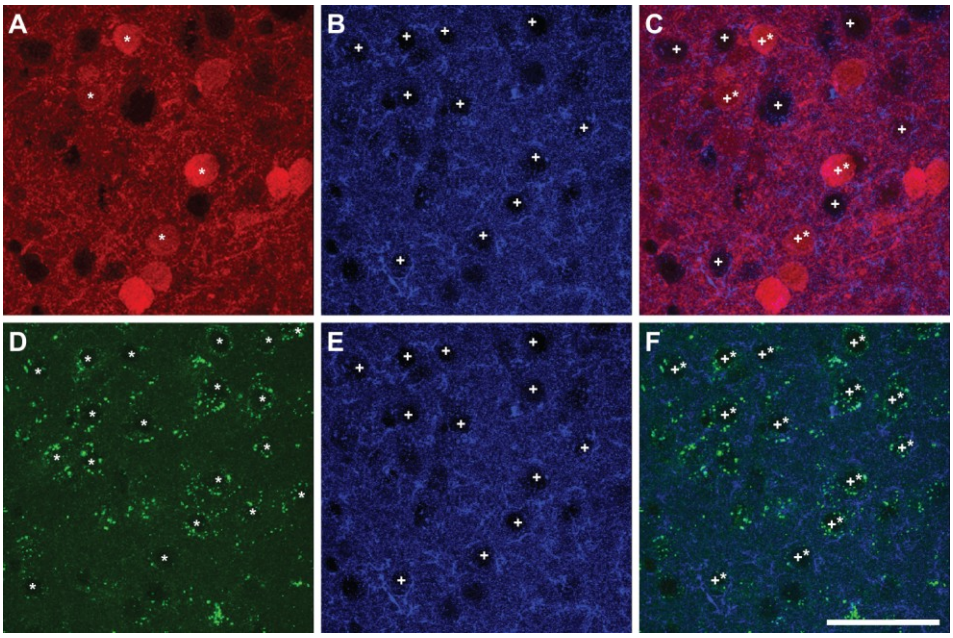

Figure 6. Colocalization of markers of D_1aR (A) or D_2R (D) expression with EAAC1 pyramidal cells (B,E) in Drd$_1$a-tdTomato/Drd$_2$-EGFP mice (overlay images, C,F). A majority of pyramidal cells expressed Drd$_2$ marker (stars in **A,C**) whereas a minority of pyramidal cells (crosses) expressed *Drd1a* marker(stars in **D,F**). Scale bar: 50 μm.

Table 7. Percentage of pyramidal cells containing Drd_1a-tdTomato and Drd_2-EGFP in the mPFC of mice.

	Infralimbic Ctx	Prelimbic Ctx	Cingulate Ctx
Layer II/III			
Drd_1a	21.1	24.2	16.5
Drd_2	92.6	94.4	93.3
Drd_1a and Drd_2	21.1	23.0	15.2
Layer V			
Drd_1a	19.3	25.6	21.5
Drd_2	94.6	92.5	92.7
Drd_1a and Drd_2	18.4	24.5	20.8

All values are mean percentage of pyramidal cells from 3 Drd_1a-TdTomato/Drd_2-EGFP transgenic mice. Abbreviations: Ctx: cortex

FIGURE 7

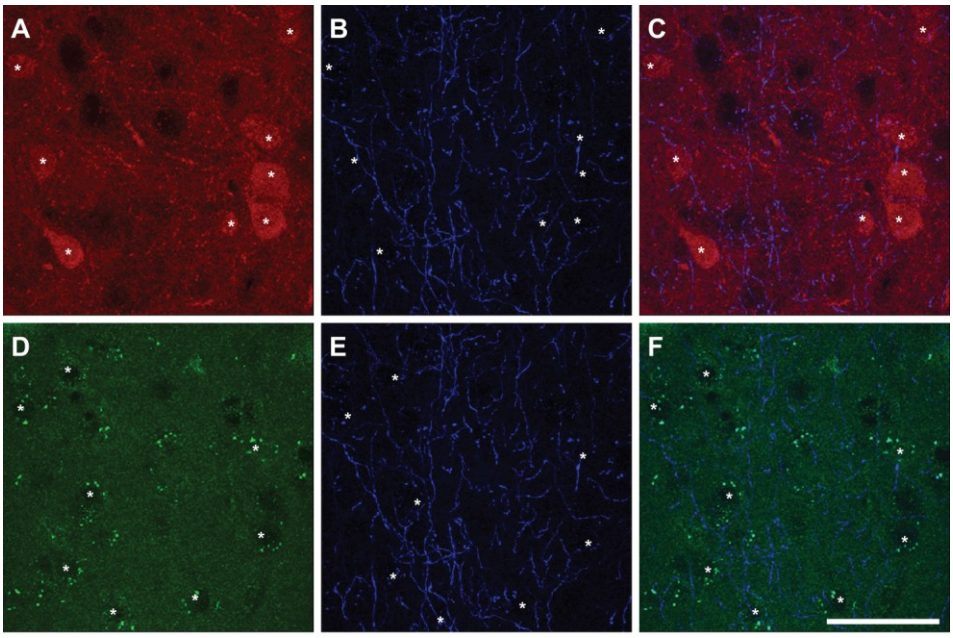

Figure 7. Colocalization of markers of D_1aR (A) or D_2R (D) expression with ChAT (B,E) in Drd$_1$a-tdTomato/Drd$_2$-EGFP mice (overlay images, C,F). The colocalization of *Drd1a* or *Drd2* markers and cholinergic fibers was very scarce. Drd$_1$a and Drd$_2$ markers were detected in cortical cell soma but not ChAT fibers. Scale bar: 50 μm.

Discussion

The goal of this study was to determine the anatomical potential for a modulatory interaction between cholinergic and TH afferents in the rodent mPFC and with the output pyramidal cells. The results indicate that the cholinergic and dopaminergic systems converge on pyramidal cells in mPFC to possibly modulate their activity. The level of dopaminergic fibers relationship with pyramidal cells is higher in the output layer compared to the cortico-cortical connection layer (layer II/III), whereas cholinergic fibers have the same extent of interaction in layers II/III and V. The mutual axo-axonal microproximity between the two neuronal systems was poor in mPFC. However, the cholinergic system appears to have more influence on the dopaminergic fibers since a larger proportion of the TH fibers are within microproximity to cholinergic fibers and the cholinergic fibers did not express markers of either d1ar or d2r expression. Moreover, ChAT fiber segments bore a higher density of varicosities compared to those outside the vicinity of TH fibers, which could account for an index of improved ACh transmission in these axonal segments. Both ChAT and TH fiber segments bore a higher density of varicosities within microproximity compared to those outside microproximity indicating a potential for elevated transmission at these sites. In addition, in the mPFC of Drd_1a-tdTomato/Drd_2-EGFP mice, pyramidal cells preferentially expressed markers of the inhibitory D_2R over D_1aR. The result of the present study suggests an important role in mPFC output via co-modulation of pyramidal cells by both cholinergic and dopaminergic fibers, and the heterogeneity of the three subregions

in mPFC regarding the neuroanatomical relationship among these three neuronal elements.

Enrichment of the Microproximities

Confocal microscopy offers a means in which to examine the neuroanatomical relationships among individual optical sections at high resolution in sequence through the specimen (Wouterlood et al., 2007, Ichinohe et al., 2008). Here we examined the frequency of microproximities between fibers and pyramidal cells to determine the possible functional interaction between the cholinergic and dopaminergic system in the PFC in the context of diffuse transmission. The primary interest of the current study was to investigate the extracellular microenvironment, where the output of mPFC is modulated by ACh and DA via diffuse transmission. Synaptic incidents were not counted since ACh terminals rarely form junctional complexes in the neocortex, and only a small proportion of DA varicosities in the neostriatum are synaptic (Descarries et al., 1997, Descarries et al., 2008). Rather, the density of varicosities in segments in microproximity were counted and compared to segments outside of microproximity. We hypothesized that the density of varicosities in an axonal segment could be related to the level of activity, like the experience-induced increase of the number of dendritic spines and axonal synaptic boutons (Stettler et al., 2006). This is in agreement with the hypothesis of the “fast form of non-synaptic transmission” of ACh in the rat mPFC. The criterion definition for the sphere of influence of ACh and DA poses a challenge due to the scarcity of

data describing the temporal and spatial parameters of diffuse transmission. The real sphere of influence for a neurotransmitter is limited by a number of factors including the initial number of molecules released, the sensitivity and location of specific receptors, the extracellular volume, the tortuosity of diffusion, the diffusion coefficient of the neurotransmitter, and the regionally distinct uptake mechanisms (Nicholson and Sykova, 1998). To our knowledge diffusion properties of DA and ACh in the extracellular space of mPFC are unknown. Based on ultrastructural studies (Chedotal et al., 1994, Vaucher and Hamel, 1995) a maximal distance of 3 μm between two fibers was used as a conservative within-limit number for efficient diffuse transmission, i.e. in which neurotransmitter concentration would be sufficient to induce a significant effect, especially taking into consideration the rapid hydrolysis of ACh by AChE (Descarries et al., 1997, Descarries, 1998, Lendvai and Vizi, 2008).

Proportion of ChAT Fibers within Microproximity of TH Fibers

Mutual interaction between cholinergic and dopaminergic axons characterized by proximity of axons within 3 μm could be observed in the mPFC. The frequency of microproximity was moderate for the ChAT fibers (9–18%) which suggests a weak resultant influence of DA on the cholinergic fibers if any, but quite consistent for the TH fibers (20–40%). However, the higher density of TH varicosities within the microproximity of ChAT fibers (ranging from 0.49 to 0.56 per μm), compared to those outside microproximity of ChAT fibers (ranging from 0.26 to 0.39 per μm) raises the possibility of a DA release site which could modulate ChAT fibers. The value of Mander's coefficient of colocalization of tdTomato linked to the *Drd1a* promoter or EGFP associated with the *Drd2* promoter with ChAT was however low (ranging from 0.10 to 0.25), suggesting that the cholinergic fibers were devoid of D_1aR and D_2R. The lack of clear labeling for markers of dopaminergic receptors might be due to a weak transport of the reporter protein, although the nigrostriatal pathway is well labeled (Shuen et al., 2008). However, the lack of clear labeling of dopaminergic receptors within cholinergic fibers indicates that the pharmacological influence of DA over ACh transmission would take place at the level of pyramidal cells or interneurons rather than in presynaptic modulation of ChAT afferents. It has been shown that DA has an influence on ACh release, which leaves open the potential for a local effect. However, the effect of DA pharmacological agents on ACh transmission might also be exerted through indirect mechanisms when administered systemically, like the involvement of other

neurotransmitters systems, instead of local mechanisms. For example, dopaminergic fibers might interact with cholinergic cell bodies in the BF (Smiley et al., 1999) or on glutamatergic input from the nucleus accumbens (Brooks et al., 2007) to exert its influence on projecting cholinergic fibers to the mPFC. Finally, it cannot be excluded that immunodetection of GFP or tdTomato is weaker in the axon compared to the cell body because the gene is expressed in the cell body. While it is possible that the lack of dopaminergic receptors on cholinergic fibers might be due to low axonal levels of the reporter protein, axonal tdTomato protein is readily detectable in the striatonigral pathway (Shuen et al., 2008).

Higher Proportion of TH Fibers within Microproximity of ChAT Fibers

The higher proportion of TH fibers in close proximity with ChAT fibers (22–40%), especially within layer V would predict a stronger influence of ACh upon dopaminergic transmission. The higher density and size of ChAT varicosities on the fiber segments that are within microproximity to TH fibers supports the possibility that ACh release modulates TH fibers in the rat mPFC. Pharmacological evidence also supports the notion that the microproximity of DA and ACh is functional since local injections of nicotine or increased level of ACh have been shown to increase DA release in mPFC (Shearman et al., 2005, Shearman et al., 2006). The highest proportion of TH and ChAT microproximity occurs in layer V, which suggests that cholinergic fibers modulate the output of mPFC through direct contact to pyramidal cells as well as modulation of DA activity. However, it should

be noted that densities and diameters of the varicosities examined under confocal microscope might be slightly overestimated compared to results obtained under electron microscope due to the airy distribution (i.e., a gradient of intensity) of edge of the biological object in bitmapped images (Wouterlood et al., 2007).

Combined Effects of ACh and DA on Pyramidal Cells

Most pyramidal cells investigated were within the proximity of both cholinergic and dopaminergic fibers. This is consistent with the findings that dopaminergic afferents to the mPFC primarily target the cortical pyramidal cells (Verney et al., 1990). This spatial closeness makes it likely that dopaminergic and cholinergic fibers can modulate mPFC output mostly by innervating the same pyramidal neurons and have a combined effect on pyramidal cell output. In layer V, microproximities between ChAT fibers and TH fibers and pyramidal cells were localized on the soma and apical dendrite. This is consistent with the findings that the majority of the D_1R and D_2R are located on cell bodies and dendrites of cells intrinsic to the mPFC (Choi et al., 1995, Tzschentke, 2001). There were relatively few microproximities localized on the basal dendrites which is of importance in spike generation (Shu et al., 2007), but the EAAC1 staining was not sensitive enough to label the extent of the dendritic tree. The observed convergence of cholinergic and dopaminergic fibers on pyramidal cells is consistent with various pharmacological evidence supporting the modulation of mPFC pyramidal cells by ACh and DA (Gulledge and Jaffe, 1998, Carr and Surmeier, 2007, Lopez-Gil et al.,

2009). Pyramidal cells may integrate inputs from both cholinergic and dopaminergic systems that in turn transmit and modulate local activity to subcortical target regions. In addition, cholinergic and dopaminergic systems may shape the excitatory output of the mPFC, since neonatal ACh or DA depletion results in layer V neurons having smaller apical tufts, reduced apical dendrites number/density and reduced basilar spine density. Furthermore, combined ACh/DA depletion produced morphological effects that were additive compared to changes produced by cholinergic and dopaminergic denervation alone (Sherren and Pappas, 2005).

Supporting the neuromodulation of pyramidal cells by DA, are findings in the *Drd1a*-td Tomato *Drd2*-EGFP mice which indicate that more than 90% of the pyramidal cells express *Drd2* and only about 20% of the pyramidal cells contain *Drd1a*. Our findings are consistent with previous findings showing that D_1R were primarily found on non-pyramidal cells, and that D_1R and D_2R showed only a partial overlap (Vincent et al., 1993, 1995). About 20% of the pyramidal cells express markers for both Drd_1a and Drd_2, suggesting a possibility of direct D_1R–D_2R association on the same cell (Dziedzicka-Wasylewska et al., 2008). This indicates that dopaminergic transmission on output pyramidal cells might be inhibitory. This is consistent with previous studies showing an excitatory action of DA on GABAergic cells and an inhibitory action on pyramidal cells (Steketee, 2003). In contrast, cholinergic fibers have the same extent of innervation in layers II/III and V. This indicates that ACh might modulate both the excitatory output and input of

the mPFC. As ACh enhances neuronal activity, an increased cholinergic transmission would enhance the excitatory output of mPFC. However, the concomitant stimulation of TH fibers, which are inhibitory in layer V, would balance the level of output. According to our anatomical data, it can be suggested that the cholinergic afferents exerts an influence on the excitability of the mPFC at both the level of input from associational areas and of output, which can justify an involvement of ACh in retention and orienting, whereas DA would act on impulsivity and selectivity by decreasing the output of layer V neurons (Steckler et al., 1998).

Regional Heterogeneity in mPFC

In this study, region-specific differences were found among the three sub-areas in the rat mPFC in terms of the length of ChAT and TH fibers, the incidents of close appositions between cholinergic and dopaminergic fibers, as well as the proportion of pyramidal cells innervated by cholinergic fibers. Regional heterogeneity in rat mPFC has been a widely-accepted view, and it was shown that IL, PrL and Cg1 each have different extrinsic connections and functions (Broersen et al., 1995, Steckler et al., 1998, Tzschentke, 2001, Heidbreder and Groenewegen, 2003, Thienel et al., 2009). The dense interaction of pyramidal cells with both ChAT and TH fibers in the mPFC did not show any significant differences among the three subregions, implicating the importance of this output mode via co-modulation of pyramidal cells by both ChAT and TH fibers throughout the mPFC. However, more appositions between cholinergic and dopaminergic fibers were

found in Cg1 despite the smallest fiber density in this area, suggesting a stronger interaction between these systems in Cg1. This is consistent with a lower concentration gradient of extracellular DA in Cg1 compared to IL and dorsal PrL (Sesack et al., 1998, Heidbreder and Groenewegen, 2003). The results also put an emphasis on the relationship of pyramidal cells with cholinergic fibers in layer V of PrL and Cg1, suggesting a greater control of the output of these regions by ACh. Pharmacological evidence suggests that an increase in tonic levels of extracellular ACh mediated enhancement of arousal or readiness for input processing in operant tasks testing attention (Briand et al., 2007, Kozak et al., 2007). Since Cg1 is involved in executive functions (Thienel et al., 2009), ACh potentially plays a role in executive function by modulating DA neurotransmission in this area. Finally, the regional difference in function of the PFC could be executed via differences in their connectivity to other brain regions (Steckler et al., 1998, Gabbott et al., 2005, Vertes, 2006, Thienel et al., 2009).

Conclusion

This study has shown that the anatomical positioning between the dopaminergic and cholinergic systems in the mPFC seems to be primarily located at the level of the intracortical cells. Contrary to dopaminergic fibers, cholinergic fibers is positioned to modulate both the input and output of mPFC and influence layer V pyramidal cells through direct microproximity and influence on dopaminergic fibers. This finding might contribute to improved pharmacological

therapies for the treatment of a series of diseases such as schizophrenia, depression, drug abuse, and attention deficit disorders that are associated with improper function of the PFC.

Conflict of Interest Statement

The authors declare that the research was conducted in the absence of any commercial or financial relationships that could be construed as a potential conflict of interest.

Acknowledgments

We wish to thank Florence Dotigny for technical assistance, Jean-François Bouchard for contribution to Image analysis, Nathalie Bouchard and Kathye Aubé for their help in the maintenance of the mouse colony.

CHAPTER III

Axonal Varicosity Density as an Index of Local Neuronal Interactions

PLoS ONE 6(7): e22543. doi:10.1371/journal.pone.0022543

Zi-Wei Zhang[1,2], Jun Il Kang[1,2], Elvire Vaucher[1]

1 School of Optometry, Université de Montréal, Montréal, Quebec, Canada,

2 Department of Physiology, Université de Montréal, Montréal, Quebec, Canada

Contributions:

I contributed to the design, experiment, statistical analysis, production and revision of this article.

Dr. Elvire Vaucher supervised, and contributed to the design, experiment, statistical analysis, production and revision of this article.

Mr. Jun IL Kang contributed to the design and experiment of this article. He was in charge of the effect of the stimulation in the visual cortex.

Abstract

Diffuse transmission is an important non-synaptic communication mode in the cerebral neocortex, in which neurotransmitters released from en passant varicosities interact with surrounding cells. In a previous study we have shown that the cholinergic axonal segments which were in the microproximity with dopaminergic fibers possessed a greater density of en passant varicosities compared to more distant segments, suggesting an activity-dependent level of en passant varicosities in the axonal zone of interaction. To further evaluate this plastic relationship, the density of cholinergic varicosities was quantified on fiber segments within the microproximity of activated or non-activated pyramidal cells of the prefrontal cortex (mPFC). Repetitive 14 days patterned visual stimulation paired with an electrical stimulation of the cholinergic fibers projecting to the mPFC from the HDB was performed to induce persistent axonal plastic changes. The c-Fos early gene immunoreactivity was used as a neuronal activity marker of layer V pyramidal cells, labeled with anti-glutamate transporter EAAC1. Cholinergic fibers were labeled with anti-ChAT (choline acetyltransferase) immunostaining. The density of ChAT+ varicosities on and the length of fiber segments within the 3 μm microproximity of c-Fos positive/negative pyramidal cells were evaluated on confocal images. More than 50% of the pyramidal cells in the mPFC were c-Fos immunoreactive. Density of ChAT+ varicosities was significantly increased within 3 μm vicinity of activated pyramidal cells (0.50±0.01 per μm of ChAT+ fiber length) compared to non-activated cells in this group (0.34±0.001; $p \leq 0.05$) or control rats

(0.32±0.02; p≤0.05). Different types of stimulation (visual, HDB or visual/HDB) induced similar increase of the density of ChAT+ varicosities within microproximity of activated pyramidal cells. This study demonstrated at the subcellular level an activity-dependent enrichment of ChAT+ varicosities in the axonal zone of interaction with other neuronal elements.

Introduction

The modulation of the cortical neuronal activity by the cholinergic system is mainly exerted via diffuse transmission by acetylcholine (ACh) released from varicosities along axons (Agnati et al., 1995, Descarries et al., 1997, Descarries, 1998, Descarries and Mechawar, 2000, Vizi et al., 2004, Lendvai and Vizi, 2008, Duffy et al., 2009, Yamasaki et al., 2010). Synaptic transmission also occurs but more rarely. This diffuse transmission has been suggested in the medial prefrontal cortex (mPFC), where cholinergic neurons of the horizontal limb of the diagonal band of Broca (HDB) send long projections to its three subareas, the anterior cingulate (Cg1), the prelimbic (PrL) and the infralimbic (IL) cortex (Golmayo et al., 2003, Vertes, 2004, Tavares and Correa, 2006, Vertes, 2006, Henny and Jones, 2008). In these cortical regions, cholinergic stimulation induces modulation of pyramidal cells activity and synaptic plasticity (Golmayo et al., 2003, Henny and Jones, 2008, Sarter et al., 2009a, Hasselmo and Sarter, 2010, Parikh et al., 2010), including neuroplasticity in layer V pyramidal neurons of mPFC (Brown and Kolb, 2001), structural alteration of the pyramidal cells (Bergstrom et al., 2008), glutamatergic transmission modulation (Gil et al., 1997, Gioanni et al., 1999, Hsieh et al., 2000, Carr and Surmeier, 2007, Gulledge et al., 2009). Through this diffuse interaction with glutamatergic cells, the prefrontal cholinergic fibers play an active role in mPFC cognitive functions (Robbins et al., 1998, Zaborszky et al., 1999, Gill et al., 2000, Passetti et al., 2000, Heidbreder and Groenewegen, 2003, Dalley et

al., 2004b, Sarter et al., 2005, Sarter et al., 2006, Carr and Surmeier, 2007, Parikh and Sarter, 2008).

Recently, it has been suggested that *en passant* boutons on axonal segments are dynamic structures and their density along the axons is not uniform (Anderson and Martin, 2001, De Paola et al., 2006, Stettler et al., 2006, Zhang et al., 2010). Particularly, we have shown that the density of cholinergic and dopaminergic varicosities was significantly higher within fiber segments in reciprocal microproximity compared to more distant segments, suggesting variations in the density of varicosities could be a useful index for neuronal interaction (Zhang et al., 2010). In stationary Macky monkeys, frequent *en passant* boutons addition and elimination along collaterals were observed with *in vivo* two-photon imaging (Stettler et al., 2006), as seen for dendritic spines plasticity (Luscher et al., 2000, Muller et al., 2000). Cell type-specific rearrangements of axonal boutons were also observed in the mouse barrel cortex *in vivo* (De Paola et al., 2006).

In the present study, we hypothesized that varicosity density along the axon can be an index of localized neuronal interactions. Cholinergic varicosities on fiber segments within the vicinity of activated pyramidal cells of mPFC were examined in visually and HDB electrically stimulated rats using triple immunolabelling and confocal microscopy. The stimulation paradigm was designed to allow both post-synaptic (visual stimulation) and pre-synaptic (HDB stimulation) activation of

pyramidal cells in the mPFC which corresponds to the mode of cholinergic system functioning, i.e. enhancement of afferent sensory inputs through Hebbs-like synaptic plasticity (Kang and Vaucher, 2009a, Hasselmo and Sarter, 2010). HDB stimulation activates the cell soma of the cholinergic projections to the mPFC to modulate pyramidal cells (Livingstone et al., 2010, Thomsen et al., 2010), whereas signal induced by visual stimulation was expected to be modulated and processed by the neuronal elements in mPFC as the final step of the visual processing hierarchy (Golmayo et al., 2003, Livingstone et al., 2010). A two weeks repetitive stimulation was designed to allow structural changes correlating this consolidated neuronal network. Activation of the glutamatergic pyramidal cells was identified by a colocalization of the early gene c-Fos expression and the excitatory amino acid carrier protein 1 (EAAC1), a neuron-specific glutamate transporter (GluT) (Rothstein et al., 1994, Dotigny et al., 2008, Zhang et al., 2010). Cholinergic fibers and varicosities were labeled by choline acetyltransferase (ChAT) (Dotigny et al., 2008). Consistent with our hypothesis, significant elevation of ChAT+ varicosity density in the vicinity of c-Fos+/GluT(EAAC1)+ cells compared to those in the vicinity of c-Fos negative pyramidal cells were observed, suggesting dynamics of varicosity density as a useful index for the neuronal activity.

Methods

Animal preparation

Thirteen male Long Evans rats (300–325 g) obtained from Charles River Canada (St-Constant, Québec, Canada) were housed in a temperature-controlled room (21–25°C) under natural daylight, and had free access to food and water. All procedures were approved by the local Animal Care Committee (Comité de déontologie de l'expérimentation sur les animaux) and were conducted in accordance with the guidelines of the Canadian Council on Animal Care (protocol number: 10-133).

For chronic electrode HDB implantation, animals were anesthetized with isoflurane (induction 5%, maintain 3%) and placed in a stereotaxic apparatus. The stimulating tungsten electrode (impedance: 2 mΩ, FHC, Bowdoinham, ME, USA) denuded at each tip was implanted in the left HDB (mm from Bregma: AP -0.3, L +2.0, DV -9.0) via a hole made by a drill. The electrode was secured by dental cement. A post-operative delay of 2 days was allowed before any further experiment.

Stimulation paradigm

Awake rats were restrained and head fixed in a frame surrounded by three monitors (one in the front and two at each side, placed 21 cm away from the eyes of the rat) during 10 min for 14 days. Three groups of rats were prepared for treatment. Control group (n = 4) received no visual stimulation (grey screen) and no HDB stimulation, visually stimulated group (n = 3) received visual stimulation (sine-wave grating) only, HDB stimulated group (n = 3) received HDB electrical stimulation only, and visual/HDB stimulated group (n = 3) received both HDB electrical stimulation and visual stimulation. All 13 animals including the controls received a chronic electrode implantation. Visual training was accomplished via exposition of the animal to a sine-wave grating stimulus (orientation 30°, contrast 90%, 0.12 cycle/deg, phase converting at 1 Hz, produced by Vpixx software, v 8.5; Sentinel Medical Research Corp., Quebec, Canada) displayed on the three computer monitors (LG, luminance 37 cd/m2) for 10 minutes. HDB electrical stimulation was performed over the same 10 min period using pulses (100 Hz, 0.5 ms, 50 μA, 1 sec on/1 sec off) generated (Pulsemaster A300, WPI, Sarasota, FL) and delivered through an isolation unit (WPI 365, WPI, Sarasota, FL) through the chronically implanted electrode.

Immunocytochemistry

One week after the last stimulation, animals were anesthetised with isoflurane, and received a 20 min visual stimulation. This one week period was allowed for consolidation of the neuronal network involved during training and also for measuring discrimination performance of rats in the visual water maze task (Prusky et al., 2000, Dotigny et al., 2008, Kang and Vaucher, 2009b) (data outside of the focus of the present paper, not shown). Rats were then deeply anesthetised with pentobarbital (54 mg/kg body weight i.p.) and perfused transcardially with 4% paraformaldehyde at room temperature. After perfusion, brains were harvested, post fixed for 2 h in fresh fixative and stored in 0.1 M phosphate buffer (PBS, pH = 7.4) overnight. Serial coronal vibratome sections (35 µm thick) from mPFC (at the level of Bregma + 2.7-2.2 mm) were cut using a vibratome (Leica microsystems), collected serially in 24 wells plates (4 sections/well) in 0.1 M phosphate buffer (PBS, pH = 7.4), so the AP level of the sections could be easily identified according to their position in the plate and anatomical references. Sections were then stored in antifreeze (30% glycerol, 30% ethylene glycol, 40% NaPB 0.24 M) solution at –20°C until further use. Selected sections were thoroughly washed in 0.1 M PBS and incubated in 0.3% H_2O_2 in 0.1 M PBS for 20 min. The sections were then washed and incubated in 1.5% donkey serum in PBS-T (0.1 M phosphate buffer, pH 7.4 and 0.25% triton x-100) for 1 h for non specific sites blockade. To examine the ChAT+ varicosities in vicinity of c-Fos expressing pyramidal cells, rat brain sections were incubated in a cocktail of primary antibodies for 24 h at room temperature (Table 1): anti-ChAT (1:200; Chemicon, Billerica, MA, USA) for

cholinergic fibers; anti-c-Fos (1:10000; Oncogene Research Products, San Diego, CA, USA) for c-Fos expressing cells (Hughes and Dragunow, 1995, Herdegen and Leah, 1998, Dotigny et al., 2008) and anti-GluT(EAAC1) (1:500, Chemicon, Billerica, MA, USA) for pyramidal cells (Rothstein et al., 1994, Dotigny et al., 2008, Zhang et al., 2010). The morphology of GluT(EAAC1)+ cells was carefully examined and the analysis was made on the cells showing a clear pyramidal cell morphology. They were thus named pyramidal cells instead of GluT(EAAC1)+ cells. After washing, the sections were incubated in secondary antibodies conjugated with fluorophore FITC, CY5, TRITC (Jackson Immunoresearch, West Grove, PA, USA) for 2 h 30 (Table 1). To examine the c-Fos+ activity and the number of pyramidal cells on a larger scale, adjacent sections were double immunostained with anti-cFos and anti-GluT(EAAC1), and coupled with TRITC and FITC. Then the sections were washed and mounted onto slides with Vectashield mounting medium (Vector Laboratories, Burlingame, CA, USA).

Table 1: Combination of primary and secondary antibodies for double and triple-fluorescent staining procedures

Series	**Primary antibodies**			**Secondary antibodies**	
	Antigen	Host	Dilution	Donkey IgG	Dilution
ChAT/c-Fos/	ChAT	goat	1:200	Anti-goat-FITC	1:200
GluT(EAAC1)	c-Fos	rabbit	1:10000	Anti-rabbit-CY5	1:200
	GluT(EAAC1)	mouse	1:500	Anti-mouse-TRITC	1:200
c-Fos/	c-Fos	rabbit	1:10000	Anti-rabbit-CY5	1:200
GluT(EAAC1)	GluT(EAAC1)	mouse	1:1000	Anti-mouse-TRITC	1:200

Abbreviations: ChAT: choline acetyltransferase; GluT(EAAC1): glutamate transporter.

Confocal microscopy and quantification

Confocal microscopy offers a good means to explore into the neuroanatomical relationships in the three dimensions (x, y, z). Argon laser (excitation at 488 nm) was used for excitation of FITC, Helium Neon laser (excitation at 543 nm) was used for excitation of TRITC and Helium Neon laser (excitation at 633 nm) was used for excitation of CY5 via the Leica SP2 confocal

microscope (Leica Microsystems, Wetzlar, Germany). The pinhole size was always set at Airy One (Beam expander 3) and the zoom factor remained at 1 throughout the imaging. On the sections with triple immunostaining, Z-series of images were taken using 100× oil lens (Plan Apochromatic; Numerical aperture: 1.4) in sequential scanning mode and with an image size of 1024 x 1024 pixels for each channel and captured by Leica Confocal Software (LCS lite). Sections with c-Fos/GluT(EAAC1) double immunostaining were imaged using 40× oil lens in sequential scanning mode and with an image size of 1024 x 1024 pixels. The step size between any two consecutive optical sections was set at 1 μm. A confocal projection was a series of horizontal optical scanning sections in the same image. When a projection was generated, the sampling points of the individual images superimposed along the projection axis were examined throughout all optical sections. In a maximum projection, the maximum intensity value was displayed. On those coronal sections, the dendrites of the pyramidal cells in layer V extended toward the direction of the pial surface and sometimes spanned into upper layers. The field size of 150 μm x 150 μm was sufficient to capture the complete shape of pyramidal soma and dendrites in the XY direction. To fully capture the full shape of soma and dendrites of pyramidal cells in the Z-direction, projection images with a total depth of 3 μm instead of single optical scanning images were used for quantification. Two ROI's (Regions of Interest) were randomly chosen within each subregion of the mPFC.

Based on functional or anatomical relationship between the mPFC and BF (Golmayo et al., 2003, Vertes, 2004, Henny and Jones, 2008), Cg1, PrL and IL were analyzed. The neuronal relationships within layer V were quantified because they constitute the principal cortical output layer (Gabbott et al., 2005, Bergstrom et al., 2008). Confocal images could be confidently ascribed to layer V on the basis of the depth of the image below the surface and the characteristics of the distribution and shape of pyramidal cells. The density of ChAT+ varicosities on fiber segments within the microproximity (3 μm or less) (Zhang et al., 2010) of pyramidal cells immunoreactive or not with c-Fos in visual/HDB animals were quantified on projection images using Leica confocal software (LAS AF lite). In contrast, only the density of ChAT+ varicosities on fiber segments within the microproximity c-Fos negative pyramidal cells were examined in control animals, since 98% of the pyramidal cells were c-Fos negative (Table 2). To see if it is possible to further differentiate the major factor(s) contributing to the morphological changes of cholinergic fibers associated with local neuronal activity, the density of ChAT+ varicosities on fiber segments within the microproximity c-Fos positive pyramidal cells in HDB stimulation only group and in visual stimulation only group were also examined in layer V of IL. Considering the rapid hydrolysis of ACh by acetyl cholinesterase (Descarries et al., 1997, Descarries, 1998, Lendvai and Vizi, 2008), the present research adopted a conservative within-limit number for efficient diffuse transmission of ACh, 3 μm in three-dimensions (x, y, z axis in confocal microscopy) (Zhang et al., 2010), as a maximal sphere of concentration for ACh to induce significant effect (Chedotal et al., 1994, Vaucher and Hamel, 1995). The varicosity

density didn't vary much with different sections or animals within the same group, indicating accurate and reliable detection of varicosities. In total, ChAT+ varicosities were counted on 4931.88 μm of ChAT+ fiber segments within the vicinity of 546 pyramidal cells (259 of which being c-Fos+). The density of c-Fos+, pyramidal and c-Fos+/pyramidal cells were quantified by visual examination using photoshop CS3. Each ROI (i.e., each single projection image) covered 3 μm in depth of the tissue and corresponded to a field size of $4.3x10^5$ μm^3. Therefore, the number of c-Fos+ cells was expressed as the number per $4.3x10^5$ μm^3. In total, 3764 pyramidal cells and 4012 c-Fos+ cells were quantified on confocal images of double immunolabeling of c-Fos+ and pyramidal cells (40X, oil), within a total sampling area of 5.20×10^7 μm^3.

Table 2: Number of c-Fos+ cells and Pyramidal cells in layer V of mPFC

	Number of c-Fos+ cells	Number of Pyramidal cells	Percentage of Pyramidal cells which are c-Fos+	Percentage of c-Fos+ cells which are GluT(EAAC1)+
Visual/HDB stimulation				
Infralimbic Ctx	87±39$^{\&▲}$	30±2$^{▲}$	73$^{\&}$	25$^{▲}$
Prelimbic Ctx	80±34$^{\&▲}$	32±12	78$^{\&▲}$	31$^{▲}$
Cingulate Ctx	53±27$^{\&}$	31±5	65$^{\&}$	38$^{\&▲}$
Visual stimulation				
Infralimbic Ctx	13±6$^{■}$	39±15	9$^{*■}$	33$^{■}$
Prelimbic Ctx	8±6$^{*■}$	33±14	5$^{■}$	23$^{■}$
Cingulate Ctx	7±6$^{■}$	30±5	8$^{*■}$	51*
HDB stimulation				
Infralimbic Ctx	39±15$^{▲■Δ}$	46±8$^{▲}$	49$^{■Δ}$	59$^{▲■Δ}$
Prelimbic Ctx	37±15$^{▲■Δ}$	42±14	48$^{▲■Δ}$	60$^{▲■Δ}$
Cingulate Ctx	22±11$^{■Δ}$	38±5	35$^{■Δ}$	62$^{▲Δ}$
Control				
Infralimbic Ctx	5±3$^{\&Δ}$	38±13	2*$^{\&Δ}$	16^{Δ}
Prelimbic Ctx	2±1*$^{\&Δ}$	37±8	2$^{\&Δ}$	24^{Δ}
Cingulate Ctx	1±1$^{\&Δ}$	38±11	0*$^{\&Δ}$	0*$^{Δ\&}$

All values are means ± SEM (number of cells / $4.3x10^5$ μm^3) or percentage of colocalization of Pyramidal and c-Fos+ cells from 13 adult rats in visual/HDB stimulation group. Abbreviations: Ctx: cortex; GluT(EAAC1): glutamate transporter; HDB: horizontal limb of the diagonal band; mPFC: medial prefrontal cortex.

* $p \leq 0.05$, Mann-Whitney U test, two-tailed, group-specific difference between control and visual stimulation.

$^{\Delta}$ $p \leq 0.05$, Mann-Whitney U test, two-tailed, group-specific difference between control and HDB stimulation.

$^{\&}$ $p \leq 0.05$, Mann-Whitney U test, two-tailed, group-specific difference between control and visual/HDB stimulation.

▲ $p \leq 0.05$, Mann-Whitney U test, two-tailed, group-specific difference between visual/HDB stimulation and HDB stimulation.

▪ $p \leq 0.05$, Mann-Whitney U test, two-tailed, group-specific difference between visual stimulation and HDB stimulation.

Statistics

All the statistics in the present study were processed with SPSS (17.0). For each biological parameter investigated in this study (varicosity density, varicosity diameter, fiber segment length, c-Fos activity, percentage of c-Fos activated pyramidal cells, etc.), region-specific comparisons were carried out between any of the subregions in the mPFC in each group (Wilcoxon signed-rank test for paired samples, $p \leq 0.05$, two-tailed), and group-specific comparisons were made between any of the groups in each subregion of the mPFC (Mann-Whitney U test, $p \leq 0.05$, two-tailed).

Results

C-Fos activation of GluT (EAAC1)+ cells in layer V of the mPFC

c-Fos immunoreactivity in layer V of the mPFC was significantly greater in visual/HDB stimulation and HDB stimulation group compared to control or to visual stimulation groups (Mann-Whitney Test, $p \leq 0.05$, two-tailed, Fig. 1, Table 2, 3). It was also significantly greater in PrL and IL of visual/HDB stimulation group compared to HDB stimulation group but not in Cg1 (Table 2), suggesting that our site of HDB stimulation exerted a modulating effect on sensory processing mainly in PrL and IL instead of Cg1. c-Fos immunoreactivity in PrL was also significantly greater in visually stimulated rats compared to control rats (Mann-Whitney Test, $p \leq 0.05$, Fig. 1, Table 2, 3). There was no regional difference in the number of c-Fos+ cells (Wilcoxon signed-rank test, $p > 0.05$, two-tailed; Fig. 1, Table 2, 3).

Consequently, the proportion of c-Fos immunoreactive pyramidal cells was significantly different (Mann-Whitney Test, $p \leq 0.05$, Table 2, 3) among the four groups of rats. In visual/HDB stimulation group, the majority of the pyramidal cells were c-Fos immunoreactive (65% in Cg1, 78% in PrL, and 73% in IL) (Fig. 2, Table 2, 3). This proportion was significantly lower in HDB stimulation group (35% in Cg1, 48% in PrL and 49% in IL). Only 0 to 2% and 5 to 9% of the pyramidal cells were c-Fos immunoreactive in the mPFC from control rats and visually stimulated rats, respectively. This was significantly lower compared to either visual/HDB stimulation

group (Mann-Whitney Test, $p \leq 0.05$, Table 2, 3) or HDB stimulation group (Mann-Whitney Test, $p \leq 0.05$, Table 2, 3), suggesting the frontal cortical representation of visual stimuli was enhanced by HDB input into mPFC. No significant difference in the number of pyramidal cells in mPFC was found among the four different groups of animals (Table 2), with the exception of IL between HDB stimulation group and visual/HDB stimulation group, which could be possibly attributed to a slight overexpression of GluT(EAAC1) protein in the HDB stimulated animals – resulting in an enhanced detectability of the glutamatergic cells. No significant regional difference in the proportion of c-Fos+ pyramidal cells was found for each group (Wilcoxon signed-rank test, $p > 0.05$, two-tailed).

The proportion of c-Fos+ cells that were glutamatergic (labeled for GluT(EAAC1)) was significantly greater in HDB stimulation group (from 59 to 62%) compared to visual/HDB stimulation groups (from 25 to 38%, Mann-Whitney Test, $p \leq 0.05$, Table 2), or visual stimulation group (from 23 to 33%, Mann-Whitney Test, $p \leq 0.05$, Table 2).

Figure 1.

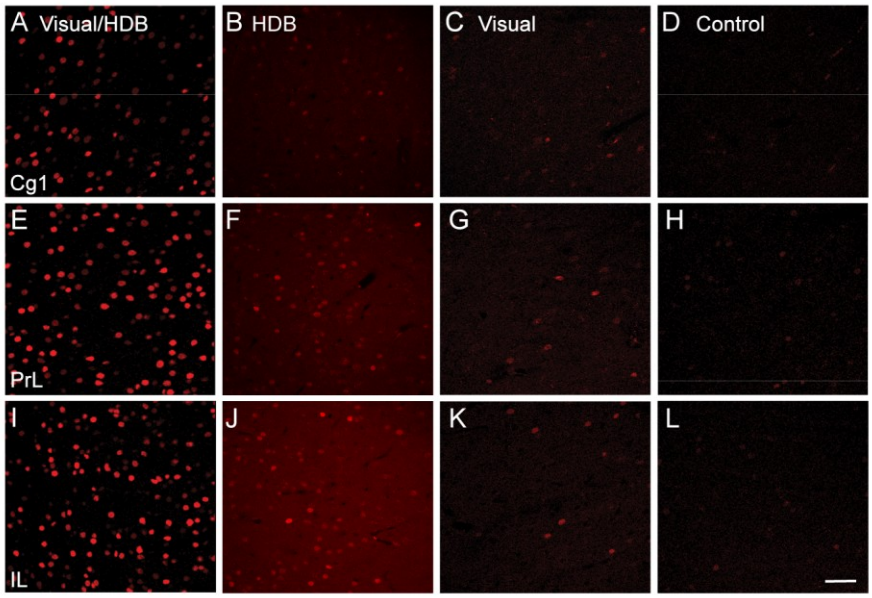

Figure 1. c-Fos immunoreactivity in layer V of the mPFC. Representative examples of c-Fos activity in layer V of Cg1 (A–C), PrL (D–F), and IL (G–I) in visual/HDB stimulated (A,D,G), visual stimulated (B,E,H) and control (C,F,I) rats. c-Fos+ cells appeared as red cores. In the visual/HDB stimulation group, there were significantly lower c-Fos+ cells in Cg1 compared to PrL or IL. There was no significant difference in c-Fos activity between PrL and IL. In all the three subregions of mPFC there was significant enhancement of c-Fos activity in visual/HDB stimulation rats compared to control or visual stimulated rats. Abbreviations: Cg1: cingulate cortex; IL: infralimbic cortex; mPFC: medial prefrontal cortex; PrL: prelimbic cortex. Scale bar: 50 μm.

Table 3. *p* values of group-specific effects.

	Control vs. Visual	Control vs. HDB	Control vs. Visual/ HDB (cFos+)	Control vs. Visual/ HDB (cFos-)	Visual vs. HDB	Visual vs. Visual/ HDB (cFos+)	HDB vs. Visual/ HDB (cFos+)	Visual/ HDB (cFos+) vs. Visual/ HDB(cFos-)
Number of cFos+ cells								
Cg1	0.077	0.034*	0.034*	—	0.050*	0.050*	0.127	—
PrL	0.034*	0.034*	0.034*	—	0.050*	0.050*	0.050*	—
IL	0.077	0.034*	0.034*	—	0.050*	0.050*	0.050*	—
Number of pyramidal cells								
Cg1	0.480	1.000	0.480	—	0.127	0.513	0.127	—
PrL	0.724	0.724	0.724	—	0.827	0.827	0.275	—
IL	0.724	0.480	0.289	—	0.376	0.513	0.050*	—
ChAT+ varicosity density								
Cg1	—	—	0.034*	0.480	—	—	—	0.050*
PrL	—	—	0.034*	1.000	—	—	—	0.050*
IL	0.032*	0.032*	0.034*	0.157	1.000	1.000	0.275	0.050*
ChAT+ varicosity diameter								
Cg1	—	—	0.724	0.289	—	—	—	0.513
PrL	—	—	0.077	0.289	—	—	—	0.827
IL	0.289	0.724	0.034*	0.034*	0.513	0.050*	0.513	0.513
ChAT+ fiber length								
Cg1	—	—	1.000	0.034*	—	—	—	0.127
PrL	—	—	0.289	0.034*	—	—	—	0.275
IL	0.034*	0.0513	0.034*	0.034*	0.513	0.275	0.827	0.275

All values are obtained *p* values of group-specific effects in the c-Fos immunoreactivity and ChAT+ varicosity density/diameter and ChAT+ fiber length within microproximity of pyramidal cells in 4 groups of rats: control, visual stimulation only, HDB stimulation only, and visual/HDB stimulation. Symbol* indicates significant *p* values (Mann-Whitney U test, $p \leq 0.05$, two-tailed).

Figure 2.

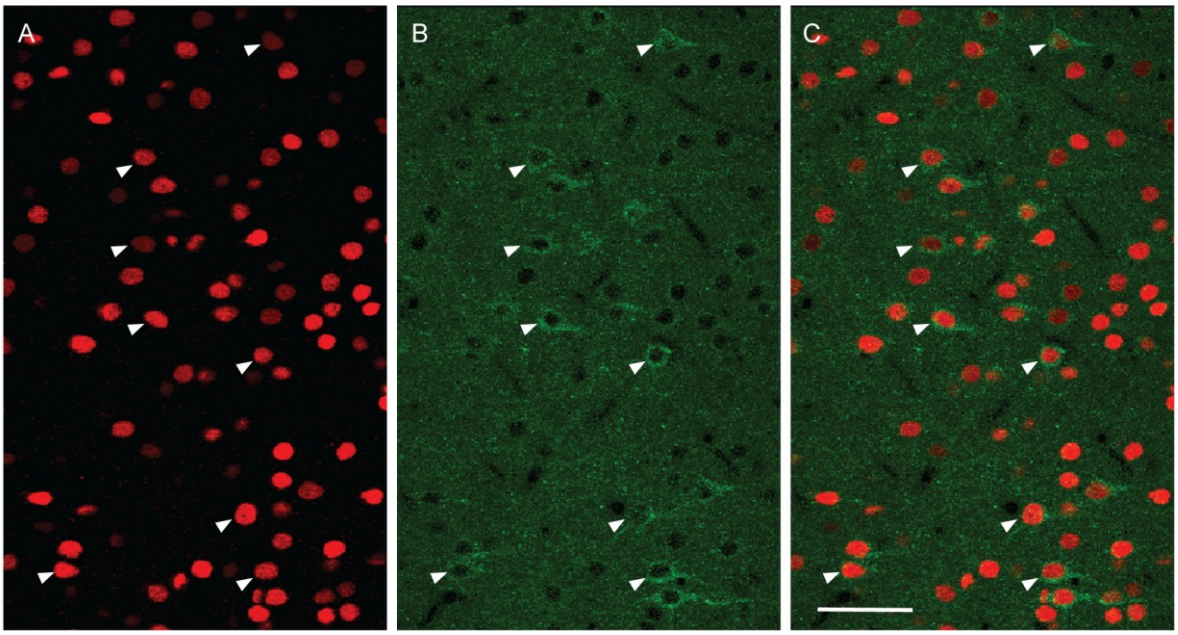

Figure 2. Colocalization of c-Fos and GluT(EAAC1) in pyramidal cells in layer V of mPFC. Representative examples of c-Fos (red, A) and GluT(EAAC1) (green, B) immunostaining and their colocalization (C) in layer V of PrL in the mPFC of visual/HDB stimulated rats. Arrowheads point to examples of colocalization of c-Fos+ cells and pyramidal cells. Note that the majority of pyramidal cells were

immunoreactive for c-Fos, whereas only a small proportion of c-Fos+ cells were stained for GluT(EAAC1). Abbreviations: ChAT: choline acetyltransferase; GluT(EAAC1): glutamate transporter; mPFC: medial prefrontal cortex; PrL: prelimbic cortex. Scale bar: 50 μm.

Activation-dependent elevation of the density of ChAT+ varicosities in layer V of the mPFC

In layer V of the mPFC of visual/HDB stimulation group, a higher density of ChAT+ varicosities was found on axonal fiber segments within the vicinity (3 μm or less) of c-Fos+ pyramidal cells compared to those within the vicinity of non-activated pyramidal cells in visual/HDB stimulation or control group, suggesting a localized activity-dependent enrichment of ChAT+ varicosities (Mann-Whitney Test, $p \leq 0.05$, two-tailed, Fig. 3, 4, Table 3, 4). No significant difference was found in the ChAT+ varicosity density within the proximity of non-activated pyramidal cells between visual/HDB stimulation group and control group in all three subareas (Mann-Whitney Test, $p = 0.034$, two-tailed, Table 3, 4, Fig. 4), indicating the increase of ChAT+ varicosity density within the proximity of c-Fos+ pyramidal cells in visual/HDB stimulation group was indeed due to relevant neuronal activity. In the control group, all the quantification was done on c-Fos negative pyramidal cells, since 98% of the pyramidal cells were c-Fos negative (Table 2).

In layer V of IL a higher density of ChAT+ varicosities was found on axonal fiber segments within the vicinity of c-Fos+ pyramidal cells of both visual stimulation group (0.47 ± 0.03 per μm of ChAT+ fiber length) and HDB stimulation group (0.45 ± 0.04 per μm of ChAT+ fiber length) compared to those within the vicinity of c-Fos negative pyramidal cells in control group (0.31 ± 0.03 per μm of ChAT+ fiber length, Mann-Whitney Test, $p = 0.032$, two-tailed, Fig. 3, Table 3, 4), suggesting either visual stimulation alone or HDB stimulation alone could induce localized activity-dependent enrichment of ChAT+ varicosities in the mPFC. The increase of the ChAT+ varicosity density within the microproximity of c-Fos+ pyramidal cells was about the same level in these groups as in visual/HDB stimulation group, since no statistical difference was found between these groups (Mann-Whitney Test, $p > 0.05$, two-tailed, Fig. 3, Table 3, 5).

Figure 3.

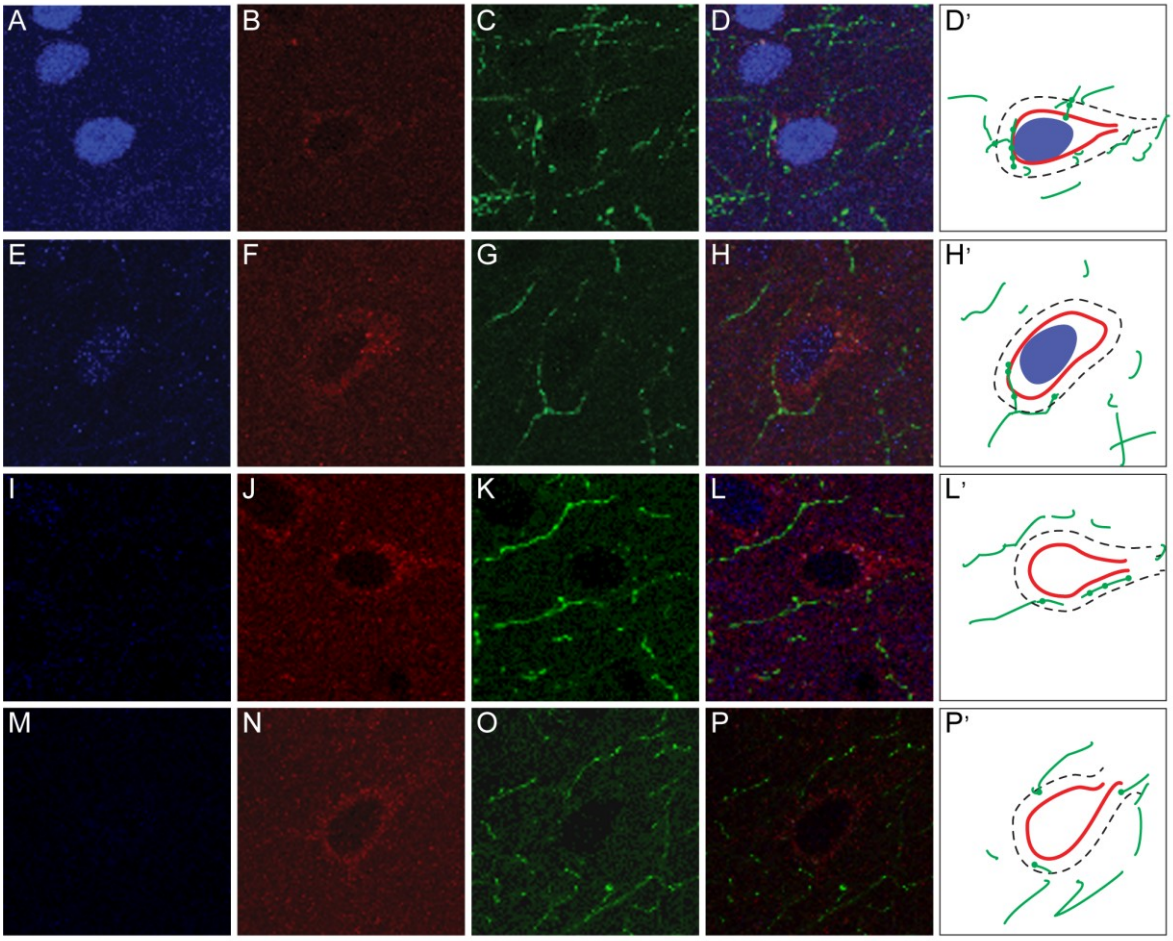

Figure 3. Evaluation of ChAT+ varicosity density on fiber segments within microproximity of activated or nonactivated pyramidal cells. Representative examples of projection images of triple immunostaining for c-Fos (blue), GluT(EAAC1) (red) and ChAT (green) in layer V of the mPFC (A–P) of ChAT+ varicosity in microproximity of activated pyramidal cells in visual/HDB stimulation group, visual stimulation only group, and HDB stimulation only group (the three top panels), and for ChAT+ varicosity in microproximity of nonactivated pyramidal cells in the visual/HDB stimulation group and the control group (the bottom two panels) D',H',L',P', T': Drawing of ChAT+ fibers (green lines) within 3 μm microproximity (dashed line) of c-Fos+ pyramidal cells (red perimeter with a blue nucleus) or non-activated pyramidal cells (red perimeter without blue nucleus) in layer V of the mPFC. Representative images were taken from IL and PrL. ChAT+ varicosities (illustrated by dots on the green ChAT+ fibers) were quantified on fiber segments within 3 μm microproximity of pyramidal cells. Note that an increased density of varicosities was seen in segments in microproximity of activated cells compared to non-activated cells. Abbreviations: ChAT: choline acetyltransferase; GluT(EAAC1): glutamate transporter; Cg1: cingulate cortex; IL: infralimbic cortex; mPFC: medial prefrontal cortex; PrL: prelimbic cortex. Scale bar: 10 μm.

Figure 4.

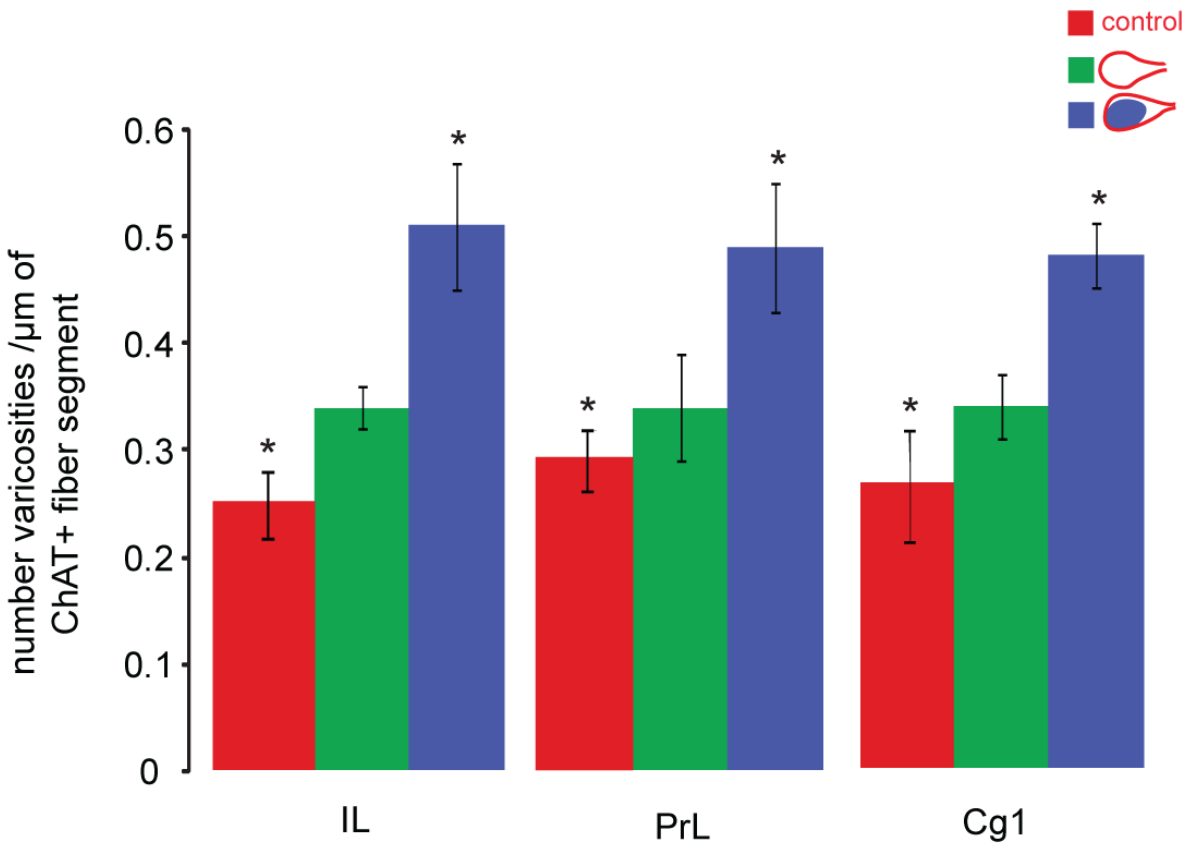

Figure 4. ChAT+ varicosities density on fiber segments within microproximity of activated or nonactivated pyramidal cells. Within the visual/HDB stimulation group, the density of ChAT+ varicosities on fiber segments within microproximity of nonactivated cells (green bars) was lower than on fiber segments within microproximity of activated pyramidal cells (blue bars) in layer V of every subregion of mPFC investigated. In contrast, the density of ChAT+ varicosities fiber segments within microproximity of nonactivated cells in the control group (red bars) was not significantly different from those within microproximity of nonactivated cells in the

visual/HDB stimulation group, but significantly lower than those within microproximity of activated pyramidal cells in the visual/HDB stimulation. Symbol * indicate significant difference in the density of ChAT+ varicosities on fiber segments within microproximity of activated pyramidal cells compared to those within microproximity of nonactivated pyramidal cells ($p \leq 0.05$, Mann-Whitney U test, two-tailed). Abbreviations: Cg1: cingulate cortex; ChAT: choline acetyltransferase; IL: infralimbic cortex; PrL: prelimbic cortex.

Table 4. Density and diameter of ChAT+ varicosities and length of ChAT+ fiber segments within microproximity of Pyramidal cells in Layer V of mPFC.

	IL	PrL	Cg1
Visual/HDB stimulation			
Microproximity with c-Fos+ pyramidal cells			
Density of ChAT+ varicosities	0.51±0.06*&	0.49±0.06*&	0.48±0.03*&
Diameter of ChAT+ varicosities(nm)	608±10&	602±14	601±28
ChAT+ fiber length(μm)	9.9±1.1	9.7±1.5	9.4±2.2*
Microproximity with non-activated pyramidal cells			
Density of ChAT+ varicosities	0.34±0.02*	0.34±0.05*	0.34±0.03*
Diameter of ChAT+ varicosities(nm)	626±36▲	598±24	608±20
ChAT+ fiber length(μm)	9.1±0.9▲	8.3±0.6▲	7.1±0.4▲
Control			
Microproximity with non-activated pyramidal cells			
Density of ChAT+ varicosities	0.31±0.03&+‡	0.34±0.02&	0.32±0.04&
Diameter of ChAT+ varicosities(nm)	581±6&▲	580±16	596±15
ChAT+ fiber length(μm)	12.9±1.1▲+	10.9±0.9▲	10.1±0.7▲

All values are means ± SEM in visual/HDB stimulation rats and control rats. Density of ChAT+ varicosities is expressed in number of varicosities / μm of ChAT+

fiber segment. Diameter of ChAT+ varicosities is expressed in nm. ChAT+ fiber length is expressed in μm. Abbreviations: Cg1: cingulate cortex; ChAT: choline acetyltransferase; IL: infralimbic cortex; PrL: prelimbic cortex; GluT(EAAC1): glutamate transporter; HDB: horizontal limb of the diagonal band; mPFC: medial prefrontal cortex.

* $p \leq 0.05$, Mann-Whitney U test, two-tailed, comparing microproximity of Pyramidal /c-Fos+ cells to microproximity of Pyramidal cells not immunoreactive to c-Fos within visual/HDB stimulation group.

& $p \leq 0.05$, Mann-Whitney U test, two-tailed, comparing microproximity of Pyramidal /c-Fos+ cells in visual/HDB stimulation group to microproximity of Pyramidal cells not immunoreactive to c-Fos in control group.

▲ $p \leq 0.05$, Mann-Whitney U test, two-tailed, comparing microproximity of Pyramidal cells not immunoreactive to c-Fos in visual/HDB stimulation group to control group.

+ $p \leq 0.05$, Mann-Whitney U test, two-tailed, comparing microproximity of Pyramidal /c-Fos+ cells in visual stimulation group to microproximity of Pyramidal cells not immunoreactive to c-Fos in control group.

ǂ $p \leq 0.05$, Mann-Whitney U test, two-tailed, comparing microproximity of Pyramidal /c-Fos+ cells in HDB stimulation group to microproximity of Pyramidal cells not immunoreactive to c-Fos in control group.

Table 5. Density and diameter of ChAT+ varicosities and length of ChAT+ fiber segments within microproximity of activated pyramidal cells in Layer V of IL.

IL	Visual stimulation	HDB stimulation	Visual/HDB stimulation
Microproximity with c-Fos+ pyramidal cells			
Density of ChAT+ varicosities	0.47±0.03*	0.45±0.04*	0.51±0.06*
Diameter of ChAT + varicosities (nm)	578±21	598±27	608±10*
ChAT+ fiber length (μm)	9.3±1.6*	10.2±1.4	9.9±1.1

All values are means ± SEM in 3 groups of rats: visual stimulation only, HDB stimulation only, and visual/HDB stimulation. No statistical significance was found among these 3 groups regarding ChAT+ varicosity density, diameter or fiber length ($p > 0.05$, Mann-Whitney U test, two-tailed). Density of ChAT+ varicosities is expressed in number of varicosities / μm of ChAT+ fiber segment. Diameter of ChAT+ varicosities is expressed in nm. ChAT+ fiber length is expressed in μm. Abbreviations: ChAT: choline acetyltransferase; IL: infralimbic cortex; HDB: horizontal limb of the diagonal band.

* $p \leq 0.05$, Mann-Whitney U test, two-tailed, comparing microproximity of Pyramidal /c-Fos+ cells to microproximity of Pyramidal cells not immunoreactive to c-Fos in control group.

Diameter of ChAT+ varicosities in layer V of the mPFC

The diameter of ChAT+ varicosities within the vicinity of c-Fos+ pyramidal cells or pyramidal cells of IL in visual/HDB stimulation group were significantly bigger than those within the vicinity of pyramidal cells of IL in control group and in visual group, which could suggest more modulation from HDB in IL compared to PrL and Cg1 (Mann-Whitney Test, $p \leq 0.05$, two-tailed, Table 3, 4).

No regional difference among Cg1, PrL, and IL was found for each parameter (Wilcoxon signed-rank test, $p > 0.05$, two-tailed).

Longer ChAT+ fiber segment within microproximity of c-Fos+ pyramidal cells in layer V of Cg1

ChAT+ fiber segments within the microproximity of c-Fos+ pyramidal cells in control group were significantly longer than those within the microproximity of c-Fos activated pyramidal cells in Layer V of IL in visual/HDB stimulation group (Mann-Whitney Test, $p = 0.034$, two-tailed, Table 3, 4), indicating that enhanced varicosity density within the vicinity of c-Fos activated pyramidal cells was not due to longer fiber length. ChAT+ fiber segments within the microproximity of pyramidal cells in mPFC in control animals were significantly longer than those within the

microproximity of pyramidal cells in visual/HDB stimulation group (Mann-Whitney Test, $p = 0.034$, two-tailed, Table 3, 4).

No significant regional difference was found among the three subareas regarding ChAT+ fiber length in the vicinity of pyramidal cells in visual/HDB stimulation group (Wilcoxon signed-rank test, $p > 0.05$, two-tailed).

Discussion

The primary interest of the current study was to verify whether the density of axonal varicosities in a specific axonal segment was related to the level of local neuronal activity. To this purpose, segments of ChAT+ fibers stimulated repetitively were analyzed in relation to their vicinity to mPFC pyramidal cells expressing or not the early gene c-Fos. The results show different level of modulation of mPFC pyramidal cells by visual and HDB cholinergic inputs. Significant elevation of the density of ChAT+ varicosities within the microproximity of c-Fos+ pyramidal cells compared to those within the microproximity of nonactivated cells was demonstrated. This suggests dynamics of the varicosities along the axon relatively to local neuronal interaction.

Activity-dependent modulation of pyramidal cells by HDB input in layer V of mPFC

5 to 9% of the pyramidal cells were c-Fos immunoreactive in the mPFC of visually stimulated rats which was significantly more than in control groups. They were significantly lower when compared either with visual/HDB stimulation group (70%) or HDB stimulation alone (50%) group, suggesting the strong c-Fos activation in the mPFC cortex was mainly due to HDB stimulation. The c-Fos activation of the pyramidal cells in the mPFC by visual stimulation alone was most probably due to post-synaptic activation brought upon by visual sensory input into the PFC from associational sensory cortices (Ongur and Price, 2000, Kim et al., 2003, Fenske et al., 2006), as already reported (Ricciardi et al., 2009, Greenberg et al., 2010, Majeed et al., 2011). The strong c-Fos+ immunoreactivity elicited by HDB stimulation, most likely resulted from direct HDB projections to the mPFC cells and local fibers (Laplante et al., 2005). Such strong c-Fos activation after acute basal forebrain stimulation has already been reported in fronto-parietal cortex of rats (Kocharyan et al., 2008). Moreover, the pairing of visual and HDB stimulation induced significantly higher c-Fos immunoreactivity in mPFC than either visual stimulation alone or HDB stimulation alone, suggesting a potentiation of mPFC pyramidal cells response to sensory stimuli by cholinergic projections, as shown in other cortical areas (Ricciardi et al., 2009, Greenberg et al., 2010). Thus, the c-Fos activation of pyramidal cells in the mPFC in visual/HDB stimulation rats represented a combination of both sensory and cholinergic activation, with HDB

stimulation contributing more than visual stimulation itself. The frontal cortical representation of visual stimuli was thus primarily enhanced by HDB input into mPFC (Dotigny et al., 2008, Thomsen et al., 2010), both of which were suggested as part of cognitive mechanism (Sarter et al., 2003, Weidner et al., 2009). Our results were consistent with the assumed role of cortical projecting cholinergic system from basal forebrain in facilitating extrinsic sensory stimuli (Sarter et al., 2006, Burk et al., 2008, Deiana et al., 2010). Visual stimulation paired with HDB stimulation enhanced c-Fos+ activity on a large scale, indicating the potential role of HDB as an important relay station in enhancing frontal cortical representation of visual stimuli, consistent with basal forebrain's role in enhancement of cognitive functions (Zaborszky et al., 1999, Zaborszky and Duque, 2000, Ramanathan et al., 2009).

In HDB stimulation group, about 60% of c-Fos+ cells were glutamatergic. It has been found that most pyramidal cells (78 – 90%) in layer V of the mPFC were within the proximity of cholinergic fibers (Zhang et al., 2010), suggesting a conjoint activation of the pyramidal cells by sensory or associative afferents and cholinergic projections. The majority (65-78%) of the pyramidal cells of layer V were c-Fos+ in visual/HDB stimulated rats, consistent with the well-documented importance of pyramidal cells in cognition in the frontal cortex (Spruston, 2008, Arnsten, 2009, Goldwater et al., 2009, Stahl, 2009, Lopez-Gil et al.). Our study was focused on the cholinergic input from the HDB, but it should be noted that GABAergic or glutamatergic projections from the HDB (Henny and Jones, 2008) could also have

contributed to the c-Fos signal in mPFC. As well, only a moderate proportion of c-Fos+ cells (40% in Cg1, 32% in PrL, and 29% in IL) were pyramidal cells in visual/HDB stimulation group, which might suggest the activation of other phenotypes of intracortical neurons (Wang et al., 2010).

Dynamics of varicosities as an index of localized neuronal activity

The density of ChAT+ varicosities within the vicinity of c-Fos+ activated pyramidal cells in visual/HDB stimulation group was significantly elevated compared to those within the vicinity of non-activated pyramidal cells either in visual/HDB stimulation group or in control group, a piece of evidence supporting the modulation of the pyramidal cell activity by HDB projections into the mPFC, and thus varicosity density being a good index for local neuronal activity. Consistently, no significant difference was found in the ChAT+ varicosity density within the microproximity of non-activated pyramidal cells between visual/HDB stimulation group and control group, indicating the increase of varicosity density within the microproximity of activated pyramidal cells in visual/HDB stimulation group was indeed due to relevant neuronal activity. Dendritic arbors of the pyramidal cell could not be visualized with our GluT(EAAC1) antibody, but it might be possible that this microproximity relationship includes axo-dendritic interactions since dendrites are filled of cholinergic receptors. It is probable that the c-Fos expression by pyramidal cells was induced by ACh, as c-Fos is not expressed in cholinergic lesioned animals in visual cortex (Dotigny et al., 2008). However, as the c-Fos

expression was maintained even one week after the last HDB stimulation, we suggest that there was also some backward crosstalk from the pyramidal cell to the cholinergic fibers. This crosstalk could involve local factors released from activated mPFC neurons, such as potassium, glutamate, neurotrophins which could maintain the state of activation of the cholinergic fibers. This is complementary to previous results suggesting that local neurons are able to induce ACh release from the cholinergic fiber terminals (Laplante et al., 2005, Parikh et al., 2008). Also, recurrent collaterals from the pyramidal cells might influence local cholinergic fibers. Stimulation paradigm is another factor which could affect the formation of new varicosities, such as the type, intensity and duration of the stimuli (Lendvai et al., 2000, De Paola et al., 2003, Nikonenko et al., 2003), as well as the age of the animals (Lendvai et al., 2000).

In order to elucidate whether the change in ChAT+ varicosity density was due to local factors or intrinsic axonal properties, the enrichment of ChAT+ varicosities in microproximity of c-Fos+ pyramidal cells in IL was quantified in visual stimulation alone or HDB stimulation alone conditions. In both cases, the density of ChAT varicosities was equivalent to the one in the visual/HDB group. This suggests both types of stimulation could contribute to the dynamics of ChAT+ varicosities and thus varicosities dynamics were due to interaction with local neurons rather than activation of the fiber *per se*. This is consistent with the fact that activation of HDB fibers did not result in increased varicosity density in microproximity to the non-activated pyramidal cells. Thus, it seems that different

types of stimuli could induce the same level of varicosity enrichment, which should be investigated further.

Our previous findings demonstrated significant elevation of ChAT+ and tyrosine hydroxylase+ varicosities on fiber segments within reciprocal microproximity of each other in the mPFC of normal adult rats (Zhang et al., 2010), sustaining ACh/DA interaction evidences in this cortex. The present study verified that dynamics of ChAT+ varicosity density was related to the level of activity of pyramidal cells in the mPFC at a subcellular level, suggesting that the density of varicosity can be used as an index for local neuronal interaction (Fig. 5). Such plastic structural changes are extensively described in the dendritic arbor of pyramidal cells, where the dynamic and number of dendritic spines is modulated by local neuronal activity. In case of dendritic spines, repetitive activation of the synapses reinforces the strength of post and presynaptic elements and lead to duplication of the synapse (Larkum et al., 2004, Shu et al., 2007, Spruston, 2008) to favor improved postsynaptic activation.

Figure 5.

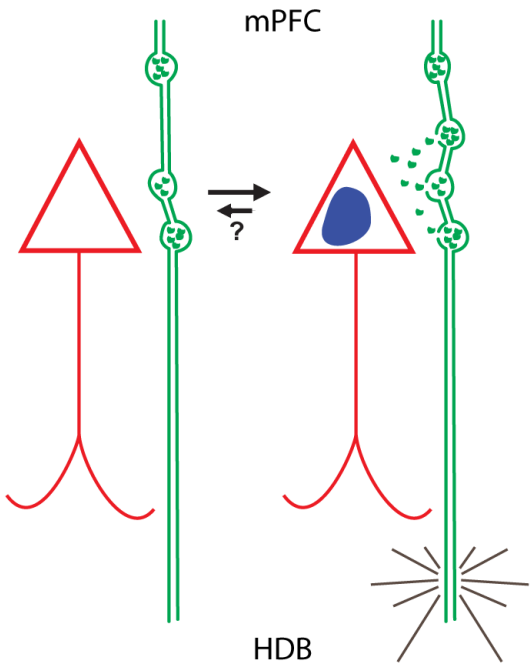

Figure 5. Schematic illustration of hypothetic duplication of the *en passant* varicosities due to repetitive neuronal activation. Repetitive activation (grey lines) of the cholinergic neurons in HDB could lead to induction of c-Fos (blue core) activation of pyramidal cells (red triangle) in mPFC and duplication of the cholinergic varicosities on their projecting fibers in vicinity of activated pyramidal cells. Whether this gain of varicosities is reversible remains to be determined (question mark). Abbreviations: HDB: horizontal limb of the diagonal band; mPFC: medial prefrontal cortex.

As well, recent studies suggest that varicosities spacing patterns seems regulated according to synaptic plasticity (Shepherd et al., 2002, Stettler et al., 2006) although some other studies propose that varicosities on axons from cortical neurons are formed and spaced in a regulated manner (Sabo et al., 2006). Varicosities on CA3-CA1 axonal shafts were found to be spaced non-uniformly along the axons. On short scales, varicosity spacing was found to be highly variable but not random (Shepherd and Harris, 1998, Shepherd et al., 2002). As well, synaptic boutons gain and loss were observed in adult visual cortex (Stettler et al., 2006). The higher density of ChAT+ varicosities on fiber segments innervating c-Fos+ activated pyramidal cells corroborate these previous hypotheses and link the density of varicosities to neuronal activity. Appearing of new *en passant* varicosities might be either due to formation de novo or mobilization of previously existing ones to new sites as fast as 1-2 h after stimulation as shown for presynaptic axonal terminals (Friedman et al., 2000, Colicos et al., 2001), and may be correlated to the turnover of other neuronal elements in the same microenvironment (Trachtenberg et al., 2002). We suggest that duplication of the *en passant* varicosities could happen in repetitive neuronal activation (Fig. 5). Whether this gain of varicosities is reversible remains to be determined, but previous studies tend to suggest it (Stettler et al., 2006). The length of the fiber segment sharing the microproximity with the activated cells was elevated in Cg1 of visually/HDB stimulated animals, suggesting that the surface of interaction between the fiber and the pyramidal cell increases after repetitive interaction. This increase of surface interaction and number of varicosity would

result in increased ACh diffusion and putatively increased cholinergic transmission efficiency, which is consistent with our previous findings of more appositions between cholinergic and dopaminergic fibers in Cg1 despite its smallest fiber density compared to PrL and IL of mPFC (Zhang et al., 2010). In contrast, the diameter of the ChAT+ varicosities did not vary significantly, which suggests these structural changes were not due to increased number of vesicles in the varicosity before it splits but rather to formation of a distinct swelling along the axon. However, no regional difference was found suggesting that the fiber/neuron interaction is similar in all the mPFC subregion examined.

Conclusion

Investigating the local variation in the density of varicosities is a useful tool to visualize at a subcellular level plastic changes induced by functional interaction between neuronal systems and better understand the specificity of the neuronal network.

CHAPTER IV

Cholinergic depletion in nucleus accumbens impairs working memory and mesocortical dopamine function in rats.

François Laplante[1]*, Zi-Wei Zhang[2], Marc M. Dufresne[3], Elvire Vaucher[2] and Ron M Sullivan[1].

[1]Dept. Psychiatry, McGill University, Montréal QC, Canada
[2]School of optometry, Université de Montréal, Montréal QC, Canada
[3]Council of Canadian Academies, Ottawa ON, Canada

Contributions:

I contribute to the experiment, statistical analysis and production of the examination on TH varicosities in this article.

Dr. François Laplante contributed to the design, experiment, statistical analysis and production of this article.

Mr. Marc Dufresne contributed to reagents/materials/analysis tools.

Dr. Elvire Vaucher supervised my work and contributed to the data analysis of this article.

Dr. Ron M Sullivan contributed to the design, data analysis and production of this article.

Abstract

In rats, selective depletion of cholinergic interneurons in the ventral striatum (nucleus accumbens or N.Acc.) results in a heightened behavioural sensitivity to amphetamine and impaired sensorimotor gating processes, suggesting a hyper-responsiveness to dopamine (DA) activation in the N.Acc. We hypothesized that local cholinergic depletion may also trigger more widespread functional alterations, particularly in prefrontal cortex (PFC). Adult male Sprague-Dawley rats were injected bilaterally in the N.Acc. with an immunotoxin targeting choline acetyltransferase (ChAT). Two weeks later, they were trained and tested for working memory performance using the delayed alternation paradigm in the T-maze. The same animals were subsequently implanted with voltammetric recording electrodes in the ventromedial PFC to measure *in vivo* extracellular DA release in response to mild tail pinch stress. The PFC was also examined for density of tyrosine hydroxylase (TH)-labelled varicosities. In parallel, we also measured *post-mortem* tissue content of dopamine in another cohort of control and lesioned rats.

Anti-ChAT lesioned rats showed significant impairments in working memory performance across delay intervals and demonstrated significant reductions in mesocortical DA activation which correlated with cognitive (memory) impairments. TH-labelled varicosities were also reduced in cortical layer V relative to controls. The basal prefrontal cortical level of DA was not significantly affected. These data

suggest that local and selective depletion of cholinergic interneurons in N.Acc. triggers widespread functional alterations in mesocorticolimbic DA systems, including cognitive processes known to be under cortical DA regulation. The functional relevance of ventral striatal cholinergic deficits for schizophrenic symptomatology is discussed.

Key words: Schizophrenia, Animal model, Immunohistochemistry, Saporin, Ventral striatum, In vivo voltammetry.

Introduction

The ventral striatum or nucleus accumbens (N.Acc.) is a convergence zone for an abundance of limbic and prefrontal inputs of vital importance in the execution of a variety of adaptive behaviours (Brog et al., 1993;Goto and Grace, 2008;Groenewegen et al., 1999;Sesack and Grace, 2010;Wright and Groenewegen, 1995). Mesolimbic dopamine (DA) neurons originating in the ventral tegmental area (VTA) interact anatomically and functionally with cholinergic interneurons of the N.Acc. to modulate the activities of GABAergic medium-sized spiny neurons (Di *et al*., 1994), which provide outputs to motor circuits for the execution of behaviour, and provide feedback to the DA cell body region of the VTA (Berendse et al., 1992;Heimer et al., 1991;Usuda et al., 1998;Zahm and Heimer, 1990).

Acetylcholine (ACh) regulates N.Acc. circuits in a manner seemingly opposite to DA, possibly by dampening the effect of excessive DA release (Hoebel *et al*., 2007), and a delicate balance between striatal DA and ACh activity is required for optimal functioning (Aosaki et al., 2010;Hikida et al., 2003;McGeer and McGeer, 1977). Using a novel cholinergic immunotoxin approach, we have shown that local and selective reduction in the number of cholinergic neurons in N.Acc. greatly enhances the behavioural activating effects of amphetamine (Laplante et al., 2011). The same lesions disrupted sensorimotor gating processes (impaired

prepulse inhibition of the acoustic startle response), an effect reversed by the DA antagonist haloperidol. Both the behavioural hyper-responsiveness and sensorimotor gating deficits are consistent with proposed roles of DA in the N.Acc. (Messier et al., 1992;Swerdlow et al., 1990).

Reduced cholinergic function in N.Acc. may be especially relevant for schizophrenia, since studies of *post mortem* schizophrenic brains reported a significant loss of cholinergic cells, selective to the ventral striatum (Holt et al., 1999;Holt et al., 2005). Given that schizophrenia is also characterized by hypo-functional prefrontal DAergic activity and prefrontally mediated working memory deficits (Goldman-Rakic, 1994;Grace, 1991;Weinberger, 1987), our purpose was to examine whether local N.Acc. cholinergic depletion could induce similar deficits in rats. In other words, could this local, subcortical manipulation cause functional alterations in prefrontal cortical circuitry.

To this end, we first measured post-mortem brain tissue content of ACh and DA and relevant metabolites in PFC and N.Acc. Secondly, we compared lesioned and control rats in a working memory task (delayed alternation in T-maze) and in the ability to activate the mesocortical DA system, as measured by the *in vivo* release of extracellular PFC DA in response to a mildly activating stressor. We also wanted to know if potential lesion-induced changes in PFC DA activation and working memory performance were correlated. Additionally, we examined immunoreactivity for tyrosine hydroxylase (TH) in PFC as further evidence of

possible functional changes in the mesocortical DA system following N.Acc. cholinergic depletion.

Materials and methods

Adult male Sprague-Dawley rats (250-275 g) were obtained from Charles River (St-Constant QC) and housed in pairs with food and water *ad libitum* in a temperature- and humidity-controlled room with a 12-h light/dark cycle. Experiments were carried out in accordance with the Canadian Council on Animal Care Guidelines and approved by our local ethics committee for animal experimentation.

Lesion of cholinergic neurons

As previously described (Laplante et al., 2011) rats were anesthetised with isoflurane 5% for induction and 3-4 % for maintenance in an oxygen flow of 0.6 l/min with a Labvet apparatus (Dispomed Ltd, Joliette QC) and secured into a stereotaxic frame. A 33 gauge needle was lowered into the N.Acc. at the coordinates: AP + 1.6 mm; ML $\pm$ 1.4 from bregma; DV – 7.5 from dura (Paxinos and Watson, 1982). A saporin-based IgG immunotoxin targeting choline acetyltransferase (ChAT; Advanced Targeting Systems Inc, San Diego CA; cat No IT-42) was administered bilaterally (0.5 μl per side, 0.5 μg/μl in PBS) at a flow rate of 0.1 μl/min for 5 min (n = 12 rats), allowing an additional five minutes for diffusion.

Because saporin is a ribosome-inactivating protein that has to be internalised to exert its toxicity (Stirpe et al., 1983), controls (n = 11) received the same amount/volume of saporin coupled to a rabbit IgG antibody (Advanced Targeting Systems Inc, cat No IT-35) with no ability to target neurons. Rats were sutured and returned to their home cage for a minimum of two weeks.

Delayed alternation testing of working memory

Delayed alternation testing was performed as previously described (Aultman and Moghaddam, 2001, Lipska et al., 2002) with modifications. The dimensions of the central arm of the T-maze, constructed with grey PVC, were 50 × 12 × 33 cm and 40 × 12 × 33 cm for each lateral arm, which were equipped with a sliding door. There was a 2 cm diameter hole at the end of each lateral arm (1 cm deep to conceal food from view). Food reward consisted of a piece of Kellogg's Froot Loops cereal.

After three days of initial handling (5 min/day), rats were habituated to the maze for 8-10 days and were food restricted to 15 g/day throughout all phases of testing. For the first three days of habituation, rats were exposed to the T-maze for a 15 min exploration with the doors raised and food available in both arms. Subsequently, animals were exposed to 10 forced-alternation trials (one arm closed) per day until they would consistently run to the ends of the open arms for food (5-7 days).

Then delayed alternation training began. After a randomly chosen forced run into a baited arm and a 10 s delay interval in the holding cage, the animal was placed back in the central arm with access to both arms but with bait only in the arm opposite to that entered in the previous forced run. Upon entering a choice arm, that door was closed. Rats received ten trials (forced run–delayed choice) per day, with a 20 s inter-trial interval. Random arm sequences were used which included five forced runs to each of the right (R) and left (L) arms (e.g., R-R-L-R-L-L-R-L-R-L). A different sequence was used each day, but sequences were the same for all rats. The maze was cleaned with 70% alcohol between rats.

Testing began for three additional days and was conducted similarly, but using three different delay intervals (1-2, 10 or 40 s). On each of the three test days, rats received 8 trials at each delay interval in random sequence (24 trials/day). Data are expressed as percentage of correct choices. After completion of testing, rats were again fed *ad libitum*.

In vivo voltammetry (chronoamperommetry)

One week following working memory testing, each rat underwent stereotaxic implantation (anesthesia as above) of a voltammetric recording electrode, optimized for the detection of DA. Electrode construction, calibration and recording parameters are similar to earlier studies (Stevenson et al., 2003, Laplante et al., 2005, Zhang et al., 2005). Each electrochemical probe consisted of three 30µm-diameter carbon fibers (Avco Specialty Materials, Lowell, MA) extending 50–100

μm beyond the epoxy-sealed tip of a pulled glass capillary. The fibers were coated with a 5% solution of the ion exchange polymer Nafion (Aldrich, Milwaukee, WI), promoting the exchange of cations like DA and repelling anions like ascorbic acid (AA) and 3,4-dihydroxyphenylacetic acid (DOPAC). Prior to implantation, electrodes were calibrated in 0.1 M PBS, pH 7.4, containing 250 μM AA to determine sensitivity and selectivity for DA against AA. All electrodes used had DA/AA selectivity ratios >1000:1 and a highly linear response ($r > 0.997$) to increasing concentrations of DA. Recording electrodes were implanted in the DA-rich terminal area of the ventromedial PFC of the right hemisphere at the following coordinates: AP + 3.2 mm (re. Bregma); ML + 0.8 and DV - 4.2 mm (dura). Rats were also implanted with a Ag/AgCl reference electrode in the posterior cortical surface. Miniature pin connectors soldered to the voltammetric and reference electrodes were inserted into a Carleton connector (Ginder Scientific, Ottawa ON). This assembly was then secured with acrylic dental cement to three stainless steel screws threaded into the cranium.

Stress testing

Four days after surgery, rats were placed in specially constructed voltametric testing chambers (40 x 40 x 75 cm high) and the rats implants were connected to a headstage attached via shielded cable to a swivel at the top of the chamber, in turn linked to a computer-controlled chronoamperometric control box (FAST, Quanteon, Lexington, KY). Rats were habituated to the test chamber for 60 min, which allowed the DA dependent signal to reach a stable baseline. A mild tail

pinch stress (5 min) was then initiated by placing a rubber-coated metal clip approximately an inch from the tip of the tail, with sufficient pressure that the rat could not shake it off. Recordings continued an additional 60 min after removal of the clip to ensure that stress-induced elevations in extracellular DA returned to baseline. The primary measure of interest was the peak or maximal increase in DA concentration relative to pre-stress baseline. Data points for DA levels were plotted at 5 min intervals over the session. A second identical test was conducted the following day to examine potential group differences in either habituation or sensitization of stress-induced DA activation.

Electrochemical recordings and data format.

An oxidative potential of +0.55 mV, with respect to the reference electrode, was applied to the electrode for 100 ms at 5 Hz. The amplitude of the resulting oxidation current was digitized and integrated over the last 80 ms of each pulse. Every 10 digitized current measures were summed, displayed on a video monitor at 2 s intervals, and converted to molar equivalent DA concentration based on the *in vitro* calibration factor for each electrode. The reduction current generated when the potential was set to 0.0 mV for 100 ms was similarly digitized and summed. With these conditions, the magnitude of the reduction current in response to increases in DA is typically 60–80% that of the oxidation current (Red/Ox ratio = 0.6-0.8). In contrast, the oxidation of AA is nearly irreversible (Red/Ox ≈ 0) and DOPAC almost completely reversible (0.9-1.0), while norepinephrine (NE) and

serotonin (5-hydroxytryptophan; 5-HT) are 0.4-0.5 and 0.1-0.3, respectively (Gratton et al., 1989, Doherty and Gratton, 1992, 1996).

As electrodes are individually calibrated *in vitro* with a DA standard, *in vivo* increases in oxidation current are expressed as μM (or nM) DA equivalents relative to the signal reference point at the onset of stress. This technique does not quantify an absolute baseline value or concentration of DA (pre-stress), rather the change in concentration as a function of stress.

It must be noted that particularly in PFC, there may be a minor contribution of NE to the "DA-dependent" signal, although we believe this to be minimal. First, all recordings in the study had Red/Ox ratios in the 0.55-0.75 range, characteristic of DA. With the same technique and location in ventromedial PFC (where DA innervation is quite dense), stress-induced "DA" increases are pronounced, whereas slightly more dorsally where there is less DA, but similar amounts of NE, the stress response is greatly diminished (Doherty and Gratton, 1996). In the same study, the selective DA reuptake blocker GBR 12909 markedly increased the stress-induced signal increases in the ventromedial regions. Finally, the electrodes themselves are 3-4 times more sensitive (*in vitro*) to the same concentration of DA as NE (personal observations). Nonetheless, a possible contribution of NE to our recorded signal should still be considered when we refer to the DA response.

Perfusion and immunohistochemistry

For complete details about tissue preparation, see Laplante et al. (2011). Rats were anesthetised with urethane (1.3 g/kg i.p., 0.25g/ml) and perfused transcardially with 0.9% NaCl (100 ml), followed by 700 ml of ice-cold 4% paraformaldehyde in 0.1 M sodium tetraborate buffer (pH 9.5). Brain coronal sections were cut at 30 µm in four one-in-four series throughout the extent of the PFC and N.Acc. Two series were immunostained for ChAT and tyrosine hydroxylase (TH) and one series was stained with thionin to confirm electrode placements in PFC.

Brain sections were incubated with the primary antibody goat anti-ChAT 1:2000 or rabbit anti-TH 1:1000 (Chemicon, Temecula CA) in KPBS with 0.3% triton X-100, 2% rabbit or goat serum for 48 h at 4º C. The primary antibodies were respectively detected using biotinylated rabbit anti-goat and goat anti-rabbit immunoglobulins (Vector Laboratories, Burlingame CA) 1:200 with avidin-DH-biotinylated horseradish peroxidase-H-complex (Vectastain Elite ABC kit, Vector Laboratories) and diaminobenzidine (DAB) reaction product was developed using glucose oxidase method with nickel enhancement.

Quantification

The number of ChAT-positive neurons throughout the N.Acc. (15-18 sections examined per rat) was quantified as previously detailed (Laplante et al., 2011). To confirm whether the cholinergic cell loss was restricted to the N.Acc., we

quantified the density of ChAT expressing neurons in two brain structures adjacent to the injection site: the diagonal band and the dorsal striatum. Images of these regions were acquired with a CX41 microscope (Olympus, Markham, ON) equipped with an Infinity 2 camera (Lumenera Corporation, Ottawa ON). For the analysis, the most anterior sections of the diagonal band have been selected because of their closest proximity to the injection sites. Regarding the dorsal striatum, we selected sections at the level of the injection sites. The cell counting and surface measurement were performed with Image J software (National Institute of Health, Bethesda, MD). The analysis was performed on the entire surface of the diagonal band, but for the dorsal striatum the measurements were done in a 0.5 mm wide strip along the border with the N.Acc.

Quantification of TH-labelled varicosities was carried out as previously described (Zhang et al., 2010, Zhang et al., 2011). Measurements were done in layer V of the ventromedial prefrontal cortex due to its high density of DA nerve terminals and the involvement of this cortical layer in the pathological states of schizophrenia (Black et al., 2004). Two sections at the level of medial PFC (2.7 mm anterior to Bregma) were examined per animal. In total, 84 photographs from 21 rats were acquired with a Leica DC 500 digital camera (Leica Microsystems, Herrbrugg, Switzerland), 40X lens (oil) and exported to Adobe Photoshop for further quantification. Each image corresponded to a field size of 0.09 mm2 (0.34 mm x 0.27 mm), and 7.71 mm2 of cortical area, 0.1 mm above the ventral border of the infralimbic cortex and the second at 0.2 mm above toward the dorsal border

of infralimbic cortex. Quantification of the number of TH varicosities (ellipsoid swellings, usually with darker staining) on fiber segments in the plane of focus were carried out on microphotographs (Figure 7). The fibers (1 pixel thick line) and varicosities were reproduced and sharpened on another optical layer using Photoshop CS3 and the length was quantified on Image J (Rasband, 1997-2009). In total, 274.51 mm of TH fiber segments were evaluated.

Post mortem tissue neurotransmitter levels.

In a second experimental cohort, lesioned and control animals (12 per group) were sacrificed two weeks post-surgery by decapitation following rapid isoflurane anesthesia and brains were quickly removed and dissected on ice. Tissue sampling was performed as described previously (Duchesne et al., 2009) with slight modification. Although the main region of interest was the N.Acc (core and shell), the neighbouring dorsal striatum (caudate and putamen), PFC (infralimbic and prelimbic) were also investigated. Tissue samples for the left and right hemispheres were obtained using a 2mm diameter stainless steel punch and rapidly frozen at −80 ºC for later neurochemical analysis. Brain samples were thawed, weighed and sonicated in 500 µl of 0.12M perchloric acid. Homogenates were centrifuged at 13,000 g for 5 min and pellet was kept for western blot analysis whereas supernatants were filtered through 22 µm microcentrifuge filters (Fisher Sci.) for neurotransmitter quantification.

To determine the tissue content of ACh from the filtered supernatant, 50 µl were injected into an ESA Coulochem III high pressure liquid chromatography (HPLC) system-equipped separating column with post column enzymatic reaction and electrochemical detection (Day et al., 2001). ACh was separated from other molecules by an ACH-250 (ESA Inc, Chelmsford MA) column (250 × 3.2 mm). From this column, the eluate then passed through an ACH-SPR enzyme reactor (ESA) containing acetylcholinesterase (AChE; EC 3.1.1.7) and choline oxidase (EC 1.1.3.17). The separated ACh and choline react with the enzymes to give stoichiometric yield of hydrogen peroxide, which is electrochemically detected with an analytical cell, model 5040 equipped with platinum electrode at a potential of +300 mV. As recommended by the manufacturer, the mobile phase consist of a 100 mM aqueous sodium phosphate buffer, pH 8.0, containing 2 mM 1-octanesulfonic acid sodium salt and 0.005% of reagent MB (provided by ESA) and is delivered at 0.35 ml/min by a dual piston pump (1525U; Waters, Milford MA) and is degassed online. With these conditions, ACh elutes at ~8.5 minutes. Sample concentrations were calculated by comparison with known standards. ACh tissue levels are expressed as pmol/mg wet tissue weight.

To quantify the catecholamines, 10 µl from the filtered supernatant were injected into an ESA Coulochem III high performance liquid chromatography system with electrochemical detection (HPLC-EC). Mobile phase and HPLC parameters were as previously described (Duchesne et al., 2009). The concentration of DA and its major metabolite DOPAC were computed based on

calibration curves with known amounts of standards. Tissue levels were expressed as pg/mg wet tissue weight. Levels of 5-HT and its metabolite 5-hydroxyindoleacetic acid (5-HIAA) were also assessed. (Levels of norepinephrine and homovanillic acid were not easily quantified with the present protocol).

Statistical analysis

For the quantification of ChAT immunoreactive neurons and the quantification of neurotransmitters and their metabolites, two-way repeated-measures analysis of variance (ANOVA) was conducted for the analysis of the main effect of experimental groups (lesion effect) and brain hemisphere as repeated-measures factor, and interaction between these two factors. Regarding TH-labelled varicosities, significant differences between experimental groups were determined by independent t-tests. For the first ten days of working memory testing, a two-way (ANOVA) was conducted with "lesion" as independent factor and "day" as repeated measures factor. On each of the three subsequent test days, similar ANOVAs were conducted with "delay interval" as the repeated measure. Voltammetry data for each day were presented and analysed as (5 min) time samples with repeated measures. The mean peak (maximal) DA responses were analysed with "day" as repeated measure. Post hoc Bonferonni tests were conducted following significant interactions. In addition, Pearson analyses were performed to examine correlations between DA responses and working memory performance within groups.

Results

Cholinergic cell loss in N. Acc.

Immunohistochemistry findings demonstrated that infusion of the anti-ChAT IgGsaporin toxin resulted in a mean reduction of 72 % in the number of neurons expressing ChAT within the N.Acc. relative to the rabbit IgG-saporin controls (Figure 1; $F(1,21) = 65.32$; $p < 0.0001$ for main effect of lesion). Depletion of cholinergic neurons was present in both core and shell of the N.Acc. but was restricted to this brain region as no reduction in ChAT neurons was observed in the diagonal band (Figure 2A; $F(1,21) = 0.58$; $p = 0.45$ for main effect of lesion) or the dorsal striatum (Figure 2B; $F(1,21) = 2.53$; $p = 0.13$ for main effect of lesion).

Figure 1

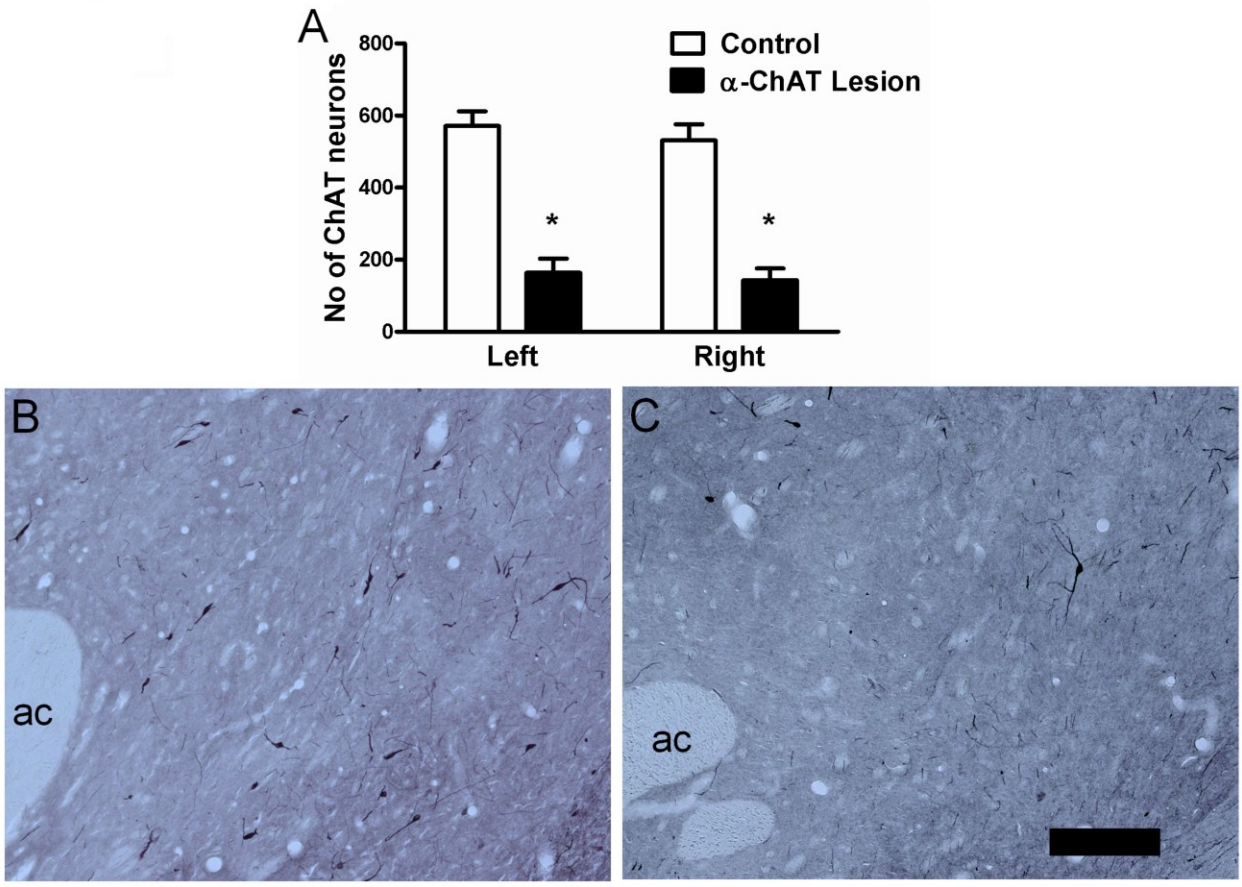

Figure 1: A) ChAT-expressing cells counted bilaterally throughout the extent of the N.Acc. Data represent mean ± SEM, (n = 11-12 in each group). Post-hoc analysis revealed significant differences between control and lesioned groups in both hemispheres (* $p < 0.001$). B) Representative sections of ChAT-immunostained tissues of N.Acc. from rabbit IgG-saporin-treated control rats and C) anti-ChAT IgG-saporin-treated rats. Scale = 200 μm. ac: anterior commissure.

Figure 2

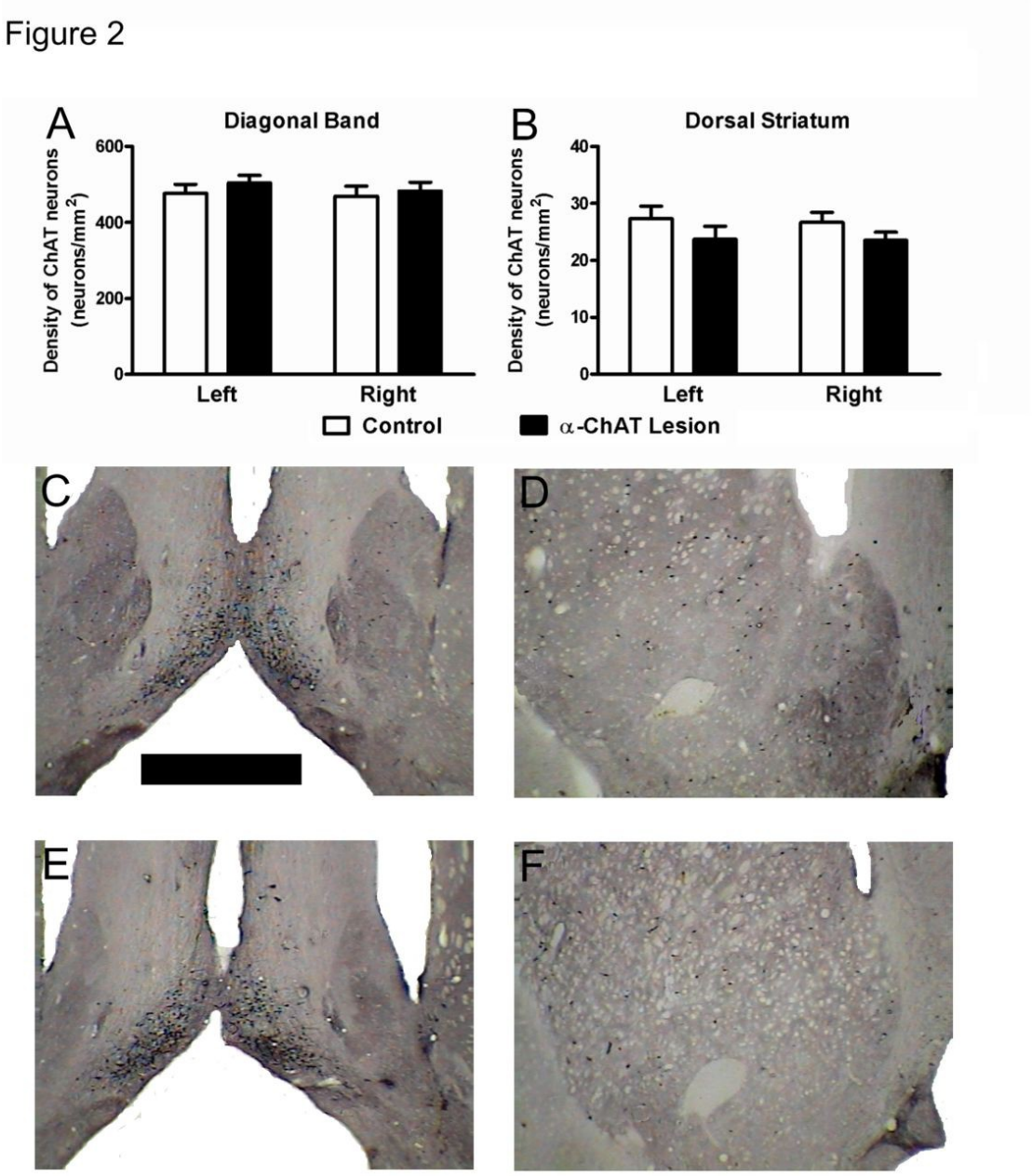

Figure 2: Density of ChAT immunolabelled cells in the left and right sides of the A) diagonal band and B) dorsal striatum. Data represent mean ± SEM, (n = 11-12 in each group). No significant differences were found between control and lesioned groups in either of these adjacent brain regions, confirming the selectivity of lesions

in the N.Acc. Representative sections of ChAT-immunostained tissues of the diagonal band of a control (C) and lesioned rat (E) and dorsal striatum control (D) and lesion (F). Scale = 1 mm

Delayed alternation performance in the T-maze

During the ten days of delayed alternation testing (10 s delays), a significant main effect of lesion was observed ($F(1,189) = 11.85$, $p = 0.0024$), with anti-ChAT lesioned rats showing a consistently lower percentage of correct choices than controls, which achieved greater than 90% correct responding by day 3 (Figure 3). A main effect of day was also seen ($F(9,189) = 4.73$, $p < 0.0001$) reflecting the general improvement in performance, and there was no significant interaction between lesion and day ($F(9,189) = 1.08$, $p = 0.377$).

Figure 3

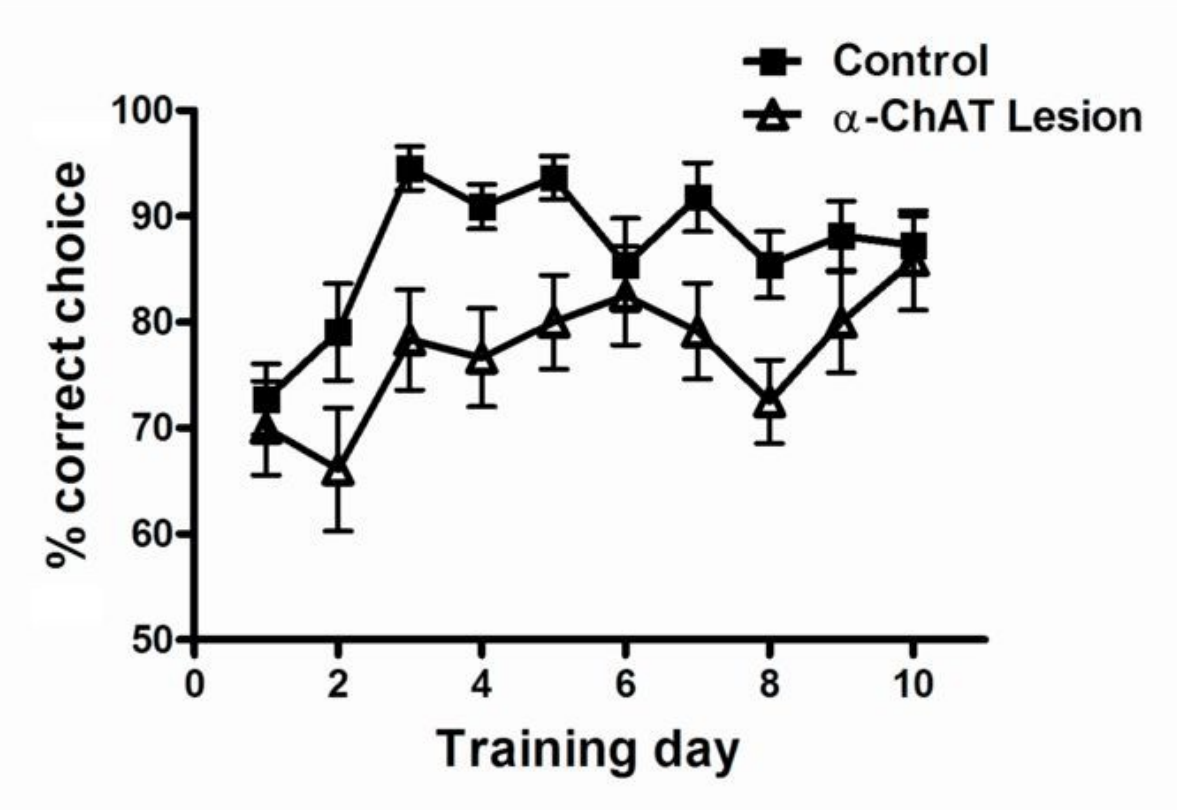

Figure 3: Performance in the T-maze for delayed-alternation training over ten consecutive days. Each rat was given 10 trials a day with an inter-trial delay of 10 s. Data are expressed as percent of correct choices and represent means ± SEM (n = 11-12). Anti-ChAT lesioned rats showed significant impairments across the training period. See text for statistical details.

Figure 4 shows the effects of lesions on working memory with different delay intervals. On day 1, controls outperformed lesioned rats across delays (lesion effect, $F(1,42) = 8.30$, $p = 0.009$). A main effect of delay ($F(2,42) = 3.60$, $p = 0.036$)

reflected the greater difficulty inherent with longer delays and there was no lesion x delay interaction ($F(2,42) = 0.91$, $p = 0.41$). Day 2 however, did not reveal a significant lesion effect ($F(1,42) = 0.32$, $p = 0.58$), as controls performed somewhat more poorly than usual, especially at short delays. The delay effect just failed to reach significance as well ($F(2,42) = 2.97$, $p = 0.062$) and the lesion x delay interaction was not significant ($F(2,42) = 0.40$, $p = 0.67$). Day 3 showed the same pattern as day 1 with significant effects of lesion ($F(1,42) = 6.73$, $p = 0.017$) and delay ($F(2,42) = 10.29$, $p = 0.0002$), but no interaction ($F(2,42) = 0.51$, $p = 0.60$). Taken together, lesioned animals showed substantial impairment in performance of the delayed alternation task.

Figure 4

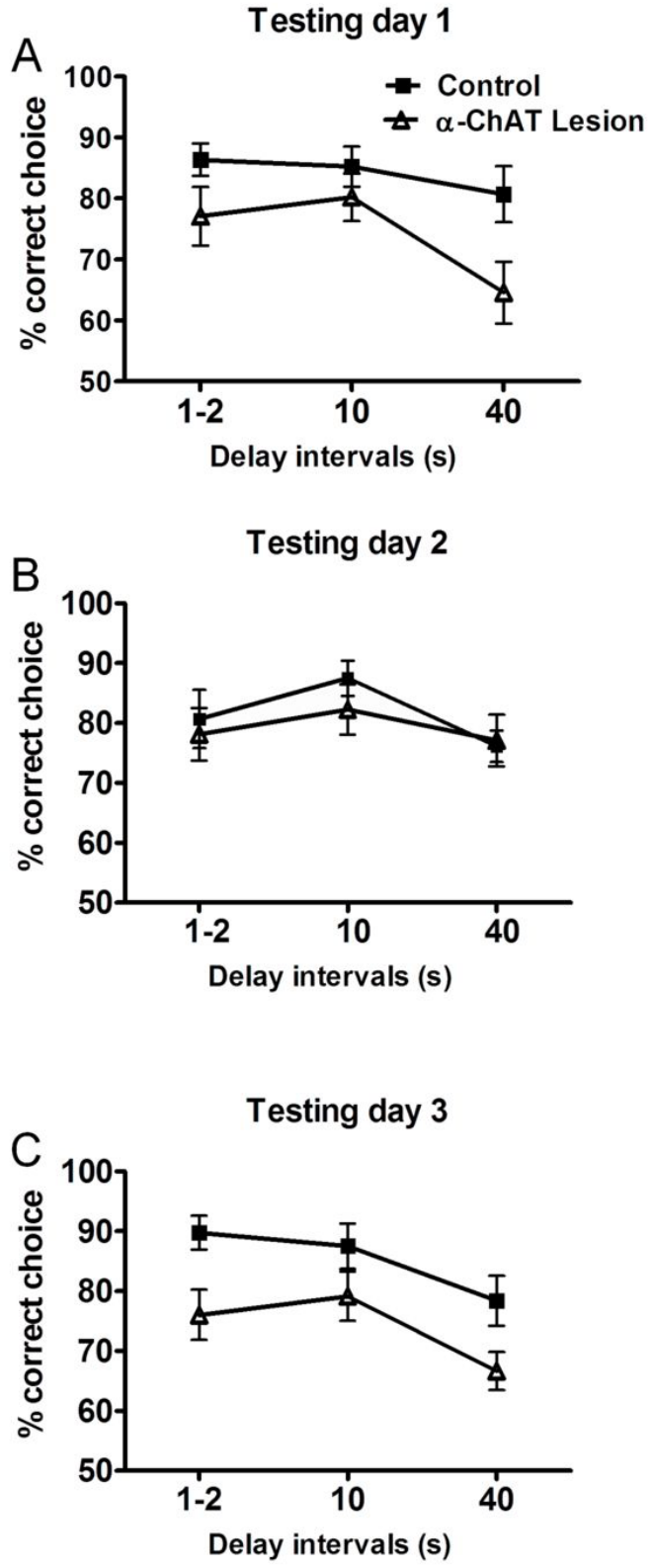
A
Testing day 1
Control
α-ChAT Lesion
% correct choice
100
90
80
70
60
50
1-2
10
40
Delay intervals (s)
B
Testing day 2
% correct choice
100
90
80
70
60
50
1-2
10
40
Delay intervals (s)
C
Testing day 3
% correct choice
100
90
80
70
60
50
1-2
10
40
Delay intervals (s)

Figure 4: Percent of correct choice during testing sessions for three consecutive days using three different delay periods within each day, A to C respectively. Data represent means ± SEM (n = 11-12). Lesioned rats were particularly impaired across delays on the first and third days of testing. See text for statistical details.

In vivo voltammetry

Three rats (2 controls, 1 lesion) were excluded from this analysis for defective or misplaced electrodes. Stress-induced increases in extracellular DA in PFC are shown in Figure 5. On the first stress test (Figure 5B), anti-ChAT lesioned rats showed significantly smaller increases in cortical DA release than controls ($F(1,216) = 4.93$, $p = 0.0394$). There were also significant effects of time ($F(12,216) = 20.95$, $p < 0.0001$) and lesion x time interaction ($F(12,216) = 2.92$, $p = 0.0009$). The group difference was especially pronounced at 5 minutes (around the time of the peak response). A similar pattern was seen on the second stress test (Figure 5C), although the main effect of lesion just missed significance ($F(1,216) = 3.99$, $p = 0.0612$). Significant effects of time ($F(12,216) = 15.97$, $p < 0.0001$) and lesion x time interaction ($F(12,216) = 1.89$, $p = 0.0369$) were again observed, with the greatest group difference seen at the 10 min point. On both days, mean DA elevations were greater in controls than lesions from the first time point at 5 minutes after stress onset until 45 minutes. Figure 5D shows the mean peaks DA responses, which typically occur for individual rats between 5 and 15 minutes from stress onset (actual data is collected every 2 s). A main effect of lesion was again

seen ($F(1,18) = 6.75$, $p = 0.018$) with no effect for days (repeated measure; $F(1,18) = 0.67$, $p = 0.42$) or lesion x day interaction ($F(1,18) = 0.23$, $p = 0.63$). Thus, anti-ChAT lesioned rats showed consistently lower levels of DAergic activation relative to controls, and neither group sensitized nor habituated to the stressor on second exposure.

Figure 5

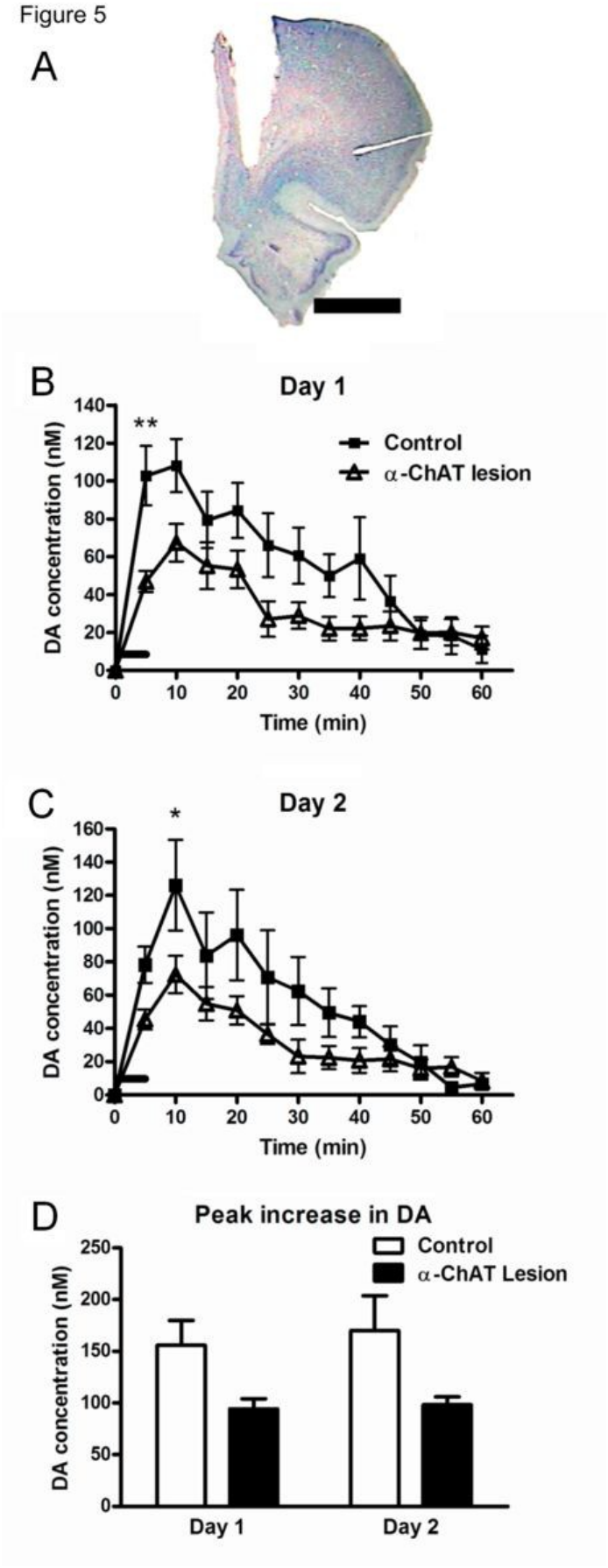
A
B
Day 1
**
Control
α-ChAT lesion
DA concentration (nM)
Time (min)
C
Day 2
*
DA concentration (nM)
Time (min)
D
Peak increase in DA
Control
α-ChAT Lesion
DA concentration (nM)
Day 1
Day 2

Figure 5: A) Histological representation of a coronal section of a rat brain stained with thionin demonstrating the location of the voltammetric recording electrode in the ventromedial prefrontal cortex (scale = 2 mm; the notch in the right lateral side is an intentional mark to identify the right hemisphere). All acceptable placements were located within the deep layers (4-6) of infralimbic or ventral prelimbic cortex. Extracellular DA release in the PFC of rats in response to 5 min tail pinch stress (black bar) on two consecutive days (B and C). Data are expressed as changes in electrochemical signal (nM DA equivalent) relative to pre-stress baseline (time 0). Anti-ChAT lesioned rats showed significant impairments in the ability to mount a mesocortical DA response to mild stress. See text for statistical details (*$p < 0.05$; **$p < 0.01$). D) Mean peak stress-induced increases in extracellular DA release. Data represent means ± SEM (n = 9-11).

Correlations with cognitive performance

As a measure of presumed working memory in the delayed alternation task, we averaged the performance on all trials with 40 s delays of the last 3 days of testing as this represents the greatest challenge to working memory. We then averaged the peak DA responses on both stress exposures. These variables were significantly correlated as shown in Figure 6, within the lesioned group ($r(11) = 0.629$, $p = 0.038$), but not controls ($r(9) = 0.238$, $p = 0.54$). This means that rats with the greatest deficits in mesocortical DA activation also showed the greatest impairments in cognitive function.

Figure 6

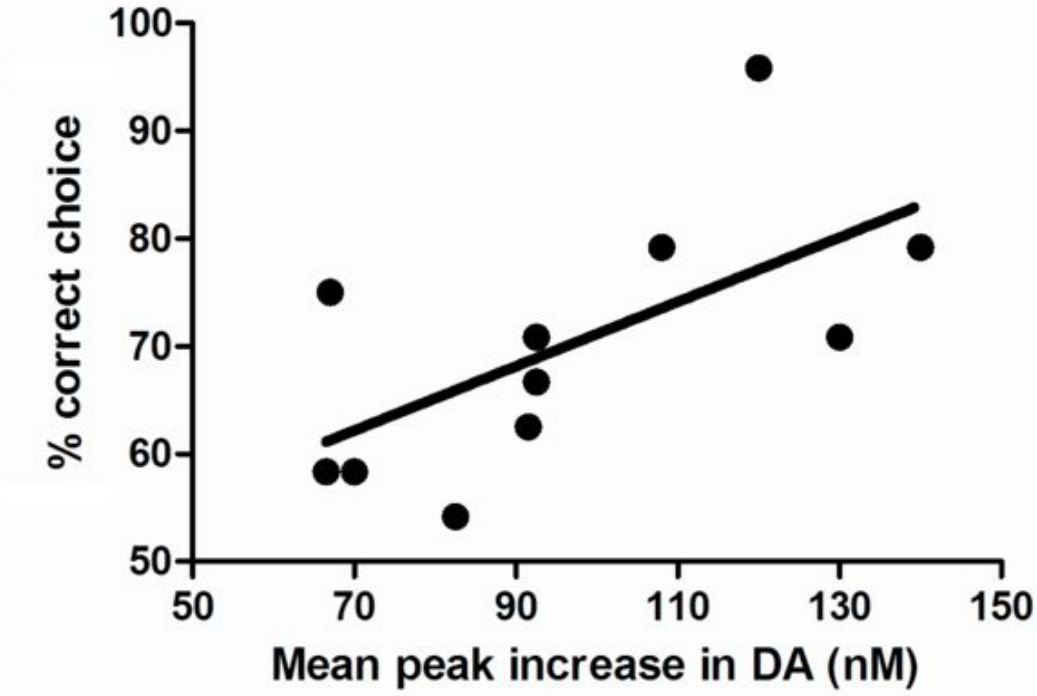

Figure 6: Working memory and mesocortical DA activation in anti-ChAT lesioned rats. Memory performance (based on 40 s delays) was significantly correlated with the degree of DAergic activation, measured separately in response to mild stress ($p = 0.038$). This suggests that cognitive impairments in rats with N.Acc. cholinergic depletion may be dependent on deficits in mesocortical DA function.

PFC tyrosine hydroxylase (TH) labelling

Layer V of infralimbic cortex was prominently innervated by TH fibers (Figure 7). These fibers were diffusedly distributed and constantly bore varicosities which appeared as ellipsoid swellings with darker staining compared to fiber segments devoid of varicosities. The density of TH varicosities was significantly decreased (11.2 %) in the lesioned rats compared to controls ($T(19) = 2.83$, $p = 0.011$). Fiber segment length also tended to be shorter in lesioned rats (2.79 ± 0.24 mm/0.09 mm2) than controls (3.79 ± 0.61 mm/0.09 mm2), but this was not significant ($T(19) = 1.58$, $p = 0.13$), indicating the variation in the density of TH varicosities was not solely due to variation in fiber length.

Figure 7

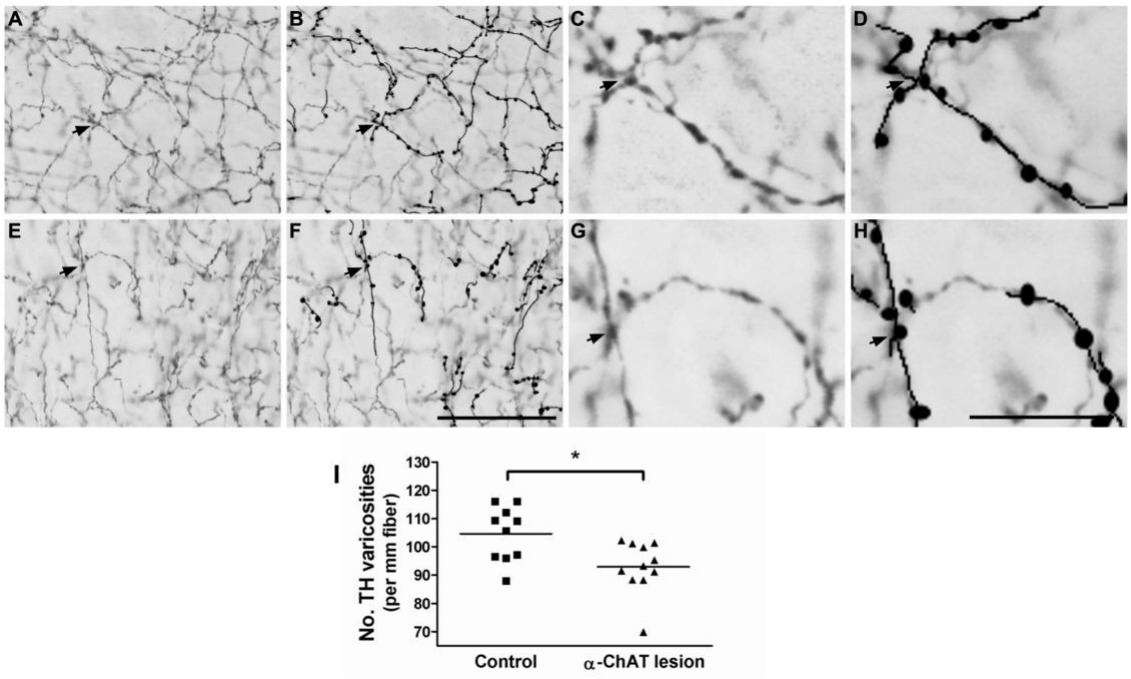

Figure 7: Quantification of TH varicosity density on fiber segments in layer V of IL cortex in control (A-D) and lesioned (E-H) animals. Microphotographs were taken

and then analyzed using Photoshop. The varicosities on fiber segments are indicated by the black dots (B, D, F, H). A decreased density of varicosities was seen in segments of lesioned animals. Scale bar: 50 μm (A, B, E, F); 10 μm (C, D, G, H). The density of TH varicosities on fiber segments in layer V (I) was lower in lesioned animals compared to controls (* $p = 0.011$). Horizontal lines represent means for each group.

Quantification of neurotransmitters in brain tissue

In our second cohort of animals, the micro-injection of the anti-ChAT IgG-saporin toxin into the N. Acc resulted in an average 33.6 % reduction in the tissue level of ACh in this area relative to controls (Figure 8A $F(1,22) = 19.17$, $p = 0.001$ for the main effect of lesion). On the other hand, the level of ACh was not affected in the ventromedial PFC, nor in the adjacent dorsal striatum (Figure 8B,C). Thus the effects of the neurotoxic injection into accumbens only affected ACh levels locally, without affecting adjacent structures, confirming again the localization of lesion effects on cholinergic function. In the N.Acc, although there is an apparent decrease in the levels of both DA and DOPAC in lesioned animals (see Table I), these trends did not reach statistical significance (for the main effect of lesion DA: $F(1,22) = 2.71$, $p = 0.11$ DOPAC: $F(1,22) = 1.81$, $p = 0.19$). In the dorsal striatum (Table II), the DOPAC/DA ratio was found to be lower in lesion rats compared to controls ($F(1,22) = 5.56$, $p = 0.028$ for the main effect of lesion). This appears to be the combined result of slightly lower DOPAC levels and slightly higher DA levels in

the lesioned group, although individually non-significant. In the PFC (Table III), no DAergic measures of basal tissue content were significantly altered as a function of N.Acc. cholinergic lesions (although serotonin turnover did appear to be slightly affected by lesions, $F(1,22) = 5.12$, $p = 0.034$). Therefore, in terms of basal tissue measures of DAergic systems, cholinergic depletion in N.Acc. appears to have somewhat greater effects on subcortical regions than on the mesocortical DA system.

Figure 8

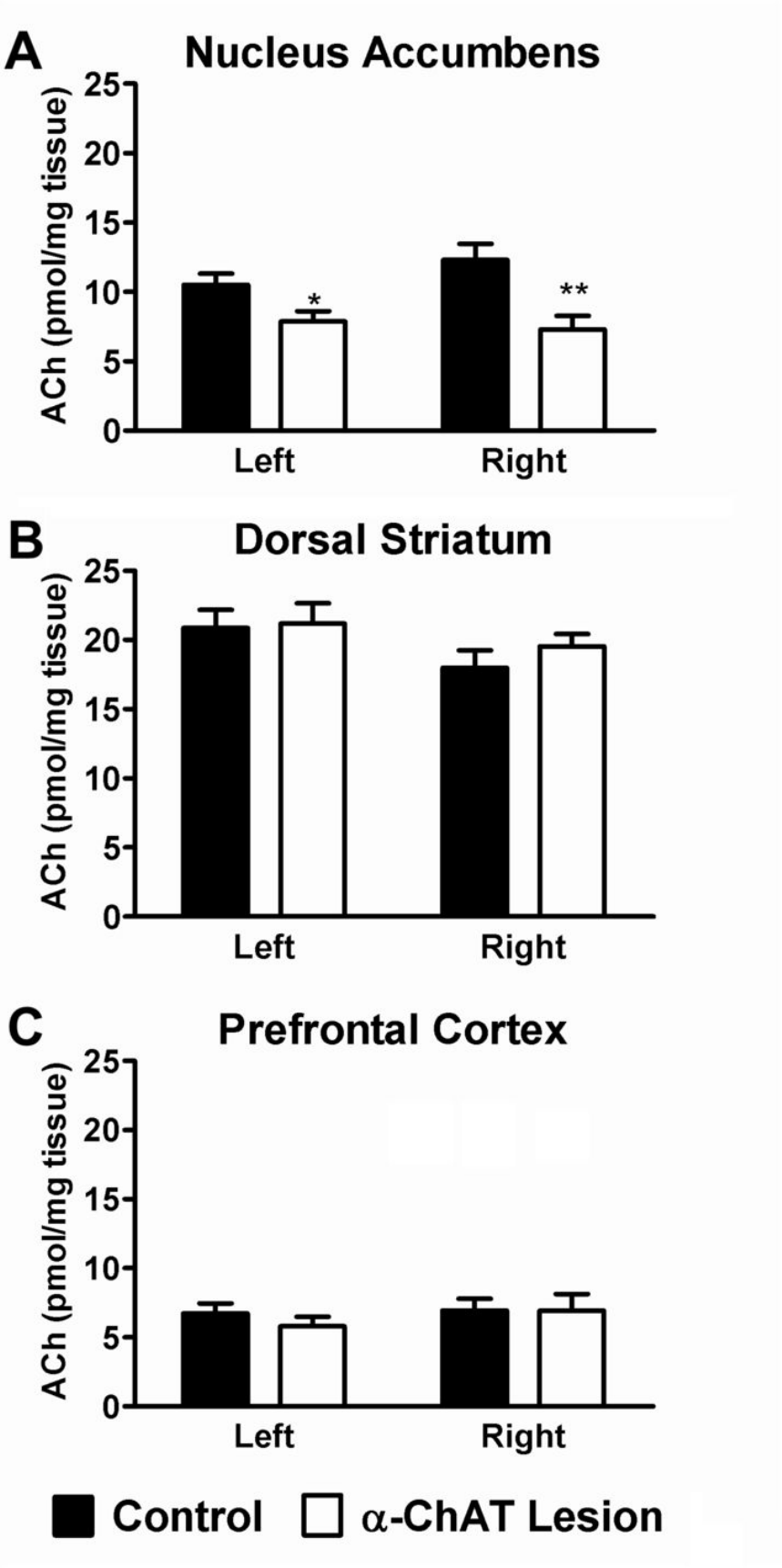
A
Nucleus Accumbens
ACh (pmol/mg tissue)
25
20
15
10
5
0
*
**
Left
Right
B
Dorsal Striatum
ACh (pmol/mg tissue)
25
20
15
10
5
0
Left
Right
C
Prefrontal Cortex
ACh (pmol/mg tissue)
25
20
15
10
5
0
Left
Right
Control
α-ChAT Lesion

Figure 8: Quantification of ACh in brain tissue sample from A) nucleus accumbens B) dorsal striatum and C) prefrontal cortex. There was a significant reduction in ACh level in the N.Acc in rats injected with the ChAT immunotoxin. Data represent mean ± SEM, (n = 12 in each group). * $p < 0.05$; **$p < 0.01$ relative to control hemisphere.

Table I : Catecholamine levels in the nucleus accumbens

Nucleus Accumbens	**Control**		**α-ChAT Lesion**	
	Left	**Right**	**Left**	**Right**
DA	8485 ± 710	8808 ± 563	7479 ± 429	7558 ± 544
DOPAC	2091 ± 154	2290 ± 181	1859 ± 119	2052 ± 148
DOPAC / DA ratio	0.263 ± 0.026	0.275 ± 0.032	0.257 ± 0.023	0.299 ± 0.042
5-HT	623.7 ± 76.1	669.0 ± 80.4	699.7 ± 58.5	754.8 ± 99.9
5-HIAA	761.7 ± 99.2	810.4 ± 82.6	902.1 ± 62.3	869.6 ± 46.4
5-HT / 5-HIAA ratio	1.29 ± 0.08	1.34 ± 0.08	1.33 ± 0.07	1.30 ± 0.12

Data represent mean ± SEM. (n = 12 per group)

H: main effect of brain hemisphere. L: main effect of lesion

Value are in pg / mg tissue

Table II: Catecholamine levels in the Dorsal Striatum

Dorsal Striatum	Control		α-ChAT Lesion		
	Left	Right	Left	Right	
DA	13857 ± 739	13447 ± 843	14016 ± 723	14047 ± 1136	
DOPAC	1928 ± 135	1841 ± 156	1651 ± 162	1653 ± 114	
DOPAC / DA ratio	0.139 ± 0.007	0.136 ± 0.006	0.117 ± 0.008	0.120 ± 0.006	
					L p = 0.028
5-HT	366.5 ± 26.3	392.9 ± 39.9	399.4 ± 38.8	392.6 ± 28.2	
5-HIAA	501.4 ± 31.1	493.1 ± 35.0	505.9 ± 40.4	509.6 ± 40.8	
5-HT / 5-HIAA ratio	1.42 ± 0.101	1.31 ± 0.084	1.32 ± 0.087	1.32 ± 0.088	

Data represent mean ± SEM. (n = 12 per group)

H: main effect of brain hemisphere. L: main effect of lesion

Table III: Catecholamine levels in the prefrontal cortex

Prefrontal Cortex	Control		α-ChAT Lesion		
	Left	Right	Left	Right	
DA	144.4 ± 9.8	138.2 ± 15.2	157.3 ± 23.7	136.0 ± 9.3	
DOPAC	39.3 ± 3.0	29.9 ± 4.4	33.7 ± 6.1	28.5 ± 2.7	
DOPAC / DA ratio	0.278 ± 0.019	0.231 ± 0.036	0.254 ± 0.054	0.217 ± 0.020	**H** p = 0.089
5-HT	650.7 ± 30.9	607.2 ± 37.6	709.0 ± 42.5	619.6 ± 38.9	**H** p = 0.033
5-HIAA	370.5 ± 16.9	405.5 ± 34.9	367.9 ± 24.9	347.4 ± 20.7	
5-HT / 5-HIAA ratio	0.579 ± 0.030	0.669 ± 0.043	0.520 ± 0.017	0.570 ± 0.025	**L** p = 0.034 **H** p = 0.009

Data represent mean ± SEM. (n = 12 per group)

H: main effect of brain hemisphere. L: main effect of lesion

Value are in pg / mg tissue

Discussion

Similar to our previous report (Laplante et al., 2011), the infusion of anti-ChAT saporin immunotoxin produced substantial depletion of cholinergic neurons (72%) within the N.Acc., but not in adjacent structures (diagonal band and dorsal striatum). The extent of local depletion was greater than in our initial study (44%), possibly due to variability in toxin efficacy or the slightly longer time between injection and sacrifice in the present study (7-8 weeks compared to 5-6 weeks). The same lesion procedure also decreased significantly the intra-accumbens level of ACh without affecting the choline level, in accordance with cholinergic cell loss. Similarly to the immunohistochemistry results, the ACh levels were unchanged in dorsal striatum and PFC, the latter receiving cholinergic input from the horizontal limb of the diagonal band (Bigl et al., 1982;Laplante et al., 2005). Together, these data indicate that lesions are restricted to the injection site.

The quantification of ACh in cerebral tissue is a suitable complementary method to immunohistochemistry to determine the extent of the lesions. These two approaches require different processing (fresh tissue dissection for the former vs fixation for the latter) and are therefore exclusive. Immunohistochemistry confers an optimal spatial resolution to assess neuronal loss in sub-regions. On the other hand, the fresh tissue sampling for HPLC analysis may include N.Acc tissue not irrigated by the toxin injection which then, might dilute the observable lesion effect.

Cholinergic depletion was associated with working memory deficits along with physiological and structural alterations in the PFC. The importance of central cholinergic systems on working memory processes is well documented, especially in relation to the hippocampus or PFC (Durkin, 1994;Givens and Olton, 1990;Granon et al., 1995;Hironaka et al., 2001). The striatum also plays a regulatory role on working memory functions as ablation of cholinergic interneurons in striatum in mice using a transgenic/immunotoxic approach also resulted in impaired spatial delayed alternation performance in the T-maze (Kitabatake *et al*., 2003). The N.Acc. has previously been implicated in memory processes as well (Setlow, 1997) and electrolytic or excitotoxic lesions of this structure result in working memory impairment (Gal et al., 1997;Jongen-Relo et al., 2003). Our results suggest that cholinergic mechanisms in the N.Acc. may be specifically involved in working memory processes. We have also observed (in separate animals) that the same cholinergic lesions impair spontaneous alternation behaviour in a cross maze as a further implication of the role of cholinergic mechanisms in N.Acc. in working memory processes (unpublished observations).

The present findings also suggest that these effects may be mediated by feedback pathways modulating mesocortical DA function. Thus cholinergic depletion in N.Acc. exerts not only local effects, but triggers a functional reorganization in corticolimbic DA circuits, reflected in a deficient response of mesocortical DA neurons (originating in the VTA) to salient stimuli such as mild stress. Neuronal projections from the N.Acc to the *substantia nigra pars compacta*

(Nauta et al., 1978), the origin of the nigrostriatal DAergic pathway, provide an anatomical substrate for a possible regulation of DA activity in the dorsal striatum by the N.Acc.

Electrophysiological studies in monkeys (Schultz et al., 1993) have shown that the DA neurons of the VTA (moreso than substantia nigra) respond phasically to salient reward and conditioned cues in a manner essential for learning delayed responding tasks. Working memory tasks like the one presently employed, rely on the functional integrity of the PFC (Aultman and Moghaddam, 2001;Sanchez-Santed et al., 1997). Prefrontal cortical DA is a key regulator of these cognitive functions in rats and monkeys (Brozoski et al., 1979;Granon et al., 2000;Seamans et al., 1998;Williams and Goldman-Rakic, 1995), and best cognitive performance requires an optimal window of cortical DA activity (D_1-mediated), as either too much or too little DA results in poor working memory (Chudasama and Robbins, 2004;Goldman-Rakic et al., 2000;Zahrt et al., 1997). This relationship is further supported by the positive correlation we report between working memory performance and PFC DA activation in response to mild stress within the lesioned animals. The fact that this correlation was not significant in controls may indicate that the latter were already performing at close to optimal levels and thus were less variable.

In the PFC and N.Acc, the tissue levels of DA, DOPAC and the DOPAC/DA ratio were not significantly affected after local lesions of cholinergic neurons

indicating an unaltered tonic DA activity. Similar observations have been reported in the striatum after cholinergic cells depletion (Kaneko et al., 2000). Our lesions have affected the serotonergic transmission only in the PFC. However, more investigations are required to fully describe this effect.

Cholinergic depletion within the N.Acc. also led to structural alterations in the PFC, reflected in reduced density of TH varicosities. It has been suggested that the density of varicosities in an axonal segment are related to the level of neuronal activity (Zhang et al., 2011;Zhang et al., 2010). Consistent with cortical plasticity, synaptic varicosities or “boutons” are dynamic structures that can be formed and removed (De, V et al., 2006;Stettler et al., 2006). Similar to experience-induced increases in the number of dendritic spines and axonal synaptic boutons (Stettler et al., 2006), it is possible that the present reduction of TH-labelled varicosities reflects a hypoactive mesocortical DA (and/or noradrenaline) system, although the nature of these effects requires further mechanistic studies.

Deficient mesocortical DA function may itself induce or exacerbate a hyper-responsivity to mesolimbic DA stimulation. In this view, several studies have demonstrated that direct depletion of PFC DA leads to heightened responsiveness of N.Acc. in response to pharmacological challenge or stress (Deutch, 1992;Mitchell and Gratton, 1992;Pycock et al., 1980). However, the notion that striatal or N.Acc. manipulations can lead to functional alterations in PFC has received less attention (Simpson et al., 2010). Some data have suggested changes

in PFC functions and innervation patterns with the latter direction of modulation (Deniau et al., 1994;Kitabatake et al., 2003;Middleton and Strick, 2002). Of particular interest, it has been shown that transient over-expression of D_2 receptors restricted to striatum of mice induced impairments in working memory and behavioural flexibility, and reduced cortical DA turnover (Kellendonk et al., 2006). Such findings are consistent with recent proposals that striatal dysfunction may be of primary importance to the cognitive deficits of schizophrenia (Simpson et al., 2010). Consistent with existing theories of schizophrenia, where a hypofunctional cortical DA state exists with hyper-responsive subcortical (striatal) DA function (Davis et al., 1991;Grace, 1991;Weinberger, 1987), the latter view proposes pathways by which the latter could causally lead to the former. One prominent possibility involves modulation of striatal outputs to the mesocortical DA cell bodies of the VTA and one proposed means of dampening this system (in addition to striatal D_2 overactivity), was diminished activity of cholinergic striatal interneurons (Simpson et al., 2010).

We presently confirm that local N.Acc. cholinergic depletion leads to impaired mesocortical DA activation in freely behaving rats, quite possibly via feedback from the N.Acc. to the VTA. If such a cholinergic deficit also leads to a similar reduction in activity in the meso*limbic* DA projection back to the N.Acc., one might expect a compensatory upregulation of postsynaptic DA receptors (prominently D_2-like) in the N.Acc. Such a scenario would explain the behavioural hyper-responsiveness to amphetamine we have previously shown as a

consequence of these lesions (Laplante et al., 2011). This would also be consistent with the lesion-induced deficits in sensorimotor gating and their reversal by the D2 antagonist haloperidol(Laplante et al., 2011). Taken together, it suggests that reduction in N.Acc. cholinergic function not only induces local effects, but is capable of inducing widespread functional changes in cortical/subcortical networks.

The present cholinergic lesions in the N.Acc. may be particularly relevant to the neuropathology of schizophrenia, as *post-mortem* studies in schizophrenic patients have revealed lower densities of ChAT immuno-labelled neurons (Holt et al., 1999) and ChAT mRNA expressing cells in the ventral striatum (Holt et al., 2005). Cholinergic cell density in the nucleus basalis of Meynert (el Mallakh et al., 1991) and the pedunculopontine nucleus (German et al., 1999) were comparatively unaffected in schizophrenic brains. Loss of intra-accumbens cholinergic interneurons (Boissiere et al., 1997;Lehericy et al., 1989;Selden et al., 1994) and working memory impairments (Kensinger et al., 2003) have also been reported in Alzheimer's disease. However, the damage to forebrain cholinergic systems is far more extensive and nonspecific (Davies and Maloney, 1976;Lehericy et al., 1993;Whitehouse et al., 1982).

In summary, selective depletion of cholinergic interneurons in N.Acc. leads to impairment in working memory and reduced activation of the mesocortical DA projection to the PFC which is consistent with theories of schizophrenia (Davis et al., 1991;Grace, 1991;Weinberger, 1987). Moreover, these lesions also reduced

the number of TH-labelled varicosities in PFC. Interestingly, reductions in TH-labeled axon length and varicosities have been observed in the DA-rich, deep cortical layers in schizophrenic patients (Akil et al., 1999;Benes et al., 1997). The present data add to previous findings that the same manipulation in N.Acc. induced a behavioural hypersensitivity to psychostimulants and impaired sensorimotor gating (reversed by antipsychotics). Given the relevance of the above processes to schizophrenia (Lipska and Weinberger, 2000), we propose that the selective loss of cholinergic neurons seen in the ventral striatum (Holt et al., 2005;Holt et al., 1999) may be of greater causal significance to a wide array of schizophrenic symptomatology than is commonly appreciated. Future studies will further investigate the mechanistic consequences of this neuropathological defect.

Abbreviations: 5-HIAA, 5-hydroxyindoleacetic acid; 5-HT, serotonin or 5-hydroxytryptophan ACh, acetylcholine; ChAT, choline acetyltransferase; DA, dopamine; DOPAC 3,4-dihydroxyphenylacetic acid; N.Acc., nucleus accumbens; PFC, prefrontal cortex; TH, tyrosine hydroxylase; VTA, ventral tegmental area.

CHAPTER V

GENERAL DISCUSSION

In the present research, the immediate microenvironment (Descarries et al., 1997) of cholinergic fibers, dopaminergic fibers, and pyramidal cells in the rat mPFC were investigated to evaluate the functional potential of their spatial interrelationships via the mode of diffuse transmission. The results demonstrated a preferential microproximity between cholinergic fibers, dopaminergic fibers and pyramidal cells in the rat mPFC. The functional importance of these spatial interrelationships was supported by the dynamics of cholinergic and dopaminergic *en passant* varicosities associated with relevant neuronal activity in these different transmitter systems.

.

V.1 Viewing and analyzing the microenvironment of ACh and DA fibers and pyramidal cells via confocal microscopy

V.1.1 Viewing 3D microenvironment via confocal microscopy

It is important to explore into three-dimensional extracellular microenvironment of a neuronal modulator to understand its position and function in a continuous neuronal network. There is a wealth of 3D information on the

immediate microenvironment of transmitters like ACh or DA. Confocal microscope offers a means to collect substantial high resolution 3D information in single slices (Hibbs, 2004), and multi-fluorophore labeling makes it possible to study the neuroanatomical interactions among multiple types of neuronal elements. Therefore, in the present studies the three-dimensional distance between each system was assessed and the plasticity of axon varicosities on ACh and DA fibers in relation to their reciprocal microproximity was examined via confocal microscopy.

V.1.2 Definition of microproximity

The 3 μm maximal distance between two neuronal elements used in this research was a conservative estimate of the radius of a sphere within which ACh concentration should be able to induce significant effects at receptors. Thus far, data on the temporal and spatial parameters of diffuse transmission are scarce. However, "fast nonsynaptic transmission" has been proposed for ACh (Lendvai and Vizi, 2008) due to the quick hydrolysis action of AChE (Descarries et al., 1997, Descarries, 1998, Sarter et al., 2009b). In addition, a variety of factors may limit the real sphere of influence from the diffusion of a diffusible neurotransmitter, such as the tortuosity of diffusion, the diffusion coefficient of the neurotransmitter, the sensitivity and location of specific receptors, and the heterogeneity of the

neurotransmitter concentrations in the microenvironment (Nicholson and Sykova, 1998, Peters and Michael, 2000).

V.2 A novel way of analyzing neuroanatomical interactions between fibers

This research provides a novel way to analyze the neuroanatomical interrelationships between fiber systems. So far as we know, these are the first studies that endeavored to analyze and quantify the three-dimensional microenvironment of different neuronal elements (Chapter II), as well of the plasticity of fiber morphology within this spatial distance associated with relevant local neuronal activities (Chapter III). Due to this novel aspect of our research, it was notpossible to apply traditional stereology to the analysis and quantification of the 3D microproximity between neuronal elements. Traditional stereology uses unbiased methods to estimate first-order stereological parameters such as length, number and surface area (Peters and Michael, 2000), but it is not adapted for analyzing or quantifying the 3D microproximity between neuronal elements (personal communication with Dr. Peter R. Mouton on his stereology workshop in Montreal, 2008). For this reason, the analysis and quantification of the neuroanatomical data in the present research were accomplished semi-manually, usingthe confocal software Leica lite and LAS AF lite. This labor intensive task was carried out in each ROI, to measure the distance between each fiber segment as

well as the diameter of each varicosity along each individual fiber segment within and outside the defined microproximity to the related element under investigation.

V.3 Axon varicosity – a link between the modulators and other elements in a neuronal network

V.3.1 Combined modulation of the pyramidal neuronal output by ACh and DA

72% to 80% pyramidal cells examined in layer V were within microproximity of both ACh and DA fibers (Chapter II), suggesting the possibility of a combined modulation by ACh and DA of the output of pyramidal cells to subcortical areas (Shipp, 2007). This was consistent with previous findings that each pyramidal neuron having D4R mRNA co-expresses M1R mRNA, which indicates combination of cholinergic and dopaminergic signaling pathways at the single cell level (Vysokanov et al., 1998). Convergence of actions from different neurotransmitters is a general feature of neurotransmitter responses in the CNS (McCormick, 1992). The prefrontal pyramidal cells in Layer V potentially process and integrate large numbers of diverse inputs to their soma, dendrites and axon to to process the extrinsic sensory stimuli and send them to subcortical structures (Spruston, 2008).

V.3.2 Functional importance of the microproximity between cholinergic fiber segments and dopaminergic fiber segments

V.3.2.1 Modulation of DA on ACh in the mPFC

Only a small proportion (9–18%) of the cholinergic fibers was observed to be within 3 μm from dopaminergic fibers in the rat mPFC (Chapter II), suggesting a relatively weak direct influence of DA on cortical cholinergic fibers. This might be because DA doesn't exhibit robust diffuse transmission features in the mPFC as ACh does. A relatively high synaptic incidence was indeed observed for the DA varicosities in rat anteromedial cortex (Seguela et al., 1988). Nevertheless, there was an enrichment of the density of dopaminergic axon varicosities (Chapter II) in the microproximity of ACh fibers, raising the probability of direct biological effects of DA on the small proportion of cholinergic fibers within such a distance.

Cortical dopaminergic activity could induce ACh release via indirect pathways in a neuronal network. Dopaminergic neurons could release glutamate as co-transmitter (Trudeau, 2004, Descarries et al., 2008) to modulate pyramidal neuronal activity, which could subsequently exert the modulatory effect on cholinergic fibers within the immediate microenvironment. In addition, nAChRs present on glutamate terminals can increase glutamate release which coordinately

induces dopamine release from neighboring boutons (Livingstone et al., 2010). Dopaminergic neurons in VTA project to BF and their axons synapse on BF cholinergic cells. Therefore, DA may modulate BF cholinergic neurons which project to innervate the mPFC (Gaykema and Zaborszky, 1996, Smiley et al., 1999).

V.3.2.2 Modulation of ACh on DA in the mPFC

20-40% of dopaminergic fibers were within the 3 μm of microproximity of cholinergic fibers in the rat mPFC, with an enrichment of cholinergic varicosities juxtaposed to those dopaminergic fibers (Chapter II), raising the possibility of direct axo-axonic modulation of ACh on DA transmission in the mPFC. nAChRs may have an extrasynaptic location on presynaptic DA terminals to exert their modulatory influence in the CNS (Jones et al., 2001, Wonnacott et al., 2006, Exley and Cragg, 2008).

On the other hand, ACh could also exert its influence on DA transmission via indirect pathways. For example, *α*7 nAChR have an indirect effect on DA release through the modulation of amino acid transmitters (Wonnacott et al., 2006). ACh may modulate GABA release onto DA neurons via nAChRs present on

presynaptic GABAergic boutons within the VTA to exert its impact on mPFC dopaminergic fibers (Yang et al., 2011).

V.3.3 Enrichment of cholinergic axonal varicosities following local neuronal activity in pyramidal cells and ascending HDB cholinergic projection in the mPFC

Concomitant visual and HDB electrical stimulation resulted in significant increases in the cholinergic varicosity density within the vicinity of c-Fos activated pyramidal cells in the rat mPFC, compared to the vicinity of nonactivated pyramidal cells in the same group and the control group (Chapter III). This observation indicated that a change in axon varicosity density is associated with neuronal activity supported by the relationship between pyramidal cells in the mPFC and ascending HDB cholinergic fibers (Luiten et al., 1987, Gaykema et al., 1990).

HDB electrical stimulation provided a major contribution to the c-Fos expression of pyramidal neurons in the mPFC of rats with visual and HDB stimulation. The facilitation of PFC pyramidal cell activity by the BF cholinergic prefrontal projection is part of the “Bottom-up” mechanism underlying attention (Sarter et al., 2003), which could be executed via ascending cholinergic fibers innervating pyramidal cells, probably through presynaptic nAChRs on

glutamatergic terminals (Fabian-Fine et al., 2001, Jones and Wonnacott, 2004, Rousseau et al., 2005), and mAChRs expressed by mPFC pyramidal neurons (Vysokanov et al., 1998).

On the other hand, the enhanced pyramidal activity could also exert some backward crosstalk to the cholinergic fibers in its vicinity and contribute to the dynamics of the cholinergic varicosities. Pyramidal neuronal activity modulates the cholinergic effects in the PFC (Briand et al., 2007, Quarta et al., 2007, Parikh and Sarter, 2008). The NMDA receptor antagonist CPP was shown to remove the tonic glutamate activity, which antagonizes the attentional enhancing properties of nicotine (Quarta et al., 2007), in keeping with a reciprocal modulation between cholinergic afferents and the pyramidal cells they innervate.

V.3.4 The association between relevant neuronal activity and dopaminergic axonal varicosity density in the rat mPFC following cholinergic depletion of the nucleus accumbens

Cholinergic depletion within the nucleus accumbens (N.Acc.) resulted in significant impairments in working memory performance and reduced density of dopaminergic varicosities in the infralimbic cortex, reflecting a hypoactive mesocortical DA system. This DA hypoactivity was probably induced via feedback from the N.Acc. to the VTA (Chapter IV).

On the other hand, decreased DA activity presumably disrupts the interaction between DA and pyramidal cells. Disruption of the glutamate-dopamine interaction may alter the function of PFC and its interconnected areas, such as the N.Acc., leading to an impairment of memory performance (Del Arco and Mora, 2005). It has been proposed that a D_2R-mGluR interaction in PFC modulates the activity of the meso-limbic dopamine system (Del Arco and Mora, 2005), consistent with our findings that the majority of pyramidal cells expressed D_2R markers in the mPFC of *Drd1a*-tdTomato/*Drd2*-EGFP transgenic mice (Chapter II).

V.3.5 Combining the modulators and the neuronal networks to achieve a delicate balance through dynamics of en passant varicosity density

The present research demonstrates that an enrichment of cholinergic and dopaminergic varicosities on fiber segments in the rat mPFC is associated with neuronal activity resulting from the interaction between the cholinergic and dopaminergic systems and pyramidal cells in a large and complex neuronal network. Although this hypothetic network is composed of subsystems interconnected at different levels such as fibers and soma from different regions (Figure V.1, and Chapter II-IV), it is still a simplistic picture. The ascending BF

cholinergic projection and the VTA dopaminergic projection converge onto the same pyramidal cells in the mPFC to co-modulate the PFC output facilitating cognitive processes. The PFC in turn sends glutamatergic (and GABAergic) projections to the BF to control its activity. The PFC also sends glutamatergic projection to the N.Acc., whose own activity is under the control of the glutamate-dopamine balance in PFC.

Figure V.1

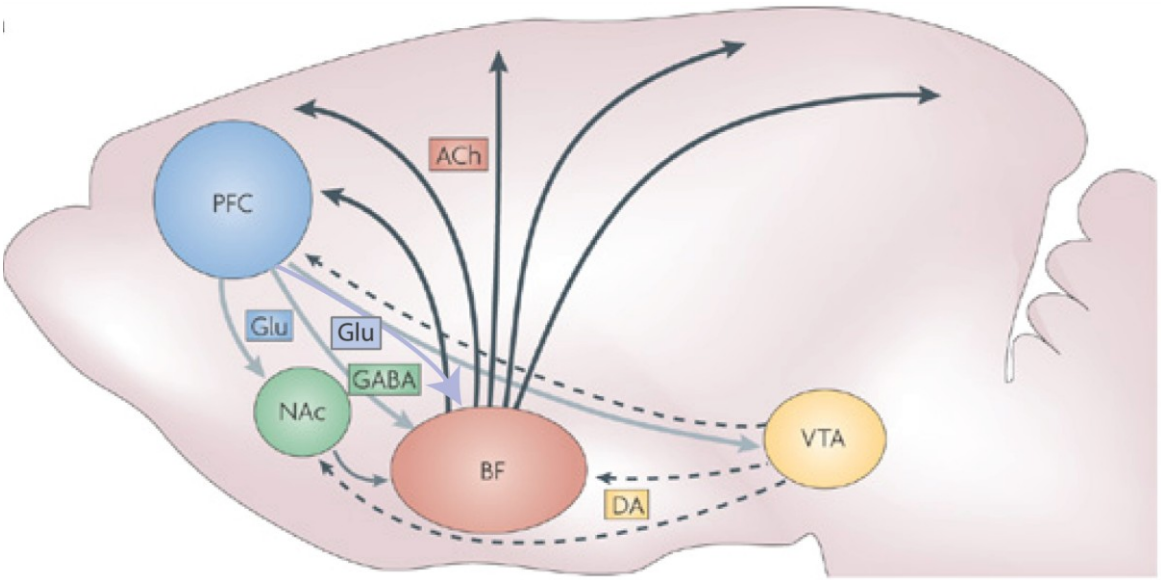

Figure V.1 Schematic illustration of a hypothetic neuronal network composed of different neuronal subsystems. The PFC receives BF cholinergic projection and VTA dopaminergic projections. These two ascending fiber systems converge on the same pyramidal cells in the PFC to co-modulate the PFC output to

facilitate cognitive processes. PFC in turn sends glutamatergic projections to the BF for its control of the subcortical areas. The PFC also sends glutamatergic projection to the nucleus accumbens, which is therefore controlled by the glutamate-dopamine balance in PFC. This figure is a modified version from (Sarter et al., 2009b) Abbreviations: ACh: acetylcholine; BF: basal forebrain; DA: dopamine; GABA: γ-aminobutyric acid; Glu: glutamate; NAc: nucleus accumbens; PFC: prefrontal cortex; VTA: ventral tegmental area

It is noteworthy that the varicosity density of cholinergic fibers depended on local neuronal activity resulting from the reciprocal interaction between cholinergic fibers and the pyramidal neurons of the mPFC (Chapter III). Thus, the structural plasticity of axon varicosities reflects how the modulators and the neuronal networks are intimately combined to achieve the processing of specific aspects of cognitive functions. The density of axon varicosities thus makes the link between different levels in a network – the cellular level (the axonal zone of interaction) and the system level (ascending cholinergic fibers from HDB and pyramidal cells of mPFC), and combines the impact of ACh diffuse transmission and the prefrontal neuronal network to achieve the required balance for cognitive processing (Figure V.2).

Figure V.2

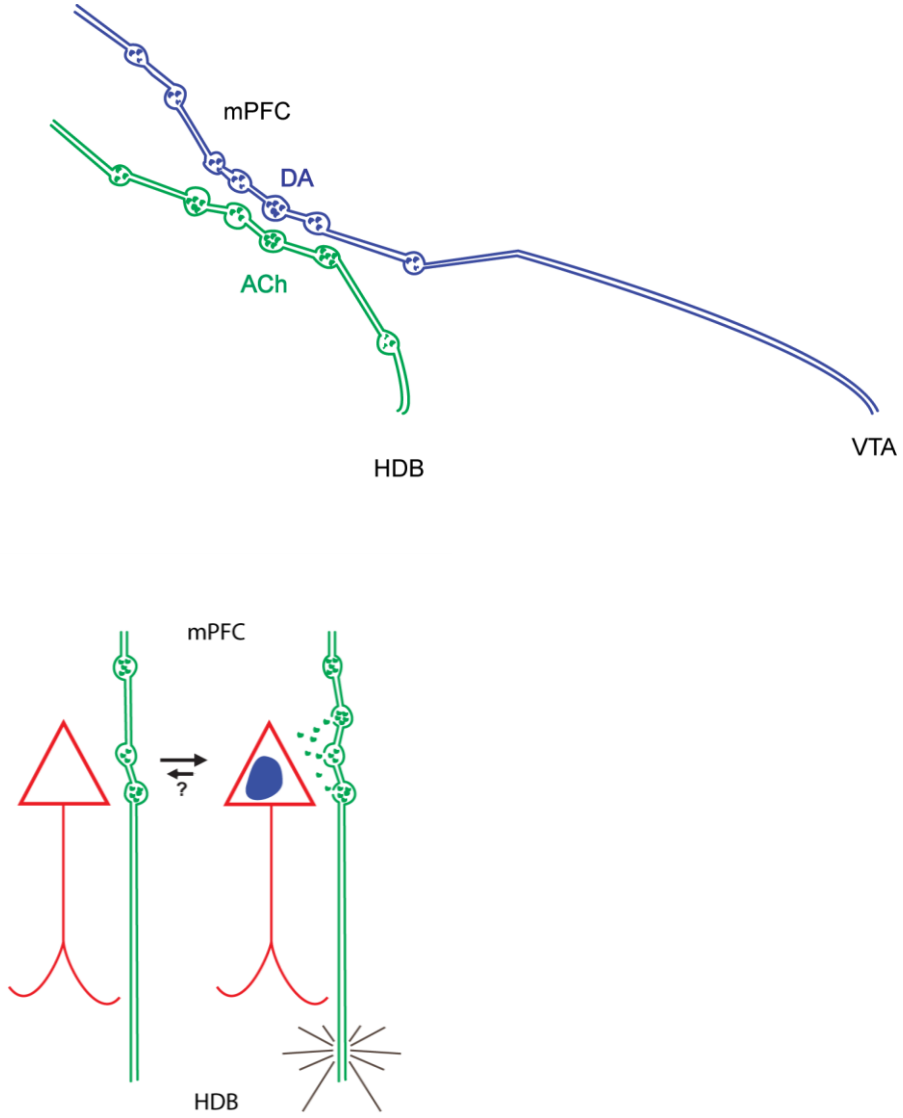

Figure V.2 Density of axon varicosities – a link between the cellular level and the systemic levels in the prefrontal neuronal network. The dynamics of cholinergic axon varicosities combines the impact of ACh diffuse transmission and the prefrontal neuronal network in the delicate processing of

cognitive functions. Top panel: Enhanced varicosity density on cholinergic and dopaminergic fiber segments within their microproximity, compared to those outside this microproximity. Bottom panel: Enrichment of cholinergic axon varicosities due to local neuronal activity from the ACh-pyramidal neuron interaction in the mPFC. Abbreviations: ACh: acetylcholine; BF: basal forebrain; DA: dopamine; HDB: horizontal limb of the diagonal band of Broca; mPFC: medial prefrontal cortex; VTA: ventral tegmental area

V.4 The importance of ACh diffuse transmission

The results from this research confirm the importance of ACh diffuse transmission in the PFC (Umbriaco et al., 1994, Descarries et al., 1997, Descarries, 1998). The enrichment of cholinergic axon varicosities within the vicinity of dopaminergic fibers (Chapter 2) or activated pyramidal cells (Chapter 3) suggests that diffuse transmission of ACh is an integral component of the prefrontal executive network. Therefore, the diffusion of ACh and its impactin the PFC should not be ignored any more, and needs to be taken into consideration in neuroscience research, particularly when trying to examine the cellular mechanisms correlated with specific aspects of cognitive functions. Denying or ignoring the existence of nonsynaptic transmission of ACh will over-simplify the principles and structures of a complex and intricate prefrontal neuronal network, and lead to incomplete and biased conclusions.

The dynamic view of axonal interactions in the present research suggests a novel way to investigate the functional role of diffuse transmission of a neuronal transmitter in brain. This might be the first step leading to novel experimental designs exploring the specific features of ACh diffuse transmission in the PFC in vivo. Novel techniques also need to be developed to suit the needs of studying the properties of diffuse transmission in the CNS. For example, much neuroanatomical software could be modified to examine and quantify certain anatomical features of the 3D extracellular space in the microenvironment.

V.5 Future perspective

V.5.1 Particularly to this research

The present Ph.D. research has analyzed the spatial interrelationships between the three transmitter-dependent systems in the mPFC, the cholinergic and dopaminergic systems and the pyramidal cells. However, there is a strong probability that for a specific aspect of cognitive function, the neuronal network involved consists of much more than these three systems. For example, the GABAergic system interacts with ACh, DA and pyramidal cells in the PFC to exert a crucial role in cognitive functions (Wang et al., 2002, Zhong et al., 2003, Guidotti

et al., 2005, Balla et al., 2009, Del Arco et al., 2011). However, the capacity of our current confocal microscopes limits the simultaneous visualization of no more than three fluorophores. It would be interesting to evaluate the reciprocal spatial distance among more than three neuronal elements in the PFC.

It would be also of great interest to design novel experiments to test if different types of extrinsic stimuli could have different impacts on the densities of axonal varicosities. In this research the visual stimulation and HDB electrical stimulation produced the same effects on the density of axon varicosities along fibers. However, better knowledge of the functional pathways in the circuits will be needed to test such a hypothesis. The pathways of visual stimulation processing in the PFC and the pathways of cholinergic activation need to be further clarified, as well as the properties of other neuronal elements induced by such stimulation, such as the cholinergic receptors present on pyramidal cells, dopaminergic fibers and other fiber systems in the PFC, and GABAergic neurons in their vicinity. Besides, knowledge of both the temporal and spatial properties of those neuronal elements induced by such stimulation is required.

V.5.2 General speculation

Much more remains to be understood about how the prefrontal neuronal components are connected with each other, and how the diffuse transmission of neuromodulators are combined at the different levels in a neuronal network to process extrinsic and intrinsic stimuli. To be able to close the explanatory gap between the local neuronal activity at the subcellular level in the PFC and the animal's behavior level, further knowledge about the diffusive properties of a neurotransmitter and the structure of the extracellular space are required, as well as extensive knowledge of the specific properties of neuronal components of the executive network at different levels (subcellular, cellular, and of the systems). Novel techniques will need to be developed to explore the network properties. Those techniques should not "truncate" some levels and limit the scientific observation at specific levels.

An open mind is also necessary to comprehend the extensive complexity of the neuronal network, which is composed of probably incredibly large numbers of systems and subsystems, plus a big variety of neuronal modulatory substances. The specific aspects of cognitive functions are generated from a delicate balance of all the components of a neuronal network. Disruption at any point in this network might lead to complication of many components, and thus detrimental to certain

cognitive processes. Innovative ways of thinking are required to link between different levels of a network and integrate all the data from different components to generate a whole picture.

REFERENCES

Agnati LF, Leo G, Zanardi A, Genedani S, Rivera A, Fuxe K, Guidolin D (2006) Volume transmission and wiring transmission from cellular to molecular networks: history and perspectives. Acta Physiol (Oxf) 187:329-344.

Agnati LF, Zoli M, Stromberg I, Fuxe K (1995) Intercellular communication in the brain: wiring versus volume transmission. Neuroscience 69:711-726.

Albuquerque EX, Pereira EF, Alkondon M, Rogers SW (2009) Mammalian nicotinic acetylcholine receptors: from structure to function. Physiol Rev 89:73-120.

Allard S, Gosein V, Cuello AC, Ribeiro-da-Silva A (2010) Changes with aging in the dopaminergic and noradrenergic innervation of rat neocortex. Neurobiol Aging.

Anderson DJ, Malysz J, Gronlien JH, El Kouhen R, Hakerud M, Wetterstrand C, Briggs CA, Gopalakrishnan M (2009) Stimulation of dopamine release by nicotinic acetylcholine receptor ligands in rat brain slices correlates with the profile of high, but not low, sensitivity alpha4beta2 subunit combination. Biochem Pharmacol 78:844-851.

Anderson JC, Martin KA (2001) Does bouton morphology optimize axon length? Nat Neurosci 4:1166-1167.

Arnsten AF (2009) Toward a new understanding of attention-deficit hyperactivity disorder pathophysiology: an important role for prefrontal cortex dysfunction. CNS Drugs 23 Suppl 1:33-41.

Aultman JM, Moghaddam B (2001) Distinct contributions of glutamate and dopamine receptors to temporal aspects of rodent working memory using a clinically relevant task. Psychopharmacology (Berl) 153:353-364.

Balla A, Nattini ME, Sershen H, Lajtha A, Dunlop DS, Javitt DC (2009) GABAB/NMDA receptor interaction in the regulation of extracellular dopamine levels in rodent prefrontal cortex and striatum. Neuropharmacology 56:915-921.

Bellgrove MA, Mattingley JB (2008) Molecular genetics of attention. Ann N Y Acad Sci 1129:200-212.

Bergles DE, Diamond JS, Jahr CE (1999) Clearance of glutamate inside the synapse and beyond. Curr Opin Neurobiol 9:293-298.

Bergstrom HC, McDonald CG, French HT, Smith RF (2008) Continuous nicotine administration produces selective, age-dependent structural alteration of pyramidal neurons from prelimbic cortex. Synapse 62:31-39.

Birrell JM, Brown VJ (2000) Medial frontal cortex mediates perceptual attentional set shifting in the rat. J Neurosci 20:4320-4324.

Black JE, Kodish IM, Grossman AW, Klintsova AY, Orlovskaya D, Vostrikov V, Uranova N, Greenough WT (2004) Pathology of layer V pyramidal neurons

in the prefrontal cortex of patients with schizophrenia. Am J Psychiatry 161:742-744.

Bohnen NI, Albin RL (2011) The cholinergic system and Parkinson disease. Behav Brain Res 221:564-573.

Breese CR, Lee MJ, Adams CE, Sullivan B, Logel J, Gillen KM, Marks MJ, Collins AC, Leonard S (2000) Abnormal regulation of high affinity nicotinic receptors in subjects with schizophrenia. Neuropsychopharmacology 23:351-364.

Briand LA, Gritton H, Howe WM, Young DA, Sarter M (2007) Modulators in concert for cognition: modulator interactions in the prefrontal cortex. Prog Neurobiol 83:69-91.

Broersen LM, Heinsbroek RP, de Bruin JP, Uylings HB, Olivier B (1995) The role of the medial prefrontal cortex of rats in short-term memory functioning: further support for involvement of cholinergic, rather than dopaminergic mechanisms. Brain Res 674:221-229.

Brooks JM, Sarter M, Bruno JP (2007) D2-like receptors in nucleus accumbens negatively modulate acetylcholine release in prefrontal cortex. Neuropharmacology 53:455-463.

Brown RW, Kolb B (2001) Nicotine sensitization increases dendritic length and spine density in the nucleus accumbens and cingulate cortex. Brain Res 899:94-100.

Brown VJ, Bowman EM (2002) Rodent models of prefrontal cortical function. Trends Neurosci 25:340-343.

Burk JA, Lowder MW, Altemose KE (2008) Attentional demands for demonstrating deficits following intrabasalis infusions of 192 IgG-saporin. Behav Brain Res 195:231-238.

Cao YJ, Surowy CS, Puttfarcken PS (2005) Different nicotinic acetylcholine receptor subtypes mediating striatal and prefrontal cortical [3H]dopamine release. Neuropharmacology 48:72-79.

Carr DB, Sesack SR (2000) Projections from the rat prefrontal cortex to the ventral tegmental area: target specificity in the synaptic associations with mesoaccumbens and mesocortical neurons. J Neurosci 20:3864-3873.

Carr DB, Surmeier DJ (2007) M1 muscarinic receptor modulation of Kir2 channels enhances temporal summation of excitatory synaptic potentials in prefrontal cortex pyramidal neurons. J Neurophysiol 97:3432-3438.

Cass WA, Gerhardt GA (1995) In vivo assessment of dopamine uptake in rat medial prefrontal cortex: comparison with dorsal striatum and nucleus accumbens. J Neurochem 65:201-207.

Chedotal A, Umbriaco D, Descarries L, Hartman BK, Hamel E (1994) Light and electron microscopic immunocytochemical analysis of the neurovascular relationships of choline acetyltransferase and vasoactive intestinal polypeptide nerve terminals in the rat cerebral cortex. J Comp Neurol 343:57-71.

Chen L, Bohanick JD, Nishihara M, Seamans JK, Yang CR (2007) Dopamine D1/5 receptor-mediated long-term potentiation of intrinsic excitability in rat

prefrontal cortical neurons: Ca2+-dependent intracellular signaling. J Neurophysiol 97:2448-2464.

Choi WS, Machida CA, Ronnekleiv OK (1995) Distribution of dopamine D1, D2, and D5 receptor mRNAs in the monkey brain: ribonuclease protection assay analysis. Brain Res Mol Brain Res 31:86-94.

Chudasama Y, Dalley JW, Nathwani F, Bouger P, Robbins TW (2004) Cholinergic modulation of visual attention and working memory: dissociable effects of basal forebrain 192-IgG-saporin lesions and intraprefrontal infusions of scopolamine. Learn Mem 11:78-86.

Colicos MA, Collins BE, Sailor MJ, Goda Y (2001) Remodeling of synaptic actin induced by photoconductive stimulation. Cell 107:605-616.

Collins TJ (2007) ImageJ for microscopy. Biotechniques 43:25-30.

Cooper JR, Bloom FE, Roth RH (2003) The Biochemical Basis of Neuropharmacology. Chapter 2.: Oxford University Press.

Couey JJ, Meredith RM, Spijker S, Poorthuis RB, Smit AB, Brussaard AB, Mansvelder HD (2007) Distributed network actions by nicotine increase the threshold for spike-timing-dependent plasticity in prefrontal cortex. Neuron 54:73-87.

Cragg SJ, Nicholson C, Kume-Kick J, Tao L, Rice ME (2001) Dopamine-mediated volume transmission in midbrain is regulated by distinct extracellular geometry and uptake. J Neurophysiol 85:1761-1771.

Dalley JW, Cardinal RN, Robbins TW (2004a) Prefrontal executive and cognitive functions in rodents: neural and neurochemical substrates. Neurosci Biobehav Rev 28:771-784.

Dalley JW, Theobald DE, Bouger P, Chudasama Y, Cardinal RN, Robbins TW (2004b) Cortical cholinergic function and deficits in visual attentional performance in rats following 192 IgG-saporin-induced lesions of the medial prefrontal cortex. Cereb Cortex 14:922-932.

Dally JJ, Schaefer M, Greenfield SA (1996) The spontaneous release of acetylcholinesterase in rat substantia nigra is altered by local changes in extracellular levels of dopamine. Neurochem Int 29:629-635.

Dani JA (2001) Overview of nicotinic receptors and their roles in the central nervous system. Biol Psychiatry 49:166-174.

Day JC, Kornecook TJ, Quirion R (2001) Application of in vivo microdialysis to the study of cholinergic systems. Methods 23:21-39.

De Paola V, Arber S, Caroni P (2003) AMPA receptors regulate dynamic equilibrium of presynaptic terminals in mature hippocampal networks. Nat Neurosci 6:491-500.

De Paola V, Holtmaat A, Knott G, Song S, Wilbrecht L, Caroni P, Svoboda K (2006) Cell type-specific structural plasticity of axonal branches and boutons in the adult neocortex. Neuron 49:861-875.

DeFelipe J, Alonso-Nanclares L, Arellano JI (2002) Microstructure of the neocortex: comparative aspects. J Neurocytol 31:299-316.

Deiana S, Platt B, Riedel G (2010) The cholinergic system and spatial learning. Behav Brain Res.

Del Arco A, Mora F (2001) Dopamine release in the prefrontal cortex during stress is reduced by the local activation of glutamate receptors. Brain Res Bull 56:125-130.

Del Arco A, Mora F (2005) Glutamate-dopamine in vivo interaction in the prefrontal cortex modulates the release of dopamine and acetylcholine in the nucleus accumbens of the awake rat. J Neural Transm 112:97-109.

Del Arco A, Mora F (2009) Neurotransmitters and prefrontal cortex-limbic system interactions: implications for plasticity and psychiatric disorders. J Neural Transm 116:941-952.

Del Arco A, Ronzoni G, Mora F (2011) Prefrontal stimulation of GABAA receptors counteracts the corticolimbic hyperactivity produced by NMDA antagonists in the prefrontal cortex of the rat. Psychopharmacology (Berl) 214:525-536.

Del Arco A, Segovia G, Fuxe K, Mora F (2003) Changes in dialysate concentrations of glutamate and GABA in the brain: an index of volume transmission mediated actions? J Neurochem 85:23-33.

Descarries L (1998) The hypothesis of an ambient level of acetylcholine in the central nervous system. J Physiol Paris 92:215-220.

Descarries L, Berube-Carriere N, Riad M, Bo GD, Mendez JA, Trudeau LE (2008) Glutamate in dopamine neurons: synaptic versus diffuse transmission. Brain Res Rev 58:290-302.

Descarries L, Gisiger V, Steriade M (1997) Diffuse transmission by acetylcholine in the CNS. Prog Neurobiol 53:603-625.

Descarries L, Lemay B, Doucet G, Berger B (1987) Regional and laminar density of the dopamine innervation in adult rat cerebral cortex. Neuroscience 21:807-824.

Descarries L, Mechawar N (2000) Ultrastructural evidence for diffuse transmission by monoamine and acetylcholine neurons of the central nervous system. Prog Brain Res 125:27-47.

Di Cara B, Panayi F, Gobert A, Dekeyne A, Sicard D, De Groote L, Millan MJ (2007) Activation of dopamine D1 receptors enhances cholinergic transmission and social cognition: a parallel dialysis and behavioural study in rats. Int J Neuropsychopharmacol 10:383-399.

Dickinson JA, Kew JN, Wonnacott S (2008) Presynaptic alpha 7- and beta 2-containing nicotinic acetylcholine receptors modulate excitatory amino acid release from rat prefrontal cortex nerve terminals via distinct cellular mechanisms. Mol Pharmacol 74:348-359.

Ding DC, Gabbott PL, Totterdell S (2001) Differences in the laminar origin of projections from the medial prefrontal cortex to the nucleus accumbens shell and core regions in the rat. Brain Res 917:81-89.

Doherty MD, Gratton A (1992) High-speed chronoamperometric measurements of mesolimbic and nigrostriatal dopamine release associated with repeated daily stress. Brain Res 586:295-302.

Doherty MD, Gratton A (1996) Medial prefrontal cortical D1 receptor modulation of the meso-accumbens dopamine response to stress: an electrochemical study in freely-behaving rats. Brain Res 715:86-97.

Dotigny F, Ben Amor AY, Burke M, Vaucher E (2008) Neuromodulatory role of acetylcholine in visually-induced cortical activation: behavioral and neuroanatomical correlates. Neuroscience 154:1607-1618.

Duchesne A, Dufresne MM, Sullivan RM (2009) Sex differences in corticolimbic dopamine and serotonin systems in the rat and the effect of postnatal handling. Prog Neuropsychopharmacol Biol Psychiatry 33:251-261.

Duffy AM, Zhou P, Milner TA, Pickel VM (2009) Spatial and intracellular relationships between the alpha7 nicotinic acetylcholine receptor and the vesicular acetylcholine transporter in the prefrontal cortex of rat and mouse. Neuroscience 161:1091-1103.

Dunnett SB, Everitt BJ, Robbins TW (1991) The basal forebrain-cortical cholinergic system: interpreting the functional consequences of excitotoxic lesions. Trends Neurosci 14:494-501.

Dziedzicka-Wasylewska M, Faron-Gorecka A, Gorecki A, Kusemider M (2008) Mechanism of action of clozapine in the context of dopamine D1-D2 receptor hetero-dimerization--a working hypothesis. Pharmacol Rep 60:581-587.

Eckenstein F, Sofroniew MV (1983) Identification of central cholinergic neurons containing both choline acetyltransferase and acetylcholinesterase and of

central neurons containing only acetylcholinesterase. J Neurosci 3:2286-2291.

Eickhoff SB, Schleicher A, Scheperjans F, Palomero-Gallagher N, Zilles K (2007) Analysis of neurotransmitter receptor distribution patterns in the cerebral cortex. Neuroimage 34:1317-1330.

Ellis S, Keswick L (2011) Medical art studio.

Everitt BJ, Robbins TW (1997) Central cholinergic systems and cognition. Annu Rev Psychol 48:649-684.

Exley R, Cragg SJ (2008) Presynaptic nicotinic receptors: a dynamic and diverse cholinergic filter of striatal dopamine neurotransmission. Br J Pharmacol 153 Suppl 1:S283-297.

Fabian-Fine R, Skehel P, Errington ML, Davies HA, Sher E, Stewart MG, Fine A (2001) Ultrastructural distribution of the alpha7 nicotinic acetylcholine receptor subunit in rat hippocampus. J Neurosci 21:7993-8003.

Fadel J, Sarter M, Bruno JP (2001) Basal forebrain glutamatergic modulation of cortical acetylcholine release. Synapse 39:201-212.

Fenske MJ, Aminoff E, Gronau N, Bar M (2006) Top-down facilitation of visual object recognition: object-based and context-based contributions. Prog Brain Res 155:3-21.

Fiorillo CD, Williams JT (2000) Cholinergic inhibition of ventral midbrain dopamine neurons. J Neurosci 20:7855-7860.

Floresco SB, Magyar O (2006) Mesocortical dopamine modulation of executive functions: beyond working memory. Psychopharmacology (Berl) 188:567-585.

Fournier GN, Semba K, Rasmusson DD (2004) Modality- and region-specific acetylcholine release in the rat neocortex. Neuroscience 126:257-262.

Franklin K, Paxinos G (2007) The Mouse Brain in Stereotaxic Coordinates.: Elsevier Inc.

Freedman R, Coon H, Myles-Worsley M, Orr-Urtreger A, Olincy A, Davis A, Polymeropoulos M, Holik J, Hopkins J, Hoff M, Rosenthal J, Waldo MC, Reimherr F, Wender P, Yaw J, Young DA, Breese CR, Adams C, Patterson D, Adler LE, Kruglyak L, Leonard S, Byerley W (1997) Linkage of a neurophysiological deficit in schizophrenia to a chromosome 15 locus. Proc Natl Acad Sci U S A 94:587-592.

Friedman HV, Bresler T, Garner CC, Ziv NE (2000) Assembly of new individual excitatory synapses: time course and temporal order of synaptic molecule recruitment. Neuron 27:57-69.

Furuta A, Noda M, Suzuki SO, Goto Y, Kanahori Y, Rothstein JD, Iwaki T (2003) Translocation of glutamate transporter subtype excitatory amino acid carrier 1 protein in kainic acid-induced rat epilepsy. Am J Pathol 163:779-787.

Gabbott PL, Dickie BG, Vaid RR, Headlam AJ, Bacon SJ (1997) Local-circuit neurones in the medial prefrontal cortex (areas 25, 32 and 24b) in the rat: morphology and quantitative distribution. J Comp Neurol 377:465-499.

Gabbott PL, Warner TA, Jays PR, Salway P, Busby SJ (2005) Prefrontal cortex in the rat: projections to subcortical autonomic, motor, and limbic centers. J Comp Neurol 492:145-177.

Galimberti I, Gogolla N, Alberi S, Santos AF, Muller D, Caroni P (2006) Long-term rearrangements of hippocampal mossy fiber terminal connectivity in the adult regulated by experience. Neuron 50:749-763.

Garris PA, Wightman RM (1994) Different kinetics govern dopaminergic transmission in the amygdala, prefrontal cortex, and striatum: an in vivo voltammetric study. J Neurosci 14:442-450.

Gaykema RP, Luiten PG, Nyakas C, Traber J (1990) Cortical projection patterns of the medial septum-diagonal band complex. J Comp Neurol 293:103-124.

Gaykema RP, Zaborszky L (1996) Direct catecholaminergic-cholinergic interactions in the basal forebrain. II. Substantia nigra-ventral tegmental area projections to cholinergic neurons. J Comp Neurol 374:555-577.

George J Siegel, Agranoff BW, Albers RW, Fisher SK, Uhler MD (1999) Basic Neurochemistry: Molecular, Cellular and Medical Aspects. : Philadelphia: Lippincott-Raven.

Giacobini E (1998) Cholinergic foundations of Alzheimer's disease therapy. J Physiol Paris 92:283-287.

Giacobini E, Zhu XD, Williams E, Sherman KA (1996) The effect of the selective reversible acetylcholinesterase inhibitor E2020 on extracellular acetylcholine and biogenic amine levels in rat cortex. Neuropharmacology 35:205-211.

Gil Z, Connors BW, Amitai Y (1997) Differential regulation of neocortical synapses by neuromodulators and activity. Neuron 19:679-686.

Gill TM, Sarter M, Givens B (2000) Sustained visual attention performance-associated prefrontal neuronal activity: evidence for cholinergic modulation. J Neurosci 20:4745-4757.

Gioanni Y, Rougeot C, Clarke PB, Lepouse C, Thierry AM, Vidal C (1999) Nicotinic receptors in the rat prefrontal cortex: increase in glutamate release and facilitation of mediodorsal thalamo-cortical transmission. Eur J Neurosci 11:18-30.

Giocomo LM, Hasselmo ME (2007) Neuromodulation by glutamate and acetylcholine can change circuit dynamics by regulating the relative influence of afferent input and excitatory feedback. Mol Neurobiol 36:184-200.

Gogolla N, Galimberti I, Caroni P (2007) Structural plasticity of axon terminals in the adult. Curr Opin Neurobiol 17:516-524.

Goldman-Rakic PS (1996) Regional and cellular fractionation of working memory. Proc Natl Acad Sci U S A 93:13473-13480.

Goldwater DS, Pavlides C, Hunter RG, Bloss EB, Hof PR, McEwen BS, Morrison JH (2009) Structural and functional alterations to rat medial prefrontal cortex following chronic restraint stress and recovery. Neuroscience 164:798-808.

Golmayo L, Nunez A, Zaborszky L (2003) Electrophysiological evidence for the existence of a posterior cortical-prefrontal-basal forebrain circuitry in

modulating sensory responses in visual and somatosensory rat cortical areas. Neuroscience 119:597-609.

Gong S, Zheng C, Doughty ML, Losos K, Didkovsky N, Schambra UB, Nowak NJ, Joyner A, Leblanc G, Hatten ME, Heintz N (2003) A gene expression atlas of the central nervous system based on bacterial artificial chromosomes. Nature 425:917-925.

Goto Y, Grace AA (2005) Dopaminergic modulation of limbic and cortical drive of nucleus accumbens in goal-directed behavior. Nat Neurosci 8:805-812.

Goto Y, Otani S, Grace AA (2007) The Yin and Yang of dopamine release: a new perspective. Neuropharmacology 53:583-587.

Gotti C, Zoli M, Clementi F (2006) Brain nicotinic acetylcholine receptors: native subtypes and their relevance. Trends Pharmacol Sci 27:482-491.

Granon S, Passetti F, Thomas KL, Dalley JW, Everitt BJ, Robbins TW (2000) Enhanced and impaired attentional performance after infusion of D1 dopaminergic receptor agents into rat prefrontal cortex. J Neurosci 20:1208-1215.

Gratton A, Hoffer BJ, Gerhardt GA (1989) In vivo electrochemical studies of monoamine release in the medial prefrontal cortex of the rat. Neuroscience 29:57-64.

Greenberg AS, Esterman M, Wilson D, Serences JT, Yantis S (2010) Control of spatial and feature-based attention in frontoparietal cortex. J Neurosci 30:14330-14339.

Gritti I, Henny P, Galloni F, Mainville L, Mariotti M, Jones BE (2006) Stereological estimates of the basal forebrain cell population in the rat, including neurons containing choline acetyltransferase, glutamic acid decarboxylase or phosphate-activated glutaminase and colocalizing vesicular glutamate transporters. Neuroscience 143:1051-1064.

Gritti I, Manns ID, Mainville L, Jones BE (2003) Parvalbumin, calbindin, or calretinin in cortically projecting and GABAergic, cholinergic, or glutamatergic basal forebrain neurons of the rat. J Comp Neurol 458:11-31.

Groenewegen HJ, Uylings HB (2000) The prefrontal cortex and the integration of sensory, limbic and autonomic information. Prog Brain Res 126:3-28.

Guidotti A, Auta J, Davis JM, Dong E, Grayson DR, Veldic M, Zhang X, Costa E (2005) GABAergic dysfunction in schizophrenia: new treatment strategies on the horizon. Psychopharmacology (Berl) 180:191-205.

Gulledge AT, Bucci DJ, Zhang SS, Matsui M, Yeh HH (2009) M1 receptors mediate cholinergic modulation of excitability in neocortical pyramidal neurons. J Neurosci 29:9888-9902.

Gulledge AT, Jaffe DB (1998) Dopamine decreases the excitability of layer V pyramidal cells in the rat prefrontal cortex. J Neurosci 18:9139-9151.

Gulledge AT, Park SB, Kawaguchi Y, Stuart GJ (2007) Heterogeneity of phasic cholinergic signaling in neocortical neurons. J Neurophysiol 97:2215-2229.

Gulledge AT, Stuart GJ (2005) Cholinergic inhibition of neocortical pyramidal neurons. J Neurosci 25:10308-10320.

Hasselmo ME, Bower JM (1992) Cholinergic suppression specific to intrinsic not afferent fiber synapses in rat piriform (olfactory) cortex. J Neurophysiol 67:1222-1229.

Hasselmo ME, Sarter M (2010) Modes and Models of Forebrain Cholinergic Neuromodulation of Cognition. Neuropsychopharmacology.

Hasselmo ME, Sarter M (2011) Modes and models of forebrain cholinergic neuromodulation of cognition. Neuropsychopharmacology 36:52-73.

He Y, Janssen WG, Rothstein JD, Morrison JH (2000) Differential synaptic localization of the glutamate transporter EAAC1 and glutamate receptor subunit GluR2 in the rat hippocampus. J Comp Neurol 418:255-269.

Heidbreder CA, Groenewegen HJ (2003) The medial prefrontal cortex in the rat: evidence for a dorso-ventral distinction based upon functional and anatomical characteristics. Neurosci Biobehav Rev 27:555-579.

Heimer L, Van Hoesen GW (2006) The limbic lobe and its output channels: implications for emotional functions and adaptive behavior. Neurosci Biobehav Rev 30:126-147.

Henny P, Jones BE (2008) Projections from basal forebrain to prefrontal cortex comprise cholinergic, GABAergic and glutamatergic inputs to pyramidal cells or interneurons. Eur J Neurosci 27:654-670.

Herdegen T, Leah JD (1998) Inducible and constitutive transcription factors in the mammalian nervous system: control of gene expression by Jun, Fos and Krox, and CREB/ATF proteins. Brain Res Brain Res Rev 28:370-490.

Hernandez LF, Segovia G, Mora F (2008) Chronic treatment with a dopamine uptake blocker changes dopamine and acetylcholine but not glutamate and GABA concentrations in prefrontal cortex, striatum and nucleus accumbens of the awake rat. Neurochem Int 52:457-469.

Hibbs AR (2004) Confocal Microscopy for Biologists. New York: Kluwer Academic / Plenum Publishers.

Hill JA, Jr., Zoli M, Bourgeois JP, Changeux JP (1993) Immunocytochemical localization of a neuronal nicotinic receptor: the beta 2-subunit. J Neurosci 13:1551-1568.

Hsieh CY, Cruikshank SJ, Metherate R (2000) Differential modulation of auditory thalamocortical and intracortical synaptic transmission by cholinergic agonist. Brain Res 880:51-64.

Huang EP (1998) Synaptic transmission: spillover at central synapses. Curr Biol 8:R613-615.

Hughes P, Dragunow M (1995) Induction of immediate-early genes and the control of neurotransmitter-regulated gene expression within the nervous system. Pharmacol Rev 47:133-178.

Hulme EC, Birdsall NJ, Buckley NJ (1990) Muscarinic receptor subtypes. Annu Rev Pharmacol Toxicol 30:633-673.

Hur EE, Edwards RH, Rommer E, Zaborszky L (2009) Vesicular glutamate transporter 1 and vesicular glutamate transporter 2 synapses on cholinergic

neurons in the sublenticular gray of the rat basal forebrain: a double-label electron microscopic study. Neuroscience 164:1721-1731.

Ichikawa J, Chung YC, Li Z, Dai J, Meltzer HY (2002) Cholinergic modulation of basal and amphetamine-induced dopamine release in rat medial prefrontal cortex and nucleus accumbens. Brain Res 958:176-184.

Ichinohe N, Hyde J, Matsushita A, Ohta K, Rockland KS (2008) Confocal mapping of cortical inputs onto identified pyramidal neurons. Front Biosci 13:6354-6373.

Ikonomovic MD, Abrahamson EE, Isanski BA, Wuu J, Mufson EJ, DeKosky ST (2007) Superior frontal cortex cholinergic axon density in mild cognitive impairment and early Alzheimer disease. Arch Neurol 64:1312-1317.

Isaacson JS (2000) Spillover in the spotlight. Curr Biol 10:R475-477.

Jacob MH, Berg DK (1983) The ultrastructural localization of alpha-bungarotoxin binding sites in relation to synapses on chick ciliary ganglion neurons. J Neurosci 3:260-271.

Javitt DC (2010) Glutamatergic theories of schizophrenia. Isr J Psychiatry Relat Sci 47:4-16.

Jimenez-Capdeville ME, Dykes RW, Myasnikov AA (1997) Differential control of cortical activity by the basal forebrain in rats: a role for both cholinergic and inhibitory influences. J Comp Neurol 381:53-67.

Jones BE (2008) Modulation of cortical activation and behavioral arousal by cholinergic and orexinergic systems. Ann N Y Acad Sci 1129:26-34.

Jones IW, Bolam JP, Wonnacott S (2001) Presynaptic localisation of the nicotinic acetylcholine receptor beta2 subunit immunoreactivity in rat nigrostriatal dopaminergic neurones. J Comp Neurol 439:235-247.

Jones IW, Wonnacott S (2004) Precise localization of alpha7 nicotinic acetylcholine receptors on glutamatergic axon terminals in the rat ventral tegmental area. J Neurosci 24:11244-11252.

Kandel ER, Schwartz JH, Jessell TM (2000) Principles of Neural Science: McGraw-Hill Health Professions Division.

Kang JI, Vaucher E (2009a) Cholinergic pairing with visual activation results in long-term enhancement of visual evoked potentials. PLoS One 4:e5995.

Kang JI, Vaucher E (2009b) Cholinergic system activation paired with visual stimulation enhance visual performance of rats in the visual water maze. In: Society of Neuroscience 39th annual meeting Chicago.

Kew JN (2004) Positive and negative allosteric modulation of metabotropic glutamate receptors: emerging therapeutic potential. Pharmacol Ther 104:233-244.

Kim MJ, Chun SK, Kim YB, Mook-Jung I, Jung MW (2003) Long-term potentiation in visual cortical projections to the medial prefrontal cortex of the rat. Neuroscience 120:283-289.

Kiss JP, Vizi ES, Westerink BH (1999) Effect of neostigmine on the hippocampal noradrenaline release: role of cholinergic receptors. Neuroreport 10:81-86.

Kiyatkin EA, Rebec GV (2001) Impulse activity of ventral tegmental area neurons during heroin self-administration in rats. Neuroscience 102:565-580.

Kocharyan A, Fernandes P, Tong XK, Vaucher E, Hamel E (2008) Specific subtypes of cortical GABA interneurons contribute to the neurovascular coupling response to basal forebrain stimulation. J Cereb Blood Flow Metab 28:221-231.

Kostrzewa RM (1995) Dopamine receptor supersensitivity. Neurosci Biobehav Rev 19:1-17.

Kozak R, Bruno JP, Sarter M (2006) Augmented prefrontal acetylcholine release during challenged attentional performance. Cereb Cortex 16:9-17.

Kozak R, Martinez V, Young D, Brown H, Bruno JP, Sarter M (2007) Toward a neuro-cognitive animal model of the cognitive symptoms of schizophrenia: disruption of cortical cholinergic neurotransmission following repeated amphetamine exposure in attentional task-performing, but not non-performing, rats. Neuropsychopharmacology 32:2074-2086.

Lacroix LP, Ceolin L, Zocchi A, Varnier G, Garzotti M, Curcuruto O, Heidbreder CA (2006) Selective dopamine D3 receptor antagonists enhance cortical acetylcholine levels measured with high-performance liquid chromatography/tandem mass spectrometry without anti-cholinesterases. J Neurosci Methods 157:25-31.

Lambe EK, Picciotto MR, Aghajanian GK (2003) Nicotine induces glutamate release from thalamocortical terminals in prefrontal cortex. Neuropsychopharmacology 28:216-225.

Lapish CC, Kroener S, Durstewitz D, Lavin A, Seamans JK (2007) The ability of the mesocortical dopamine system to operate in distinct temporal modes. Psychopharmacology (Berl) 191:609-625.

Laplante F, Lappi DA, Sullivan RM (2011) Cholinergic depletion in the nucleus accumbens: effects on amphetamine response and sensorimotor gating. Prog Neuropsychopharmacol Biol Psychiatry 35:501-509.

Laplante F, Morin Y, Quirion R, Vaucher E (2005) Acetylcholine release is elicited in the visual cortex, but not in the prefrontal cortex, by patterned visual stimulation: a dual in vivo microdialysis study with functional correlates in the rat brain. Neuroscience 132:501-510.

Laplante F, Srivastava LK, Quirion R (2004) Alterations in dopaminergic modulation of prefrontal cortical acetylcholine release in post-pubertal rats with neonatal ventral hippocampal lesions. J Neurochem 89:314-323.

Larkum ME, Senn W, Luscher HR (2004) Top-down dendritic input increases the gain of layer 5 pyramidal neurons. Cereb Cortex 14:1059-1070.

Lendvai B, Stern EA, Chen B, Svoboda K (2000) Experience-dependent plasticity of dendritic spines in the developing rat barrel cortex in vivo. Nature 404:876-881.

Lendvai B, Vizi ES (2008) Nonsynaptic chemical transmission through nicotinic acetylcholine receptors. Physiol Rev 88:333-349.

Lester DB, Rogers TD, Blaha CD (2010) Acetylcholine-dopamine interactions in the pathophysiology and treatment of CNS disorders. CNS Neurosci Ther 16:137-162.

Lewis DA, Cruz DA, Melchitzky DS, Pierri JN (2001) Lamina-specific deficits in parvalbumin-immunoreactive varicosities in the prefrontal cortex of subjects with schizophrenia: evidence for fewer projections from the thalamus. Am J Psychiatry 158:1411-1422.

Lewis DA, Glantz LA, Pierri JN, Sweet RA (2003) Altered cortical glutamate neurotransmission in schizophrenia: evidence from morphological studies of pyramidal neurons. Ann N Y Acad Sci 1003:102-112.

Li Q, Lau A, Morris TJ, Guo L, Fordyce CB, Stanley EF (2004) A syntaxin 1, Galpha(o), and N-type calcium channel complex at a presynaptic nerve terminal: analysis by quantitative immunocolocalization. J Neurosci 24:4070-4081.

Li Z, Bonhaus DW, Huang M, Prus AJ, Dai J, Meltzer HY (2007) AC260584 (4-[3-(4-butylpiperidin-1-yl)-propyl]-7-fluoro-4H-benzo[1,4]oxazin-3-one), a selective muscarinic M1 receptor agonist, increases acetylcholine and dopamine release in rat medial prefrontal cortex and hippocampus. Eur J Pharmacol 572:129-137.

Li Z, Snigdha S, Roseman AS, Dai J, Meltzer HY (2008) Effect of muscarinic receptor agonists xanomeline and sabcomeline on acetylcholine and dopamine efflux in the rat brain; comparison with effects of 4-[3-(4-butylpiperidin-1-yl)-propyl]-7-fluoro-4H-benzo[1,4]oxazin-3-one (AC260584) and N-desmethylclozapine. Eur J Pharmacol 596:89-97.

Lipska BK, Aultman JM, Verma A, Weinberger DR, Moghaddam B (2002) Neonatal damage of the ventral hippocampus impairs working memory in the rat. Neuropsychopharmacology 27:47-54.

Livingstone PD, Dickinson JA, Srinivasan J, Kew JN, Wonnacott S (2010) Glutamate-dopamine crosstalk in the rat prefrontal cortex is modulated by Alpha7 nicotinic receptors and potentiated by PNU-120596. J Mol Neurosci 40:172-176.

Livingstone PD, Srinivasan J, Kew JN, Dawson LA, Gotti C, Moretti M, Shoaib M, Wonnacott S (2009) alpha7 and non-alpha7 nicotinic acetylcholine receptors modulate dopamine release in vitro and in vivo in the rat prefrontal cortex. Eur J Neurosci 29:539-550.

Livingstone PD, Wonnacott S (2009) Nicotinic acetylcholine receptors and the ascending dopamine pathways. Biochem Pharmacol 78:744-755.

Lopez-Gil X, Artigas F, Adell A (2009) Role of different monoamine receptors controlling MK-801-induced release of serotonin and glutamate in the medial prefrontal cortex: relevance for antipsychotic action. Int J Neuropsychopharmacol 12:487-499.

Lopez-Gil X, Artigas F, Adell A (2010) Unraveling monoamine receptors involved in the action of typical and atypical antipsychotics on glutamatergic and serotonergic transmission in prefrontal cortex. Curr Pharm Des 16:502-515.

Lorrain DS, Baccei CS, Bristow LJ, Anderson JJ, Varney MA (2003) Effects of ketamine and N-methyl-D-aspartate on glutamate and dopamine release in the rat prefrontal cortex: modulation by a group II selective metabotropic glutamate receptor agonist LY379268. Neuroscience 117:697-706.

Luiten PG, Gaykema RP, Traber J, Spencer DG, Jr. (1987) Cortical projection patterns of magnocellular basal nucleus subdivisions as revealed by anterogradely transported Phaseolus vulgaris leucoagglutinin. Brain Res 413:229-250.

Luscher C, Nicoll RA, Malenka RC, Muller D (2000) Synaptic plasticity and dynamic modulation of the postsynaptic membrane. Nat Neurosci 3:545-550.

Majeed W, Magnuson M, Hasenkamp W, Schwarb H, Schumacher EH, Barsalou L, Keilholz SD (2011) Spatiotemporal dynamics of low frequency BOLD fluctuations in rats and humans. Neuroimage 54:1140-1150.

Manders EM, Stap J, Brakenhoff GJ, van Driel R, Aten JA (1992) Dynamics of three-dimensional replication patterns during the S-phase, analysed by double labelling of DNA and confocal microscopy. J Cell Sci 103 (Pt 3):857-862.

Marchi M, Risso F, Viola C, Cavazzani P, Raiteri M (2002) Direct evidence that release-stimulating alpha7* nicotinic cholinergic receptors are localized on human and rat brain glutamatergic axon terminals. J Neurochem 80:1071-1078.

Marti M, Sbrenna S, Fuxe K, Bianchi C, Beani L, Morari M (2000) Increased responsivity of glutamate release from the substantia nigra pars reticulata to striatal NMDA receptor blockade in a model of Parkinson's disease. A dual probe microdialysis study in hemiparkinsonian rats. Eur J Neurosci 12:1848-1850.

Martin LJ, Blackstone CD, Levey AI, Huganir RL, Price DL (1993) Cellular localizations of AMPA glutamate receptors within the basal forebrain magnocellular complex of rat and monkey. J Neurosci 13:2249-2263.

McCormick DA (1992) Neurotransmitter actions in the thalamus and cerebral cortex. Journal of clinical neurophysiology : official publication of the American Electroencephalographic Society 9:212-223.

Mechawar N, Cozzari C, Descarries L (2000) Cholinergic innervation in adult rat cerebral cortex: a quantitative immunocytochemical description. J Comp Neurol 428:305-318.

Meshul CK, Emre N, Nakamura CM, Allen C, Donohue MK, Buckman JF (1999) Time-dependent changes in striatal glutamate synapses following a 6-hydroxydopamine lesion. Neuroscience 88:1-16.

Millan MJ, Di Cara B, Dekeyne A, Panayi F, De Groote L, Sicard D, Cistarelli L, Billiras R, Gobert A (2007) Selective blockade of dopamine D(3) versus D(2) receptors enhances frontocortical cholinergic transmission and social memory in rats: a parallel neurochemical and behavioural analysis. J Neurochem 100:1047-1061.

Millan MJ, Loiseau F, Dekeyne A, Gobert A, Flik G, Cremers TI, Rivet JM, Sicard D, Billiras R, Brocco M (2008) S33138 (N-[4-[2-[(3aS,9bR)-8-cyano-1,3a,4,9b-tetrahydro[1] benzopyrano[3,4-c]pyrrol-2(3H)-yl)-ethyl]phenyl-acetamide), a preferential dopamine D3 versus D2 receptor antagonist and potential antipsychotic agent: III. Actions in models of therapeutic activity and induction of side effects. J Pharmacol Exp Ther 324:1212-1226.

Miller EK, Cohen JD (2001) An integrative theory of prefrontal cortex function. Annual review of neuroscience 24:167-202.

Miner LH, Schroeter S, Blakely RD, Sesack SR (2003) Ultrastructural localization of the norepinephrine transporter in superficial and deep layers of the rat prelimbic prefrontal cortex and its spatial relationship to probable dopamine terminals. J Comp Neurol 466:478-494.

Muir JL, Everitt BJ, Robbins TW (1994) AMPA-induced excitotoxic lesions of the basal forebrain: a significant role for the cortical cholinergic system in attentional function. J Neurosci 14:2313-2326.

Muller D, Toni N, Buchs PA (2000) Spine changes associated with long-term potentiation. Hippocampus 10:596-604.

Mundorf ML, Joseph JD, Austin CM, Caron MG, Wightman RM (2001) Catecholamine release and uptake in the mouse prefrontal cortex. J Neurochem 79:130-142.

Murphy ER, Dalley JW, Robbins TW (2005) Local glutamate receptor antagonism in the rat prefrontal cortex disrupts response inhibition in a visuospatial attentional task. Psychopharmacology (Berl) 179:99-107.

Neuman RJ, Lobos E, Reich W, Henderson CA, Sun LW, Todd RD (2007) Prenatal smoking exposure and dopaminergic genotypes interact to cause a severe ADHD subtype. Biol Psychiatry 61:1320-1328.

Nicholson C, Sykova E (1998) Extracellular space structure revealed by diffusion analysis. Trends Neurosci 21:207-215.

Nieoullon A, Canolle B, Masmejean F, Guillet B, Pisano P, Lortet S (2006) The neuronal excitatory amino acid transporter EAAC1/EAAT3: does it represent a major actor at the brain excitatory synapse? J Neurochem 98:1007-1018.

Nikonenko I, Jourdain P, Muller D (2003) Presynaptic remodeling contributes to activity-dependent synaptogenesis. J Neurosci 23:8498-8505.

Okuda T, Haga T (2003) High-affinity choline transporter. Neurochem Res 28:483-488.

Ongur D, Price JL (2000) The organization of networks within the orbital and medial prefrontal cortex of rats, monkeys and humans. Cereb Cortex 10:206-219.

Onn SP, Wang XB, Lin M, Grace AA (2006) Dopamine D1 and D4 receptor subtypes differentially modulate recurrent excitatory synapses in prefrontal cortical pyramidal neurons. Neuropsychopharmacology 31:318-338.

Parikh V, Ji J, Decker MW, Sarter M (2010) Prefrontal beta2 subunit-containing and alpha7 nicotinic acetylcholine receptors differentially control glutamatergic and cholinergic signaling. J Neurosci 30:3518-3530.

Parikh V, Kozak R, Martinez V, Sarter M (2007) Prefrontal acetylcholine release controls cue detection on multiple timescales. Neuron 56:141-154.

Parikh V, Man K, Decker MW, Sarter M (2008) Glutamatergic contributions to nicotinic acetylcholine receptor agonist-evoked cholinergic transients in the prefrontal cortex. J Neurosci 28:3769-3780.

Parikh V, Sarter M (2008) Cholinergic mediation of attention: contributions of phasic and tonic increases in prefrontal cholinergic activity. Ann N Y Acad Sci 1129:225-235.

Passetti F, Dalley JW, O'Connell MT, Everitt BJ, Robbins TW (2000) Increased acetylcholine release in the rat medial prefrontal cortex during performance of a visual attentional task. Eur J Neurosci 12:3051-3058.

Paxinos G, Watson C (1997) The Rat Brain in Stereotaxic Coordinates. : Elsevier Inc.

Perry KW, Nisenbaum LK, George CA, Shannon HE, Felder CC, Bymaster FP (2001) The muscarinic agonist xanomeline increases monoamine release

and immediate early gene expression in the rat prefrontal cortex. Biol Psychiatry 49:716-725.

Peters JL, Michael AC (2000) Changes in the kinetics of dopamine release and uptake have differential effects on the spatial distribution of extracellular dopamine concentration in rat striatum. J Neurochem 74:1563-1573.

Prusky GT, West PW, Douglas RM (2000) Behavioral assessment of visual acuity in mice and rats. Vision Res 40:2201-2209.

Quarta D, Naylor CG, Morris HV, Patel S, Genn RF, Stolerman IP (2007) Different effects of ionotropic and metabotropic glutamate receptor antagonists on attention and the attentional properties of nicotine. Neuropharmacology 53:421-430.

Ragozzino ME, Kesner RP (1998) The effects of muscarinic cholinergic receptor blockade in the rat anterior cingulate and Prelimbic/Infralimbic cortices on spatial working memory. Neurobiol Learn Mem 69:241-257.

Raizada RD, Grossberg S (2003) Towards a theory of the laminar architecture of cerebral cortex: computational clues from the visual system. Cereb Cortex 13:100-113.

Ramanathan D, Tuszynski MH, Conner JM (2009) The basal forebrain cholinergic system is required specifically for behaviorally mediated cortical map plasticity. J Neurosci 29:5992-6000.

Rao TS, Correa LD, Adams P, Santori EM, Sacaan AI (2003) Pharmacological characterization of dopamine, norepinephrine and serotonin release in the

rat prefrontal cortex by neuronal nicotinic acetylcholine receptor agonists. Brain Res 990:203-208.

Ricciardi E, Pietrini P, Schapiro MB, Rapoport SI, Furey ML (2009) Cholinergic modulation of visual working memory during aging: a parametric PET study. Brain Res Bull 79:322-332.

Robbins TW (2005) Chemistry of the mind: neurochemical modulation of prefrontal cortical function. J Comp Neurol 493:140-146.

Robbins TW, Granon S, Muir JL, Durantou F, Harrison A, Everitt BJ (1998) Neural systems underlying arousal and attention. Implications for drug abuse. Ann N Y Acad Sci 846:222-237.

Robinson L, Platt B, Riedel G (2011) Involvement of the cholinergic system in conditioning and perceptual memory. Behav Brain Res 221:443-465.

Rockland KS (1998) Complex microstructures of sensory cortical connections. Curr Opin Neurobiol 8:545-551.

Rossi S, Singer S, Shearman E, Sershen H, Lajtha A (2005) The effects of cholinergic and dopaminergic antagonists on nicotine-induced cerebral neurotransmitter changes. Neurochem Res 30:541-558.

Rotaru DC, Lewis DA, Gonzalez-Burgos G (2007) Dopamine D1 receptor activation regulates sodium channel-dependent EPSP amplification in rat prefrontal cortex pyramidal neurons. J Physiol 581:981-1000.

Rothstein JD, Martin L, Levey AI, Dykes-Hoberg M, Jin L, Wu D, Nash N, Kuncl RW (1994) Localization of neuronal and glial glutamate transporters. Neuron 13:713-725.

Rousseau SJ, Jones IW, Pullar IA, Wonnacott S (2005) Presynaptic alpha7 and non-alpha7 nicotinic acetylcholine receptors modulate [3H]d-aspartate release from rat frontal cortex in vitro. Neuropharmacology 49:59-72.

Rusakov DA, Kullmann DM (1998) Extrasynaptic glutamate diffusion in the hippocampus: ultrastructural constraints, uptake, and receptor activation. J Neurosci 18:3158-3170.

Rye DB, Wainer BH, Mesulam MM, Mufson EJ, Saper CB (1984) Cortical projections arising from the basal forebrain: a study of cholinergic and noncholinergic components employing combined retrograde tracing and immunohistochemical localization of choline acetyltransferase. Neuroscience 13:627-643.

Sabo SL, Gomes RA, McAllister AK (2006) Formation of presynaptic terminals at predefined sites along axons. J Neurosci 26:10813-10825.

Sanacora G, Zarate CA, Krystal JH, Manji HK (2008) Targeting the glutamatergic system to develop novel, improved therapeutics for mood disorders. Nat Rev Drug Discov 7:426-437.

Santha E, Lendvai B, Gerevich Z (2001) Low temperature prevents potentiation of norepinephrine release by phenylephrine. Neurochem Int 38:237-242.

Sarter M, Bruno JP (2000) Cortical cholinergic inputs mediating arousal, attentional processing and dreaming: differential afferent regulation of the basal forebrain by telencephalic and brainstem afferents. Neuroscience 95:933-952.

Sarter M, Bruno JP, Givens B (2003) Attentional functions of cortical cholinergic inputs: what does it mean for learning and memory? Neurobiol Learn Mem 80:245-256.

Sarter M, Gehring WJ, Kozak R (2006) More attention must be paid: the neurobiology of attentional effort. Brain Res Rev 51:145-160.

Sarter M, Hasselmo ME, Bruno JP, Givens B (2005) Unraveling the attentional functions of cortical cholinergic inputs: interactions between signal-driven and cognitive modulation of signal detection. Brain Res Brain Res Rev 48:98-111.

Sarter M, Parikh V (2005) Choline transporters, cholinergic transmission and cognition. Nat Rev Neurosci 6:48-56.

Sarter M, Parikh V, Howe WM (2009a) nAChR agonist-induced cognition enhancement: integration of cognitive and neuronal mechanisms. Biochem Pharmacol 78:658-667.

Sarter M, Parikh V, Howe WM (2009b) Phasic acetylcholine release and the volume transmission hypothesis: time to move on. Nat Rev Neurosci 10:383-390.

Scanziani M, Salin PA, Vogt KE, Malenka RC, Nicoll RA (1997) Use-dependent increases in glutamate concentration activate presynaptic metabotropic glutamate receptors. Nature 385:630-634.

Schultz W (1997) Dopamine neurons and their role in reward mechanisms. Curr Opin Neurobiol 7:191-197.

Schultz W (2002) Getting formal with dopamine and reward. Neuron 36:241-263.

Schultz W, Dayan P, Montague PR (1997) A neural substrate of prediction and reward. Science 275:1593-1599.

Seamans JK, Yang CR (2004) The principal features and mechanisms of dopamine modulation in the prefrontal cortex. Prog Neurobiol 74:1-58.

Seguela P, Watkins KC, Descarries L (1988) Ultrastructural features of dopamine axon terminals in the anteromedial and the suprarhinal cortex of adult rat. Brain Res 442:11-22.

Semyanov A (2008) Can diffuse extrasynaptic signaling form a guiding template? Neurochem Int 52:31-33.

Sesack SR, Hawrylak VA, Matus C, Guido MA, Levey AI (1998) Dopamine axon varicosities in the prelimbic division of the rat prefrontal cortex exhibit sparse immunoreactivity for the dopamine transporter. J Neurosci 18:2697-2708.

Shearman E, Rossi S, Sershen H, Hashim A, Lajtha A (2005) Locally administered low nicotine-induced neurotransmitter changes in areas of cognitive function. Neurochem Res 30:1055-1066.

Shearman E, Rossi S, Szasz B, Juranyi Z, Fallon S, Pomara N, Sershen H, Lajtha A (2006) Changes in cerebral neurotransmitters and metabolites induced by acute donepezil and memantine administrations: a microdialysis study. Brain Res Bull 69:204-213.

Shepherd GM, Harris KM (1998) Three-dimensional structure and composition of CA3-->CA1 axons in rat hippocampal slices: implications for presynaptic connectivity and compartmentalization. J Neurosci 18:8300-8310.

Shepherd GM, Raastad M (2003) Axonal varicosity distributions along parallel fibers: a new angle on a cerebellar circuit. Cerebellum 2:110-113.

Shepherd GM, Raastad M, Andersen P (2002) General and variable features of varicosity spacing along unmyelinated axons in the hippocampus and cerebellum. Proc Natl Acad Sci U S A 99:6340-6345.

Sherren N, Pappas BA (2005) Selective acetylcholine and dopamine lesions in neonatal rats produce distinct patterns of cortical dendritic atrophy in adulthood. Neuroscience 136:445-456.

Shipp S (2007) Structure and function of the cerebral cortex. Curr Biol 17:R443-449.

Shu Y, Duque A, Yu Y, Haider B, McCormick DA (2007) Properties of action-potential initiation in neocortical pyramidal cells: evidence from whole cell axon recordings. J Neurophysiol 97:746-760.

Shuen JA, Chen M, Gloss B, Calakos N (2008) Drd1a-tdTomato BAC transgenic mice for simultaneous visualization of medium spiny neurons in the direct and indirect pathways of the basal ganglia. J Neurosci 28:2681-2685.

Siegel GJ, Agranoff BW, Albers RW, Fisher SK, Uhler MD (1999) Basic Neurochemistry: Molecular, Cellular and Medical Aspects. Philadelphia: Lippincott-Raven.

Silman I, Sussman JL (2005) Acetylcholinesterase: 'classical' and 'non-classical' functions and pharmacology. Curr Opin Pharmacol 5:293-302.

Smiley JF, Subramanian M, Mesulam MM (1999) Monoaminergic-cholinergic interactions in the primate basal forebrain. Neuroscience 93:817-829.

Sokoloff P, Giros B, Martres MP, Bouthenet ML, Schwartz JC (1990) Molecular cloning and characterization of a novel dopamine receptor (D3) as a target for neuroleptics. Nature 347:146-151.

Spruston N (2008) Pyramidal neurons: dendritic structure and synaptic integration. Nat Rev Neurosci 9:206-221.

Stahl SM (2009) The prefrontal cortex is out of tune in attention-deficit/hyperactivity disorder. J Clin Psychiatry 70:950-951.

Steckler T, Sahgal A, Aggleton JP, Drinkenburg WH (1998) Recognition memory in rats--III. Neurochemical substrates. Prog Neurobiol 54:333-348.

Steketee JD (2003) Neurotransmitter systems of the medial prefrontal cortex: potential role in sensitization to psychostimulants. Brain Res Brain Res Rev 41:203-228.

Stettler DD, Yamahachi H, Li W, Denk W, Gilbert CD (2006) Axons and synaptic boutons are highly dynamic in adult visual cortex. Neuron 49:877-887.

Stevenson CW, Sullivan RM, Gratton A (2003) Effects of basolateral amygdala dopamine depletion on the nucleus accumbens and medial prefrontal cortical dopamine responses to stress. Neuroscience 116:285-293.

Sunahara RK, Guan HC, O'Dowd BF, Seeman P, Laurier LG, Ng G, George SR, Torchia J, Van Tol HH, Niznik HB (1991) Cloning of the gene for a human dopamine D5 receptor with higher affinity for dopamine than D1. Nature 350:614-619.

Sydserff S, Sutton EJ, Song D, Quirk MC, Maciag C, Li C, Jonak G, Gurley D, Gordon JC, Christian EP, Doherty JJ, Hudzik T, Johnson E, Mrzljak L, Piser T, Smagin GN, Wang Y, Widzowski D, Smith JS (2009) Selective alpha7 nicotinic receptor activation by AZD0328 enhances cortical dopamine release and improves learning and attentional processes. Biochem Pharmacol 78:880-888.

Sykova E, Chvatal A (2000) Glial cells and volume transmission in the CNS. Neurochem Int 36:397-409.

Tam SY, Roth RH (1997) Mesoprefrontal dopaminergic neurons: can tyrosine availability influence their functions? Biochem Pharmacol 53:441-453.

Tavares RF, Correa FM (2006) Role of the medial prefrontal cortex in cardiovascular responses to acute restraint in rats. Neuroscience 143:231-240.

Thienel R, Voss B, Kellermann T, Reske M, Halfter S, Sheldrick AJ, Radenbach K, Habel U, Shah NJ, Schall U, Kircher T (2009) Nicotinic antagonist effects on functional attention networks. Int J Neuropsychopharmacol 12:1295-1305.

Thomsen MS, Hay-Schmidt A, Hansen HH, Mikkelsen JD (2010) Distinct neural pathways mediate alpha7 nicotinic acetylcholine receptor-dependent activation of the forebrain. Cereb Cortex 20:2092-2102.

Todd RD, Huang H, Smalley SL, Nelson SF, Willcutt EG, Pennington BF, Smith SD, Faraone SV, Neuman RJ (2005) Collaborative analysis of DRD4 and DAT genotypes in population-defined ADHD subtypes. J Child Psychol Psychiatry 46:1067-1073.

Trachtenberg JT, Chen BE, Knott GW, Feng G, Sanes JR, Welker E, Svoboda K (2002) Long-term in vivo imaging of experience-dependent synaptic plasticity in adult cortex. Nature 420:788-794.

Trantham-Davidson H, Neely LC, Lavin A, Seamans JK (2004) Mechanisms underlying differential D1 versus D2 dopamine receptor regulation of inhibition in prefrontal cortex. J Neurosci 24:10652-10659.

Trudeau LE (2004) Glutamate co-transmission as an emerging concept in monoamine neuron function. J Psychiatry Neurosci 29:296-310.

Tseng KY, Lewis BL, Lipska BK, O'Donnell P (2007) Post-pubertal disruption of medial prefrontal cortical dopamine-glutamate interactions in a developmental animal model of schizophrenia. Biol Psychiatry 62:730-738.

Tseng KY, O'Donnell P (2004) Dopamine-glutamate interactions controlling prefrontal cortical pyramidal cell excitability involve multiple signaling mechanisms. J Neurosci 24:5131-5139.

Turchi J, Sarter M (1997) Cortical acetylcholine and processing capacity: effects of cortical cholinergic deafferentation on crossmodal divided attention in rats. Brain research Cognitive brain research 6:147-158.

Tzschentke TM (2001) Pharmacology and behavioral pharmacology of the mesocortical dopamine system. Prog Neurobiol 63:241-320.

Tzschentke TM (2002) Glutamatergic mechanisms in different disease states: overview and therapeutical implications -- an introduction. Amino Acids 23:147-152.

Ullian EM, Sargent PB (1995) Pronounced cellular diversity and extrasynaptic location of nicotinic acetylcholine receptor subunit immunoreactivities in the chicken pretectum. J Neurosci 15:7012-7023.

Umbriaco D, Watkins KC, Descarries L, Cozzari C, Hartman BK (1994) Ultrastructural and morphometric features of the acetylcholine innervation in adult rat parietal cortex: an electron microscopic study in serial sections. J Comp Neurol 348:351-373.

Uylings HB, Groenewegen HJ, Kolb B (2003) Do rats have a prefrontal cortex? Behav Brain Res 146:3-17.

Vaucher E, Borredon J, Bonvento G, Seylaz J, Lacombe P (1997) Autoradiographic evidence for flow-metabolism uncoupling during

stimulation of the nucleus basalis of Meynert in the conscious rat. J Cereb Blood Flow Metab 17:686-694.

Vaucher E, Borredon J, Seylaz J, Lacombe P (1995) Autoradiographic distribution of cerebral blood flow increases elicited by stimulation of the nucleus basalis magnocellularis in the unanesthetized rat. Brain Res 691:57-68.

Vaucher E, Hamel E (1995) Cholinergic basal forebrain neurons project to cortical microvessels in the rat: electron microscopic study with anterogradely transported Phaseolus vulgaris leucoagglutinin and choline acetyltransferase immunocytochemistry. J Neurosci 15:7427-7441.

Verney C, Alvarez C, Geffard M, Berger B (1990) Ultrastructural Double-Labelling Study of Dopamine Terminals and GABA-Containing Neurons in Rat Anteromedial Cerebral Cortex. Eur J Neurosci 2:960-972.

Vertes RP (2004) Differential projections of the infralimbic and prelimbic cortex in the rat. Synapse 51:32-58.

Vertes RP (2006) Interactions among the medial prefrontal cortex, hippocampus and midline thalamus in emotional and cognitive processing in the rat. Neuroscience 142:1-20.

Vidal F, Hidalgo J (1993) Effect of zinc and copper on preimplantation mouse embryo development in vitro and metallothionein levels. Zygote 1:225-229.

Vincent SL, Khan Y, Benes FM (1993) Cellular distribution of dopamine D1 and D2 receptors in rat medial prefrontal cortex. J Neurosci 13:2551-2564.

Vincent SL, Khan Y, Benes FM (1995) Cellular colocalization of dopamine D1 and D2 receptors in rat medial prefrontal cortex. Synapse 19:112-120.

Vizi ES (2000) Role of high-affinity receptors and membrane transporters in nonsynaptic communication and drug action in the central nervous system. Pharmacol Rev 52:63-89.

Vizi ES, Kiss JP, Lendvai B (2004) Nonsynaptic communication in the central nervous system. Neurochem Int 45:443-451.

Voytko ML, Olton DS, Richardson RT, Gorman LK, Tobin JR, Price DL (1994) Basal forebrain lesions in monkeys disrupt attention but not learning and memory. J Neurosci 14:167-186.

Vysokanov A, Flores-Hernandez J, Surmeier DJ (1998) mRNAs for clozapine-sensitive receptors co-localize in rat prefrontal cortex neurons. Neurosci Lett 258:179-182.

Wallace TL, Ballard TM, Pouzet B, Riedel WJ, Wettstein JG (2011) Drug targets for cognitive enhancement in neuropsychiatric disorders. Pharmacol Biochem Behav.

Wang X, Zhong P, Yan Z (2002) Dopamine D4 receptors modulate GABAergic signaling in pyramidal neurons of prefrontal cortex. J Neurosci 22:9185-9193.

Wang Y, Neubauer FB, Luscher HR, Thurley K (2010) GABAB receptor-dependent modulation of network activity in the rat prefrontal cortex in vitro. Eur J Neurosci 31:1582-1594.

Weidner R, Krummenacher J, Reimann B, Muller HJ, Fink GR (2009) Sources of top-down control in visual search. J Cogn Neurosci 21:2100-2113.

Wonnacott S, Barik J, Dickinson J, Jones IW (2006) Nicotinic receptors modulate transmitter cross talk in the CNS: nicotinic modulation of transmitters. J Mol Neurosci 30:137-140.

Woolf NJ (1991) Cholinergic systems in mammalian brain and spinal cord. Prog Neurobiol 37:475-524.

Wouterlood FG, Boekel AJ, Meijer GA, Belien JA (2007) Computer-assisted estimation in the CNS of 3D multimarker 'overlap' or 'touch' at the level of individual nerve endings: a confocal laser scanning microscope application. J Neurosci Res 85:1215-1228.

Wu WR, Li N, Sorg BA (2002) Regulation of medial prefrontal cortex dopamine by alpha-amino-3-hydroxy-5-methylisoxazole-4-propionate/kainate receptors. Neuroscience 114:507-516.

Xu TX, Sotnikova TD, Liang C, Zhang J, Jung JU, Spealman RD, Gainetdinov RR, Yao WD (2009) Hyperdopaminergic tone erodes prefrontal long-term potential via a D2 receptor-operated protein phosphatase gate. J Neurosci 29:14086-14099.

Yamahachi H, Marik SA, McManus JN, Denk W, Gilbert CD (2009) Rapid axonal sprouting and pruning accompany functional reorganization in primary visual cortex. Neuron 64:719-729.

Yamasaki M, Matsui M, Watanabe M (2010) Preferential localization of muscarinic M1 receptor on dendritic shaft and spine of cortical pyramidal cells and its anatomical evidence for volume transmission. J Neurosci 30:4408-4418.

Yang CR, Mogenson GJ (1990) Dopaminergic modulation of cholinergic responses in rat medial prefrontal cortex: an electrophysiological study. Brain Res 524:271-281.

Yang K, Buhlman L, Khan GM, Nichols RA, Jin G, McIntosh JM, Whiteaker P, Lukas RJ, Wu J (2011) Functional nicotinic acetylcholine receptors containing alpha6 subunits are on GABAergic neuronal boutons adherent to ventral tegmental area dopamine neurons. J Neurosci 31:2537-2548.

Yung KK, Bolam JP, Smith AD, Hersch SM, Ciliax BJ, Levey AI (1995) Immunocytochemical localization of D1 and D2 dopamine receptors in the basal ganglia of the rat: light and electron microscopy. Neuroscience 65:709-730.

Zaborszky L, Cullinan WE, Braun A (1991) Afferents to basal forebrain cholinergic projection neurons: an update. Adv Exp Med Biol 295:43-100.

Zaborszky L, Duque A (2000) Local synaptic connections of basal forebrain neurons. Behav Brain Res 115:143-158.

Zaborszky L, Gaykema RP, Swanson DJ, Cullinan WE (1997) Cortical input to the basal forebrain. Neuroscience 79:1051-1078.

Zaborszky L, Pang K, Somogyi J, Nadasdy Z, Kallo I (1999) The basal forebrain corticopetal system revisited. Ann N Y Acad Sci 877:339-367.

Zahniser NR, Sorkin A (2004) Rapid regulation of the dopamine transporter: role in stimulant addiction? Neuropharmacology 47 Suppl 1:80-91.

Zhang L (2006) Cholinergic Receptor Knockout Mice.

Zhang TY, Chretien P, Meaney MJ, Gratton A (2005) Influence of naturally occurring variations in maternal care on prepulse inhibition of acoustic startle and the medial prefrontal cortical dopamine response to stress in adult rats. J Neurosci 25:1493-1502.

Zhang ZW, Burke MW, Calakos N, Beaulieu JM, Vaucher E (2010) Confocal Analysis of Cholinergic and Dopaminergic Inputs onto Pyramidal Cells in the Prefrontal Cortex of Rodents. Front Neuroanat 4:21.

Zhang ZW, Kang JI, Vaucher E (2011) Axonal varicosity density as an index of local neuronal interactions. PLoS One 6:e22543.

Zhong P, Gu Z, Wang X, Jiang H, Feng J, Yan Z (2003) Impaired modulation of GABAergic transmission by muscarinic receptors in a mouse transgenic model of Alzheimer's disease. J Biol Chem 278:26888-26896.

Zoli M, Jansson A, Sykova E, Agnati LF, Fuxe K (1999) Volume transmission in the CNS and its relevance for neuropsychopharmacology. Trends Pharmacol Sci 20:142-150.